2012

Decision support system for sensor-based autonomous filling of grain containers

Andrew Thomas Jennett
Iowa State University

Decision support system for sensor-based autonomous filling of grain containers

by

Andrew Thomas Jennett

A thesis submitted to the graduate faculty

in partial fulfillment of the requirements for the degree of

MASTER OF SCIENCE

Major: Agricultural Engineering

Program of Study Committee:

Matthew J. Darr, Major Professor
D. Raj Raman
Brian L. Steward

Iowa State University

Ames, Iowa

2012

Table of Contents

List of Figures

List of Tables

Acknowledgements

I would like to thank Deere and Company for providing the funding and equipment for this research. I would like to thank Dr. Matt Darr for his direction and guidance through my work on this project. My program of study committee members, Drs. Matt Darr, Raj Raman, and Brian Steward, deserve my thanks for helping shape the research objectives of this work into important scientific knowledge.

Special thanks are given to Bob McNaull for writing and developing code in the embedded controllers of the ultrasonic data acquisition system and for his expertise in initiating functionality on the dSPACE development platform. Thanks are given to my other fellow graduate students and staff on the Smart Unloading project, Alex Nykamp, Ben Potter, and John Kruckeberg, who have spent countless hours in the office and in the field patiently developing software. I would also like to thank the undergraduate students who assisted with my research, Jeff Askey, Darin Goza, Chris Hoffman, Joe Klaes, and Kent Thoreson.

Deserving my most sincere thanks and appreciation is my wife, Nicole, who has not only contributed love, support, and patience throughout my graduate education, but continues to impress me as one of the brightest engineers I have ever met.

Abstract

Autonomous technology in agriculture offers many products that reduce distractions and fatigue experienced by machinery operators, including automatic path guidance, variable rate product delivery, and precision seed placement. However, the size and complexity of modern mechanical harvesting operations have limited the ability of autonomous technology to significantly reduce total negative effects on grain combine operators. Combine operators are highly susceptible to fatigue because several tasks must be performed simultaneously to ensure safe machine operation. These duties include monitoring internal threshing and crop flow intake, maintaining row alignment, avoiding foreign material intake, and overseeing unloading grain.

The primary goal of this project was to design a decision support system for autonomous unloading of combines. When unloading grain on-the-go, operators divert more attention away from critical tasks to focus on grain delivery to the adjacent cart. An autonomous system eliminating the need for combine operators to focus on unloading on-the-go potentially reduces operator stress and grain spillage.

Critical to the decision support system for autonomous unloading was the input of a two-dimensional fill grid used to describe the grain height in the cart. The inverse distance weighting method, an estimation technique common to spatial data modeling, was used to estimate points in the fill grid of a grain cart prone to being immeasurable or highly variable. This method was successful in estimating missing points in a grain cart under difficult delivery conditions to within 15 cm of underestimation and 25 cm of overestimation. A model to predict the weight of grain in a grain cart was developed using the average grain height measured in the cart. The model demonstrated high robustness by producing mean errors that changed by less than 2% of the total cart volume when the delivery conditions strayed from typical conditions to highly biased conditions. The decision support system that was developed exhibited robust performance when critical features of the system were tested at typical levels. Field testing validated the potential to apply the decision support system to autonomous combine unloading systems by producing predictable and consistent final cart volumes that were within 5% of the total volume.

Chapter 1 Introduction

Increasing productivity has been an important focus in the last century for agricultural producers. Technology from other industries is continuously finding new applications in agriculture, and new ideas are being generated within the agricultural sector to help solve the challenge of satisfying the world's ever-increasing demand for food, fiber, and fuel. Traditionally, increased productivity has been achieved with more powerful tractors and larger implements, but heavy machinery traffic has adverse effects on soil structure and future yield potential. Higher productivity also can be obtained with genetic hybrids, but this often requires a supply of more nutrients than lands naturally carry, creating the demand for additional nutrient application. When misapplied, chemicals and fertilizers can damage the fragile environmental systems upon which production agriculture relies. For these reasons, recent developments in agriculture have specifically focused on measures that reduce waste and increase productivity while using fewer resources. Precision agriculture encompasses several technologies focused on accomplishing this goal.

Spatial field management and variable rate application are two complementary precision agriculture technologies commonly used today. Before spatial management, seeding and nutrient application were conducted at a field level with no regard to changes in soil characteristics across a field. Spatial data analysis allowed management to take place in areas smaller than the width of an implement or applicator. Knowledge at the sub-implement level allowed seeding and application rate decisions to be made as machinery moves through a field, not just at the start of a field.

Management at the sub-implement level requires control at least at the same level of precision. Sub-implement soil data without sub-implement control capabilities is impractical and a waste of resources. Variable rate application (VRA) technology provides sub-implement control solutions in many ways, such as individually adjusting seeding rates across row units or by changing flow rates through specific liquid applicator nozzles. However, these systems will not precisely guide machinery along the best path of travel which would reduce operator fatigue. An auto guidance system is required to accomplish this.

Auto guidance systems have developed as part of the drive for more intelligent vehicles that offer optimized functionality and increased productivity. Auto steering is a specific type of auto

guidance system that controls machine trajectory by changing the vehicle's heading. Today, most machinery comes from the factory with hardware already installed to support auto steering systems. Otherwise, universal auto steering units can also be installed on almost any vehicle already in use, making self-guided vehicles readily available.

Auto steering technology in agriculture has transitioned to cover almost all agricultural machines. Tractors experienced the first application of auto steering because tractors typically make several passes over a field in one year. Auto steering was later applied to vehicles that travel through the field just once in a growing season, such as combines and sprayers. These vehicles created a unique challenge in that they cannot simply follow their own paths dictated by global positioning system (GPS) data. Since plants are already growing in the field, their position in relation to the existing crop must be monitored to keep from destroying plants. The impact of an auto guidance path being offset so the wheels travel directly over the existing crop could severely impact yields. To solve this issue row feeling technology was been implemented to measure the lateral distance a wheel or snout is from the adjacent plant rows. This distance is controlled by an auto steering system which aims to maintain equal distance from the plants on both sides.

Once sprayers are outfitted with VRA systems and can be safely guided through the field with row feelers, they are ready for full autonomous operation with minimal operator interaction beyond start up. Combines equipped with auto row guidance, however, still have the opportunity for more automation because several internal and external processes require close monitoring. A few of these processes include watching crop flow intake, monitoring internal grain thrashing and separating, and staying alert for unexpected machine behavior. It is difficult to apply autonomous technology to these functions since they are heavily dependent on crop conditions but, during normal operation, periodic events occur which divert operator attention away from these processes, such as unloading on-the-go.

Unloading grain on-the-go is the process of transferring grain from the combine's on-board storage hopper to an adjacent grain cart or trailer while the combine continues traveling through the field harvesting grain. Unloading on-the-go versus unloading stationary minimizes the amount of time the combine spends doing functions other than harvesting. This is important for maximizing productivity because the grain harvester is typically the bottle-neck of harvesting operations. The extra functions that must be monitored during unloading on-the-go include:

1. Maintaining a constant relative position to the adjacent grain cart;
2. Filling to a desired level in the grain cart and moving to a new position when full;
3. Disengaging the auger to prevent spillage when the cart moves from underneath the auger.

Unloading on-the-go has been identified by many original equipment manufacturers (OEMs) as an opportunity for automation to benefit operators. Control systems have already been developed by OEMs that use GPS position data to position a tractor relative to a combine. This relative position is maintained throughout the unloading event by controlling the speed and trajectory of the tractor towing the grain cart. A master-slave relationship is maintained until the system relinquishes control to the operator at the end of an unloading cycle. This autonomous control system effectively removes Function #1 from the operator's responsibility, but Functions #2 and #3 still require close monitoring.

The primary goal of this project was to completely automate unloading on-the-go for grain harvesters. Specifically, this thesis focuses on estimating the grain height in grain carts and determining the impact of grain height data on an autonomous filling system. By accomplishing this goal, a decision support algorithm was implemented in an autonomous filling system with robust field performance.

Chapter 2 Literature Review

2.1 Background

The 2010-2011 estimated area of land harvested for corn, soybeans, and wheat in the United States was more than 200 million acres, and this land produced an estimated yield of more than 17 billion bushels (United States Department of Agriculture, 2011). Since farming operations in the United States typically use mechanized harvesters, nearly all this grain was, at some point, unloaded from a combine into a separate transportation container before leaving the field. With such a large volume yield, the unloading process becomes an event of high importance and poses an opportunity for substantial engineering advancement.

The interaction between combine and tractor operators involves many phases in order for a successful unloading event to occur. The first communication is a signal from the combine operator that notifies the tractor operator the hopper needs to be unloaded. When this signal is received, the tractor operator will drive toward the combine until it has a parallel direction of travel with the combine. When the combine operator feels safe to deliver grain, the operator will engage the auger and start emptying the hopper. This process can be conducted while the combine is stationary or while it continues traveling through the field. Stationary unloading adds little distraction to combine operators because they do not need to monitor crop intake anymore. However, if it is desirable to continue harvesting grain, the process can be very distracting as the combine operator watches crop intake and unloading simultaneously.

Although unloading on-the-go adds risk to the harvest process, it poses the more substantial benefit of gaining productivity versus unloading stationary in the field. The time spent unloading can be substantial, especially in high yielding crops such as corn, as shown in Equation 1, which estimates the proportion of time spent unloading grain from a combine based on the harvest rate and unloading capacity:

$$p = \frac{w \cdot n \cdot v \cdot Y}{356400 \cdot Q} \tag{1}$$

Where p = proportion of harvesting time spent unloading grain

w = row spacing, in/row

n = number of rows on head

v = combine velocity, mi/h

Y = crop yield, bu/ac

Q = combine unload rate, bu/sec

Unloading on-the-go was less critical when combines were smaller and had slower travel speeds and narrower heads. However, when harvesting corn yielding 180 bu/ac with a 12-row head, crop intake can reach as high as 60 lb/sec at normal field speeds. Typical Class 8 (279+ kW; 375+ HP) harvesters are equipped with unloading augers that have a 3.5 bu/sec unload rate. The result is approximately 20% of the total harvest time spent unloading. Not having the capability to unload on-the-go would significantly decrease combine productivity and increase harvesting costs.

An economic model developed at Iowa State University uses these parameters to predict harvesting costs (Webster, 2011). By unloading 90% of the total harvested grain on-the-go versus stationary, the model predicts a reduction in harvesting costs of more than 25% (Webster, 2011). After realizing such a large reduction in costs, the economic benefits of unloading on-the-go become apparent.

2.2 Current Autonomous Technology

2.2.1 Agricultural machine positioning

2.2.1.1 CLAAS Assistant System for the Unloading Process

CLAAS GmbH began significant development of a control system to automatically position an agricultural trailer next to a harvester in 2007 with the launch of the Assistant System for the Unloading Process (ASUL) project (Happich et al., 2009). The concept of autonomous unloading started much earlier when CLAAS filed a United States patent application in 1996 for a device for automatic filling of containers. From the patent description, it is evident for more than a decade there has been interest in engineering a solution for autonomous grain and forage harvesting by OEMs. The application reads:

> *A device for automatic filling of a mobile container with a material stream from a harvester moving alongside a discharge knee/discharge pipe which is controllably pivotable around a vertical and/or horizontal axis, with a*

pivotable discharge flap at the end from the harvester to the container ***(Pollklas, 1996)****.*

The relative position control system developed by CLAAS required seven GPS receivers in the early stages of development. This system maintained relative positional deviation of the two vehicles of around 5 cm. However, the ability of the system to deliver material to a specific point in the adjacent container was only accurate to within 50 cm (Happich et al., 2009). This meant there could be 50 cm of error between the control system's calculated material delivery location and the actual delivery location. An update on the performance of the ASUL relative positioning system was not available, and this system has not been commercially released. Several competing OEMs have announced similar technologies that have not been released.

2.2.1.2 Case IH Vehicle-to-Vehicle

Case IH announced its autonomous vehicle position control system at the end of 2010 (CNH Global N.V., 2010). Its product was called Vehicle-to-Vehicle. Through wireless communication, Vehicle-2-Vehicle allows the combine to control tractor speed and trajectory when the tractor moves into a defined "active" zone.

2.2.1.3 John Deere Machine Sync

John Deere announced its version of automatic vehicle positioning in late summer 2011 as a product called Machine Sync (Deere & Company, 2011). Machine Sync allows the combine operator to control the location of the adjacent grain cart via radio communication between the two vehicles. From the combine or tractor cab, operators can send small adjustment commands to change the tractor position. This functionality allows the operator to evenly distribute grain in the cart as opposed to delivering grain only to a single point.

2.2.1.4 Loader-dumper positioning

Agriculture is not the only industry developing control systems to automate routine machine operations. The construction and mining industry involves many repeated processes that open opportunities for automation. A patent filed by Pulli et al. (2010) involves automation in quarry mining. In quarry mining, large volumes of rock must be removed from the mining pit to an offsite location. Typically, this is done with large dump trucks designed to carry heavy loads.

The system patented by Pulli et al. proposed automating the repetitive cycle of using a front-end loader to move rock from a pile to a dump truck. Specifically, the patent applied to autonomously positioning the loader in the correct position with respect to an adjacent dump truck. The loader autonomously drives into the zone near the dump truck, and the loader dumps its load of rock into the dump truck bed (Pulli et al., 2010).

The dump truck transports its load to the offsite destination and returns to the quarry. When the dump truck gets close to its original location, the autonomous control system engages to position the truck exactly where it was before. Although this system likely will not bring the level of automation required to remove an operator from either machine, it should create a safer work environment by allowing the loader operator to monitor surroundings instead of driving the machine.

2.2.2 Distance measurement sensors

Fill measurement sensors have been used by liquid container filling manufacturers for precise volume delivery to consumer products. Enander (1984) patented a machine to deliver precise quantities of liquid to bottles. It uses ultrasonic pulses directed downward toward the liquid surface which measures the fill height and determines when the filling machine needs to begin closing the control valve (Enander, 1984).

Performance of the ultrasonic sensor-based measurement system is much more accurate than vision-based systems, which will be discussed later in this thesis. The ultrasonic system was able to achieve final container fill height accuracies of 0.02 cm for containers 0.12 L to 18 L in size (Enander, 1984). No standard deviation was given for the height accuracy of the system.

Applying ultrasonic sensors to measure grain fill height produced several challenges outlined in Enander's patent. The first challenge was finding sensors that fit the desired range of operation. The liquid container filling system has a sensing range of 1.5 in to 9 in (Enander, 1984). Although this range is perfectly acceptable for fixed machines, it is not practical for grain and forage harvesting applications. The other challenge stems from interference from other sensors or peripheral objects. When a pulse travels through the air, part of the wave can mistakably reflect off other objects. Most of the erroneous reflection is undetectable by the sensor, but sometimes environmental acoustics will cause incorrect readings.

2.2.3 Vision systems in agriculture

Machine vision has been a promising technology in the effort to automate agriculture. It is compact, and it offers flexible mounting options, making it a viable technology to be used across different machine platforms and field operations (Moller, 2010). Several common applications of vision sensors in agriculture include mechanical weed control, machine auto guidance, and trailer filling control.

2.2.3.1 Mechanical weeding

Mechanical weed control research has gained attention due to increased restrictions on pesticide application and an increased demand for organic foods. Most vision-based weed control systems use 2D imagery to identify weeds growing between rows of plants. Once inter-row plants are identified, a mechanical cultivator uproots the plant with an automated tillage attachment. Moller reports these systems can provide up to ±3 cm accuracy at operating speeds of 10 km/h (6.2 mi/h) (Moller, 2010). When weed control automation is combined with machinery auto steering systems, mechanical cultivation can be optimized in fields with established plants. This combined technology also allows less experienced operators to be hired for labor because the only field tasks involved would be turning the tractor around at the end of the row and lining it up with the next row as the autonomous systems resume control.

2.2.3.2 Auto guidance systems

GPS auto guidance technology has a much longer history in agriculture than vision systems, but vision-based auto guidance has seen extensive development recently in applications not suited for traditional GPS guidance systems (Moller, 2010). GPS is useful for field operations before and after crops have been harvested, such as tillage, seeding, and mowing. However, when machinery must be guided through existing crops, such as mowing vineyards or baling hay swaths, it is important for machinery to have the capability to adapt to the non-linear paths along which the existing plants lie.

Stereovision cameras have been widely adopted for auto guidance. Stereovision requires two cameras separated by a known distance that capture images simultaneously. Because each image represents a different viewpoint, features will be offset in each image as a function of the distance to that feature. This disparity can be calculated by an internal computer and used to determine the distance from the camera pair to the detected feature, giving the stereo system 3D

imagery capabilities. With the ability to capture 3D data, object tracking in the field is the main application of stereovision technology today. Tracking algorithms usually reference objects, such as hay swaths, with respect to a ground plane that can be determined from the camera's mounting height and angle (Moller, 2010).

Two commercially available products utilizing stereovision technology include the Clemens VineScout and CLAAS CAMPilot. The Clemens system is used to guide tractors along vineyard rows to mow unwanted vegetation growth. Precision guidance is important because the impact of mow decks can fatally wound grape vines. This system has seen accuracy of around ±3 cm (Moller, 2010).

The CAMPilot system from CLAAS uses variation in the ground plane to detect raked swaths of hay on the ground. This system allows operators to divert attention away from driving while the CAMPilot system takes control. This allows operators to focus on optimizing vehicle and implement settings instead. CAMPilot systems are accurate to about ±5 cm at field speeds up to 10 km/h and ±10 cm at 20 km/h (Moller, 2010).

2.2.3.3 CLAAS AutoFill

One of the most advanced autonomous systems using stereovision is an unloading system called AutoFill developed by CLAAS for self-propelled forage harvesters (SPFHs). AutoFill is the only product announced to the public that uses information about the fill level of the adjacent container in its control decisions. Because the ideal material delivery location changes during a typical unloading cycle and the material height is used as feedback to the system, AutoFill is the only fully autonomous unloading system currently available for SPFHs or combines. All the positioning systems described earlier required operator interaction to change the material delivery point.

2.2.4 Model-based fill estimation

Aside from being the only product that automatically commands new relative positions during an unloading cycle, the AutoFill system is also unique because the basis for a decision to change relative positions does not come only from the measured material height. Instead, a mass flow rate model is used to estimate the accumulating volume in a container. Advanced imaging techniques with stereovision have seen success in other agricultural applications, making it a viable option to detect material height instead of estimating it. However, the designers of the system, Happich et al., decided not to immediately investigate visual sensors because the agricultural

engineering community is more accustomed to physical sensing and data logging techniques (Happich et al., 2010).

The material flow model for fill estimation has the advantage of using sensors already prevalent on agricultural machines, such as a rotary potentiometer to estimate material flow through a chamber. The volume flow is then translated into a volume of material delivered to an empty space. The system relies on bulk material models to estimate the fullness of the container. The crucial input to this model besides flow rate is the delivery point. Highly accurate delivery location information is required for acceptable system performance; however, poor delivery location data could result in the loading model erroneously generating full areas of the container where it is actually empty and moving to new locations that are actually full (Happich et al., 2009).

One modeling approach Happich et al. considered using was computational fluid dynamics (CFD) and discrete element methods (DEM) to predict bulk material piles. However, after initial testing it was determined the inhomogeneous material properties of forage required more computing power than would be available on off-road agricultural machinery (Happich et al., 2009).

A simplified geometric modeling approach was used instead of CFD and DEM. Hyperbolas, cones, and parabolas were used because their shapes and boundaries could be described with established mathematical equations. Also, modeling the shape of a cumulative pile of material only required three dynamic inputs. The first input was a single vector in 3D space defining the direction of travel of the harvested material. The second and third inputs were the front and rear slopes of a conic volume created from accumulating material (Happich et al., 2010).

Accuracy of the model-based fill estimation technique was quantified with field tests. Each test included completely filling a forage trailer to the desired level using the fill estimation model. A laser scanner mounted on a tractor loader was used to collect actual height data. Once the trailer was completely full, it drove under the raised loader while data collection software stored distance measurements. Using a known length, width, and height of the trailer, surface plots were created of the material. The mean maximum error in height across the length of the trailer for all 29 trials that were conducted was 0.60 cm. It was concluded this level of error for a container with 2.5 m sides was acceptable for satisfactory system performance (Happich et al., 2010).

2.2.5 Sensor-based filling strategies

2.2.5.1 CLAAS AutoFill

The CLAAS patent application of 1996 (Pollklas) was the first document describing a control strategy for filling a container by automatically deciding a material delivery point. It explained the need for a desired material delivery point and an input maximum fill level to define when a container was full. With the CLAAS filling strategy, once the current material delivery location was full, the control system used fill data from the rest of the container to determine the next desired location.

Happich et al. (2010) briefly described early research on the ability to make requests for new relative positions based on results of fill modeling. Fill modeling allows the autonomous system to transition from one delivery point to the next based on the height of material in the container being loaded. An initial delivery point must be defined at the very front or very rear of the container and the targeted delivery point shifts a defined distance to the next delivery location when the current location becomes full.

2.2.5.2 Loader-dumper positioning

The open quarry autonomous positioning system presented earlier also used a fill strategy. Discussion earlier mentioned the automatic positioning function of the system, but that is only part of system's capabilities. The entire system includes incremental movements of each machine to fill the entire length and width of the dump truck bed. The loader will change its dumping position while the dump truck also moves forward. Since there is no fill height information provided by sensors to measure the fill level in the dump truck bed, a model-based fill estimation technique was used to predict how many loads can be delivered to the same (Pulli et al., 2010).

The loader-dumper system is similar to the fill strategy algorithm designed by Happich et al. for self-propelled forage harvesters, except the loader-dumper system included the means for distributing the load of the container in the longitudinal and lateral directions. Varying lateral material delivery may not have been necessary for self-propelled forage harvesters because of natural movement in the system while traveling through the field.

2.2.6 John Deere Smart Unloading

John Deere has also been developing an autonomous unloading system for combines that closes the loop on unloading on-the-go similar to the CLAAS AutoFill system on SPFHs. This system,

called Smart Unloading, utilizes two stereovision-based cameras. One is mounted on the side shield of the combine, and the other is mounted on the unloading auger. These cameras track an adjacent grain cart and measure the height of grain inside the cart with respect to the cart opening. This information allows Smart Unloading to include fill strategy functionality. For combines, a fill strategy means autonomous positioning of the end of the unloading auger in a desired location relative to the grain cart edges. Similar to AutoFill, this feature will interpret the measured grain height and request movements of the boot in an incremental manner to fill a grain cart from the front to the back. On the unloading system of the combine, two degrees of freedom are available to achieve fill strategy requests: the unloading auger can be engaged or disengaged, or the auger can be swung forward or backward. Critical to performance is information about the fullness status of the entire grain cart. Missing or highly variable fullness data can cause undesirable system behavior, including excessive cycling of the auger engagement or swinging systems and sporadic movements of the auger to places in the cart already filled.

2.3 Spatial Modeling

Spatial modeling is used extensively in agriculture for site-specific crop management (SSCM). SSCM is the practice of breaking a large area, such as a field, into smaller regions called cells. Field operations, such as nutrient application and planting, are then managed on a cell by cell basis instead of field by field basis. Each cell is populated with characteristics that are assumed uniform for the entire cell, such as organic matter or nitrate level. In most fields, soil properties can change dramatically over short lengths, but it often does not make economic sense to take soil samples at a close enough spacing to capture these small variations. Instead, a practical number of samples are collected and the remaining cells must use a technique to estimate the missing data points.

Spatial modeling techniques were investigated in this review because spatial models have been used extensively in agriculture in a variety of applications to estimate unknown points in a data set. Estimating unknown points in a spatial data set was important to this research because the fullness of the grain cart was described with a two-dimensional fill grid of grain height measurements. The fill grid was rarely fully populated and was prone to producing highly-variable measurements. A spatial model could be implemented to fill in missing points in the fill grid and overwrite highly-variable ones.

2.3.1 Types of spatial models

2.3.1.1 Deterministic

In some modeling situations the scientific processes that generated a data set might be known to a sufficient degree that an accurate description of the entire data set can be made using only a few sample points. This type of estimation problem typically calls for a deterministic model. An example of a deterministic model is shown in Figure 1 where the dots on the left are the only known points in a plane and must be used to interpolate other points. Knowing these dots represent the height of a bouncing ball collected at specific time intervals allows a deterministic model to be created using simple 2D physical trajectory equations (Isaaks & Srivastava, 1989).

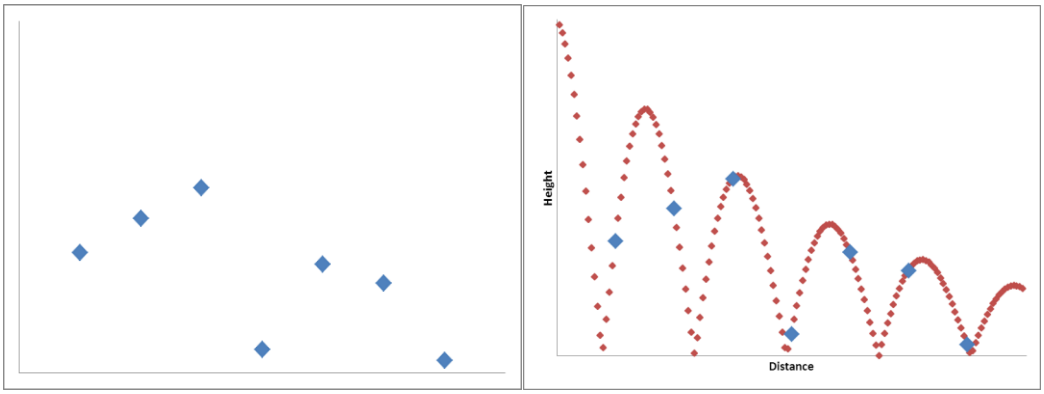

Figure 1: Deterministic model used to describe data set of known physical characteristics

A deterministic model could be used to estimate unknown points in the fill grid of a grain cart because information is known about properties of delivered grain. Grain is typically delivered to the lateral center of the grain cart and accumulates in a pile at the delivery location. This creates a symmetrical profile where the height along the far edge is typically the same as the near edge. The slope of the pile, called the angle of repose, is dependent on the type of grain harvested and the moisture content of the grain. For transport containers in the field, there is also substantial dependency on the roughness of the terrain.

2.3.1.2 Probabilistic

The probabilistic approach to estimation is used more often in geostatistics than the deterministic method. This is because geology involves complex physical processes that are not well-understood by scientists. Probabilistic models are governed by the assumption that all known

data points were the result of random processes. This assumption is often not true. However, because there is so much uncertainty in prediction methods, the randomness assumption is commonly adopted by researchers and scientists.

2.3.2 Point estimation methods

Most geostatistical models estimate a mean for an area in which multiple samples were taken. However, more precise data is often preferred so methods must be designed for estimating unknown points using neighboring known points. Four common methods used are the polygon method, triangulation, local sample mean, and the inverse distance method (Isaaks & Srivastava, 1989).

2.3.2.1 Polygon method

The polygon method is a point estimation method that searches for the closest known point to the data point being estimated and sets the estimated point equal to the closest point. The estimate is not impacted by known points farther away than the closest point. Polygon estimation of points on a two-dimensional plane usually causes discrete changes in the estimates at the polygon boundaries (Isaaks & Srivastava, 1989). These abrupt changes reflect the size and shape of the polygons created. Oftentimes, two points can be very near each other but in different polygon regions. When this occurs extreme value gradients are created.

The polygon method is expected to be useful in modeling points in the fill grid when a single point is missing between two nearby known points. When a limited number of data points are available to describe a system with high-resolution and low-amplitude variability, the polygon method can be implemented as a simple estimation technique that performs equally well as advanced geostatistical methods.

2.3.2.2 Triangulation method

Triangulation is a more complex estimation method that removes discontinuities the polygon estimation method could produce. Triangulation uses the three closest points to the point being estimated. A graphical approach to understanding this method is to draw lines to connect the three close points, *I*, *J*, and *K*. The three lines create the boundary of a plane, *IJK*, extruded into the third dimension of the original two-dimensional spatial data plane. The perpendicular distances from the spatial data plane to Plane *IJK* represent the estimated values of the triangulation method

(Isaaks & Srivastava, 1989). The mathematical technique to calculate this distance is to connect Points *I*, *J*, and *K* to the estimated point, *O*. The triangular areas created by these lines are used in Equation 2 to estimate point *O* (Isaaks & Srivastava, 1989).

$$\hat{v} = \frac{A_{OIJ} \cdot v_K + A_{OIK} \cdot v_J + A_{OJK} \cdot v_I}{A_{IJK}} \quad (2)$$

where A = area created by two known points and the estimated point

v = known point

$\hat{v}$ = estimated point

Triangulation is a robust method for estimating points surrounded by known points. The algorithm is capable of extrapolation beyond the range of the known data set, but the accuracy can be extremely poor. This is because the triangles created at the boundaries of the known data still require three points, even if they reside on the same line. When this occurs, the planar slope of the triangle becomes zero, and all estimated points beyond the data boundary become constant (Isaaks & Srivastava, 1989).

2.3.2.3 Local sample mean method

The local sample mean method uses the mean of all data points in the entire sample area to estimate the missing point (Isaaks & Srivastava, 1989). This method is the opposite of the polygon method. The polygon method gives 100% of the weight to the nearest point and 0% to all other points. The local sample mean gives each point equal weight regardless of distance to the point being estimated. A pure local sample mean usually produces poor accuracy and, as a result, is rarely used without placing a limit on the distance a known point can be from the unknown point to be included in calculation (Isaaks & Srivastava, 1989).

2.3.2.4 Inverse distance weighting method

A common estimation method that resides between the polygon and local sample mean methods is called the inverse distance weighting method. The inverse distance method uses normalized weights of all sample points in a data set to estimate the unknown point. Equation 3 governs this method. As *p*, the distance weighting exponent, approaches zero, the weighting factors for all points become equal, causing the point estimation method to resemble the local sample mean method. As the distance exponent approaches infinity, nearly all of the weight is given to the

closest point while the weight of all other points is nearly zero so the estimation method closely resembles the polygon method.

$$\hat{v}_1 = \frac{\sum_{i=1}^{n} \frac{1}{d_i^p} v_i}{\sum_{i=1}^{n} \frac{1}{d_i^p}} \quad (3)$$

Where n = number of known points in sample

d_i = distance to each known sample point

p = distance weighting exponent

v_i = known sample point value

$\hat{v}$ = estimated point

The distance weighting method has the advantage of allowing the distance exponent to be tuned to a specific application. In most applications of the inverse distance weighting method, an exponent of two is used. The choice of the distance exponent is arbitrary, but having an inverse squared relationship generally produces estimates nearest the true value than simple inverse relationships with an exponent of one (Isaaks & Srivastava, 1989).

2.3.2.5 Soil sampling case study

Han et al. (1993) compared the inverse distance weighting method to a more advanced geostatistical technique called kriging. Kriging is a much more complex estimation algorithm, rather than a formula, with several variations that have been implemented across the geological field. Kriging uses the momentum of spatial data to weight its estimation of unknown points. Unlike the other methods discussed, this allows kriging to output estimates that are higher than the highest value of a data set and lower than the lowest value of a data set.

The research was conducted on a 120-m by 73-m plot divided into 6.1-m by 6.1-m cells. Soil samples were collected for each cell and tested for the potassium chloride (KCl) extractable nitrate level. Knowing the actual nitrate levels in each cell from the samples, a percentage of the total points were randomly removed from the data set. The inverse distance weighting method and kriging were used to estimate each point removed from the data set. Results were recorded for the error in each method at increasing percentages of removed data.

The results of the research showed both methods were equally accurate when about 27% of the data was removed (Han et al., 1993). However, the inverse distance weighting method was more accurate than kriging for data sets with more than 27% of the original data removed, while kriging was more accurate when less than 27% of the data was removed. However, the accuracy of each method was so similar that the researchers concluded the inverse distance weighting method was comparable to kriging in estimation accuracy.

2.3.2.6 Yield monitor case study

Yield mapping is one of the most widely used site-specific crop management technologies used today (Han et al., 2004). Yield mapping technology involves a crop yield sensor, a positioning device, and an electronic data storage computer. The yield sensor measures the current yield coming into a harvester and transmits the data to the data storage device. At the same time the positioning system, usually a GPS receiver, sends position data to the data storage device. The storage device uses the machine's position history to account for time delay caused by thrashing the grain and measuring the yield. Once this correction is made, the computer displays updated crop yield information to the operator and saves the data in a spatial format for later analysis.

The spatial data saved by the computer is not guaranteed to be free of errors. The two most common sources of error in saved yield data are caused by a varying harvest width and poor estimation by the computer that matches data from the crop yield sensor to the positioning system (Blackmore & Marshall, 1996). Because these errors are common, the software analyzing spatial data often has the ability to estimate erroneous data points that were manually removed.

Han et al. examined the use of geostatistical algorithms to estimate missing yield data. It was concluded the inverse distance weighting method often used for yield monitor interpolation produced comparable accuracy to kriging. Kriging is traditionally used in geostatistical applications and has the capability of assigning a confidence level for each estimated point. A confidence level output may be desired in some applications, but the computing power required to solve kriging equations was impractical for the large data sets used in yield plots (Han et al., 2004).

2.3.3 Model evaluation techniques

When developing any estimation model, it is important to determine which model is best. When estimating a single point, the criterion is simple. Whichever model produced the least error is

best. However, most often an estimation model is used to predict several points, and the best model for estimating a given point may not be the best for all points (Isaaks & Srivastava, 1989). Because this situation often occurs, several techniques have been developed to evaluate model accuracy for sets of data instead of single points.

A histogram of a model's estimation error is a common means to convey model accuracy. A histogram visually captures any difference in variation between models and shows any biasing in the estimation error. However, it is not possible to conclude from a histogram whether one model is more accurate than another at larger or smaller numeric values of a data set. This level of analysis is important when modeling a system in which data points change over time. A common means to evaluate these types of models is to plot the estimated values against the true values (Isaaks & Srivastava, 1989). This approach is visual, like a histogram, except the estimation error of each point can be seen over the entire range of estimated values. A perfect estimation model would have all points located on a line at 45 degrees. Although no quantitative results with respect to the model's accuracy at higher or lower values are produced, it is easy to see more or less variation at different values.

2.4 Conclusion

The massive volume of grain harvested each year in the United States opens the opportunity for a system to autonomously unload combines on-the-go. Many agricultural OEMs already have control systems that position the tractor and combine next to one another, but none of these products fully automate the process of filling a grain container. Filling containers has been automated on self-propelled forage harvesters, but the technology has not been applied to conventional grain harvesting.

Stereovision technology has been successfully applied to auto guidance systems and distance measurement systems. Ultrasonic sensors have also been used in agriculture as object detection devices. Both technologies show promise of being capable to provide the necessary information to automate unloading on-the-go.

Also required to automate unloading on-the-go is a reliable estimate of the grain height of the container being filled. The data set will likely have unknown or highly variable points due to environmental conditions such as dust, moisture, and sunlight. A model to estimate missing points

and override bad measurements will ensure more robust performance of the autonomous filling system under the harshest conditions. Geostatistical models typically use probabilistic algorithms, but sometimes deterministic models can be used. Several estimation methods are used today to estimate unknown points, but the inverse distance weighting method has been a popular method in agriculture for applications that require short computing time. Kriging was removed from consideration for this application because studies were conducted where the accuracy of kriging was compared to inverse distance weighting in the estimation of unknown points in a spatial data set. Inverse distance weighting achieved nearly the same accuracy as kriging but with a simpler model and much less computing time.

To evaluate one estimation model against another, one summary statistic is typically not enough to evaluate all facets of a model's performance. Instead, multiple plots must be created to uniquely evaluate each case based on its unique modeling objectives. Typically, plots showing residual error and variance of the error can be analyzed to decide which model fits best.

Chapter 3 Objectives

3.1 Research Objectives

The long term goal of this project was to design and evaluate a decision support system for sensor-based autonomous filling of grain containers. The main objectives of this research were to understand the key factors that influenced fill measurement of grain containers and quantify how these factors affected the performance of the decision support system. Three specific objectives outlined below must be completed in order to validate autonomous grain container filling decision support systems.

Specific Objective #1: Develop a technique to model the height of grain in grain carts.

Specific Objective #2: Quantify the influence of grain delivery location within the grain cart on the ability to estimate total grain weight.

Specific Objective #3: Identify a decision process required to support systems for autonomous filling of grain containers and quantify the repeatability of the system during dynamic field testing.

3.2 Terminology

Throughout the process of designing a decision support system for autonomous filling of grain containers, many terms and phrases were developed to describe specific functions of the system and evaluate behavior under different conditions. It is important to fully define the terminology used to provide a better understanding of key concepts and results as they are discussed.

3.2.1 Fullness of a grain container

The fullness of a grain container describes the volume of material inside the container walls. This thesis expresses fullness as a height and a percentage. Container fullness was used in both respects throughout the document depending on when appropriate. Height-based fullness was used to describe the grain height at specific points in a grain cart while percentage-based fullness measurements described the overall general grain level relative to the entire cart capacity.

3.2.1.1 Height-based fullness

When a container is described as full based on height, this refers to the height of material measured with respect to a horizontal datum laid on the same plane as the container opening. Any reference to a fill height is the distance from the horizontal datum straight downward to the material. As an example, a fill height of -20 cm in a grain cart means the vertical distance from the referenced datum to the surface of the grain is 20 cm downward. Grain above the datum has a positive fill height. Figure 2 shows a grain cart design widely adopted in the United States where the opening of the grain cart is not horizontal. In this case, the elevation of the datum was placed at the height of the edge that would be nearest the combine during unloading on-the-go.

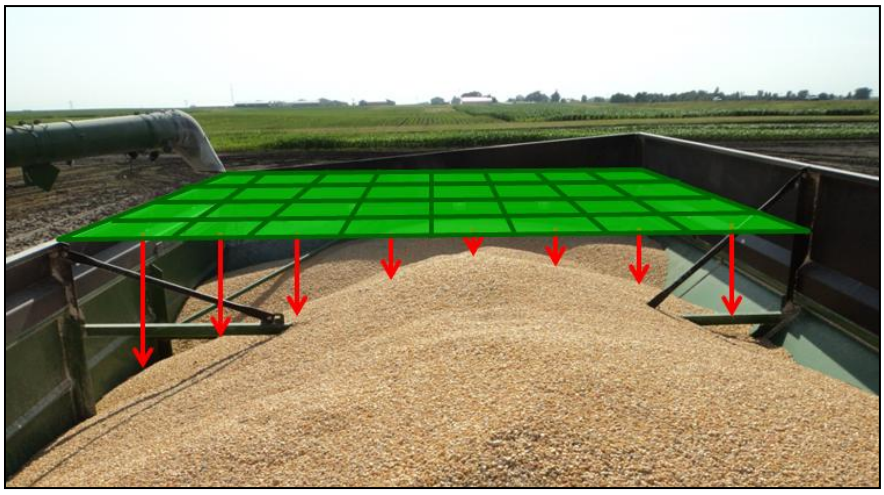

Figure 2: Grain cart overlaid with the fill height reference plane and arrows indicating the measurement direction of one row of cells; the cart opening was not parallel to the ground so the fill height reference plane was placed at the same height as the edge that would be nearest the combine during unloading on-the-go.

3.2.1.2 Percentage-based fullness

When a container's average fullness is expressed as a percentage of the total cart capacity, such as 80% or 100%, this is also a distance reference to the datum at the container opening, where 100% means the height is equal to the datum elevation. Any percentages lower than 100% mean the fill level is below the datum plane, and percentages greater than 100% are above the datum. The measurements in Figure 2 are all lower than 100%. Fill heights reference a plane located at the opening of a container because the purpose of the autonomous system was to fill containers to a specified level respective to that container, not with respect to the ground plane or another feature.

Using percentages to describe grain height in a cart developed as an intuitive description of autonomous system behavior. It was decided percentages would be used as a means for combine

operators to input a target level of fullness for the autonomous unloading system to achieve. However, since percentages are not real distances, a reference needed to be defined so 0% to 100% could be scaled to a physical dimension. The first attempt at defining 0% to 100% as an engineering unit was to set 100% equal to the total container volume, and any container not completely full would be less than 100%. However, complex environments and limitations of measurement technology did not allow for the accurate calculation of container volumes for each unique cart that could be experienced in the field.

The next approach was to set 100% equal to the volume capacity of a medium-sized grain cart. Testing at Iowa State University was conducted on a Kinze dual-auger grain cart with a nominal 840-bu capacity (Figure 3) so this cart became the standard container size used. The cart capacity was converted from bushels to cubic feet using 1.245 ft^3/bu (Bern et al., 2010). The resulting volume in cubic feet was assumed to be a rectangular cube with length and width dimensions matching the length and width of the Kinze 840 grain cart (Table 1). Knowing the length and width, the height of the theoretical rectangular cube was calculated using Equation 4 to be 165 cm. This meant grain measured 165 cm below the opening of the cart was considered 0%, and a height of -82.5 cm was 50% full. With this relationship the percentage-based fullness of a cart could be converted to a physical dimension using 1.65 cm/%.

Figure 3: Kinze 840 bu grain cart used at Iowa State University as the standard size container to serve as the baseline for percentage-based fill height calculations

Table 1: Iowa State University Kinze 840 grain cart dimensions

Dimension	Value	Units
Length	610	cm
Width	290	cm

$$h = \frac{1.245 \cdot 30.5^3 \cdot C_b}{w \cdot l} \tag{4}$$

where C_b = rated bushel capacity of grain cart, bu

w = width of grain cart, cm

l = length of grain cart, cm

h = height of grain scaled to 0-100%, cm

Preliminary testing of the autonomous filling system was conducted with a stereovision sensor that had a measurement resolution of 5 cm/bit, and zero was always set to the height of the grain cart opening. Using 1.65 cm/% and a height measurement that incremented by 5 cm, the calculated percent fullness followed the third column of Table 2 for a range of sensor outputs. It was desirable to use increments of 10% to describe the fullness of the grain cart, and the measurements needed to match the sensor outputs so the conversion factor was modified to 1.50 cm/%. With the new conversion factor, the percent fullness of the cart followed the last column in Table 2.

Table 2: Output from the stereovision sensor converted to the actual measured grain height and into percentage-based fullness using a conversion factor 1.65 cm/% and 1.50 cm/%

Sensor Output (bits)	Actual Grain Height (cm)	Percent Fullness with 1.65cm/% (%)	Percent Fullness with 1.50cm/% (%)
0	0	100	100
-1	-5	97	97
-2	-10	94	93
-3	-15	91	90
-4	-20	88	87
-5	-25	85	83
-6	-30	82	80
-7	-35	79	77
-8	-40	76	73
-9	-45	73	70
-10	-50	70	67

3.2.2 Decision Support System and Fill Zones

Since the overall goal of this project was to autonomously unload grain from a combine to a grain cart, the control architecture was divided into subsystems so major functionalities could be separated. The major subsystems were:

1. A decision support system for interpreting grain height information and making movement requests to a desired location in the cart;
2. A control implementation model that used movement requests from the decision support system to output control commands to the hydraulic actuation systems;
3. An over-arching state machine governing system behavior.

The decisions support system was responsible for determining where grain needed to be delivered within the cart. Fill zones are areas of a cart larger than individual cells of the fill grid but smaller than the entire cart area. Figure 4 shows a cart divided into three fill zones outlined in blue. Red regions at the front and rear of the cart do not make up part of the fillable area. These zones were added to prevent spilling by keeping grain delivery away from the front and back edges. Red zones were not located at the lateral edges because movement of the combine during grain harvesting only allows one degree of freedom that is oriented along the path of travel.

Figure 4: Grain cart overlaid with front and rear edge dead bands and three fill zones; grain can be delivered to the fill zones highlighted green, but the auger moving into a red zone causes it to disengage

During normal operation the of the decision support system algorithm, commands keep the end of the unloading auger in the front fill zone. Assuming a vehicle speed control system that was

discussed the review of literature, such as Machine Sync, was not available, the auger would drift out of the front fill zone from difference in vehicle velocities. When this occurs, the decision support system outputs a request to move the auger back into the intended zone and commence filling. The size of the fill zones should allow the grain delivery point to remain in a localized area while preventing the auger from constantly actuating.

Chapter 4 Grain Cart Data Acquisition System Development

4.1 Introduction

The goal of this phase of the research was to design a data acquisition system which would provide the data necessary to create a two-dimensional fill grid and transmit the grids to a controller on the combine. Several factors were considered during the early stages of designing the data acquisition system including grain detection range and resolution, system robustness, and long-term implementation potential. Several goals were set early in the design process pertaining to the collection of grain height data:

- Measure grain height at least up to the elevation of the cart opening
- Detect grain height in a grid pattern with less than 75 cm between sensors
- Resolution of the grain height measurement must be at least 5 cm
- All sensing points must update at a rate of at least 5 Hz

Additionally, several constraints of the data acquisition system were formed:

- Sensors must not fail from impact with a continuous stream of grain from the combine
- Sensor placement must not inhibit parallel development of a stereovision camera by occluding the view of the grain from the sensor
- System must reliably transfer data to the combine without restricting independent machine movements
- System must provide graphical tools to validate the accuracy of generated fill grids

Successful completion of these goals within the defined constraints would ensure data could be collected for the future phases of this research and, ultimately, the fulfillment of the overall research objectives.

4.2 Materials and Methods

A distributed data acquisition system, where each component of the system had a specific function, was developed to meet the constraints highlighted. If it was not possible to achieve all the goals listed without violating at least one constraint, it was decided to sacrifice achieving a goal of the data acquisition system instead of violating a constraint. Violating one of the constraints would

more likely lead to a complete failure in the system; whereas not meeting one of the goals would likely only result in a decrease in data acquisition system capabilities.

4.2.1 Machinery selection

To test the data acquisition system, three pieces of machinery were required: a combine, a grain cart, and a tractor. A John Deere 9860 prototype combine (Figure 5) was used to deliver grain into the grain cart. The combine was equipped with a nominal 6.9-m auger and could achieve a grain flow rate of 3.3 bu/sec (4.1 ft^3/s) with the engine at full throttle.

Figure 5: John Deere 9860 combine harvesting corn

A Kinze 840 dual-auger grain cart (Figure 6) was used to hold grain. Sheet metal and wire mesh extensions were added to the side walls to increase grain capacity by about 150 bu to a total of 1000 bu.

Figure 6: Kinze 840 bushel capacity grain cart with white side wall extensions increasing the capacity to about 1000 bushels

Permanent covers of the top opening were mounted at the front and rear (Figure 7) as part of an after-market kit that allowed a tarp to roll over the entire cart opening and protect grain from

dew and rain. The front and rear covers reduced the fillable length of the cart from 610 cm to 520 cm but left the width unchanged.

Figure 7: Tarp covers on Kinze grain cart

The tractor attached to the grain cart during testing was the John Deere 8245R in Figure 8. It was equipped with auxiliary hydraulics to power basic functions on the grain cart and a power take-off (PTO) shaft to drive the unloading auger. The tractor electrical bus was used to supply power to all the data acquisition equipment mounted on the grain cart.

Figure 8: John Deere 8245R tractor used to tow the grain cart and power the onboard electronics

4.2.2 Grain height sensor selection

In addition to following the constraints discussed in the previous section, several important criteria were considered when selecting the sensors including the sensing range, the input and output voltage ranges, and the robustness to environmental conditions. Options that were considered included a three-dimensional laser scanning system and a system of multiple ultrasonic acoustic wave emitting sensors.

The laser scanning systems researched were not designed to withstand conditions associated with being mounted outdoors on a grain cart for long periods of time. Laser distance sensors also perform poorly under heavy dust conditions because of the short wavelength of the emitted light. However, a purchased laser scanning system would have had the advantage of being nearly plug-and-play, thus reducing the integration time compared to developing a system of ultrasonic sensors.

Most ultrasonic sensors that were found fell into two categories. They could either read a narrow range of distances with high accuracy or a wide range of distances with poorer accuracy. The wide-range sensors were more applicable to this project because it was only desired to achieve 5 cm of resolution. Also, ultrasonic sensor performance does not diminish under heavy dust conditions because of the relatively long wavelength of the emitted sound. Due to deficiencies of the laser scanning system, ultrasonic sensors were chosen to be the distance sensors for the experiment.

Two ultrasonic sensor models were chosen for this application: a short-range sensor that was 18mm in diameter (20-150 cm sensing range) and a long-range sensor that was 30mm in diameter (30-250 cm sensing range). The short-range sensor was ideal for measuring close distances, such as along the near and far edges of a grain cart when the grain neared a point of overflowing and spilling. Although the grain tended to peak in the middle of the cart, the long-range sensors were best fitted for the middle because tarp structures installed on the cart as part of the tarp kit raised the sensor mounting height in the middle.

Both sensors required an input voltage of 24VDC in order to utilize their entire sensing ranges. The tractor power supply was only 12VDC, so a DC-DC boost chopper was used to step up the input voltage. Both sensor models also output a 0-10VDC analog signal proportional to the measured distance. Since the data acquisition platform used had an analog-digital (A/D) reference range of 0-5VDC, voltage dividers were used on all output signals so the full sensing range could be utilized.

Since two types of sensors were used in the final layout, two equations were needed to convert from bits to millimeters. A manufacturer's datasheet was available for each sensor and included calibration curves for each model (Figure 9). The datasheets for both models showed a

0VDC output voltage at their respective defined minimum sensing points and an output of 10VDC at their defined maximum sensing points. The equations provided by the manufacturer were verified in the lab before installation on the grain cart.

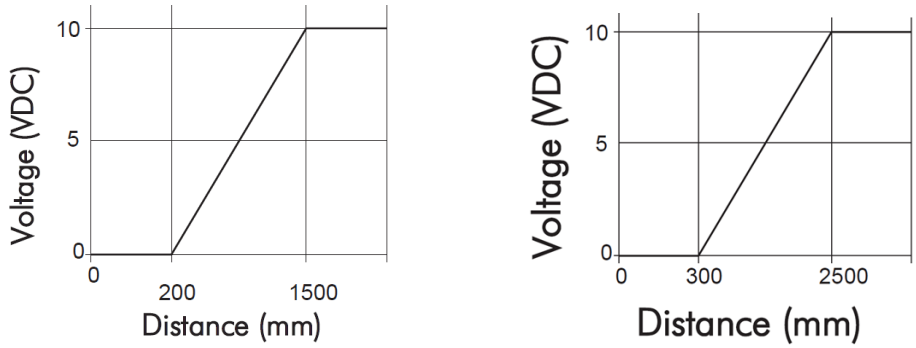

Figure 9: Sensor manufacturer calibration curves for 18mm model (left) and 30mm model (right)

The lab tests verified the same minimum sensing points on the datasheet were accurate and showed the same linear output characteristics as the manufacturer's datasheet. However, the maximum sensing points for both sensors were 500mm farther for the lab tests than the datasheet showed. Data points collected in the lab were fitted with a trend line to determine the actual calibration curves for each sensor (Figure 10) instead of the supplied data sheets. The equations in Figure 10 were used as the sensor calibration curves for the remainder of this research.

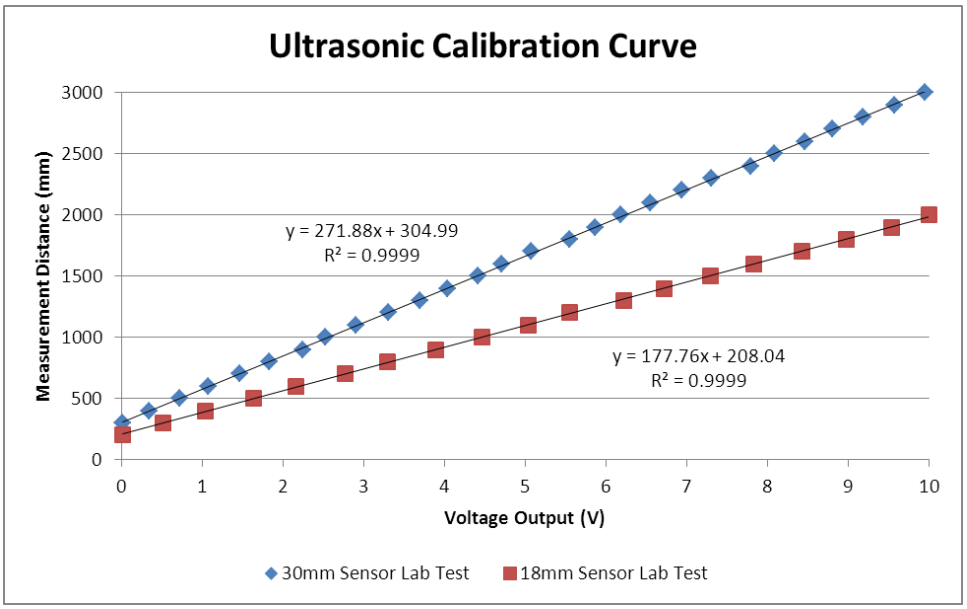

Figure 10: Calibration curves to convert output voltage to distance for both models of ultrasonic sensors

A load-cell weighing system was also installed on the Kinze grain cart. The installed system used three load-cells mounted on each wheel hub and on the tongue (Figure 11) to measure the vertical force at each point. The signal from each load-cell was routed to a multi-function scale head (Figure 12). The scale head served as the user-interface to calibrate and tare the system, specify data output options, and many more functions.

Figure 11: Kinze grain cart with arrows indicating the locations of load cells for the weighing system

Figure 12: Scale head for weighing system mounted in grain cart enclosure

4.2.3 Populating a fill grid

The ultrasonic sensors were mounted on the grain cart in a grid layout so that each cell of the fill grid could be populated with the measured grain height from its corresponding sensor. The long-range sensors were mounted at elevated locations along the middle row of the cart to measure the height of the grain before a peak had built up. The short-range sensors were mounted along the near and far edges. The smaller minimum range allowed the sensor to be mounted lower while maintaining the ability to detect the grain height close to the top of the near and far edges before overflowing.

Grain heights at the near and far edges were the most important data points to collect during the experiment. Knowing the grain height along these edges will allow the decision support system to know when the grain was about to spill and make the appropriate decisions to prevent it. Knowledge of the grain height along the near and far edges, however, would not allow the system to construct accurate estimations of the surface profile toward the center due to high variability in the angle of repose. Accurately reproducing the entire surface profile of the grain cart was not critical to prevent spilling grain over the edges, but it was required by the decision support system to detect empty and full regions of the grain cart. To accomplish this, the long-range sensors were needed along the lateral center of the grain cart to measure the height of the grain peak. Using these three points, a two-dimensional cut section could be drawn (Figure 13) at every group of sensors along the entire length of the cart to produce a surface profile representative of the actual grain height.

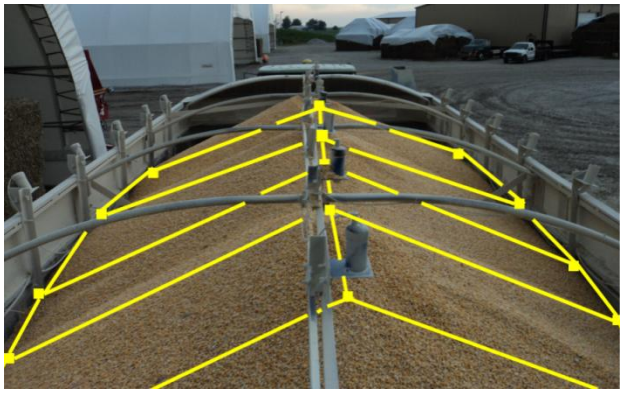

Figure 13: Using grain height measurements at three points to estimate the grain surface profile

The length-wise spacing of each group of three sensors was decided by the minimum distance the unloading auger could be swung by the combine. The autonomous fill system changed the location grain was being delivered by swinging the auger to a new location. Preliminary testing concluded 50-75 cm was the shortest distance the auger could be swung because of the on-off solenoid valve that controlled pressure to the actuation cylinder. Grain height data with finer resolution would not be significantly beneficial. It was decided to use a grid five cells wide and nine cells long to approximate the cart opening. Nine columns resulted cell widths of 67 cm, which met the goal of using cells less than 75 cm wide. Five rows were chosen because a 9:5 ratio was close to the ratio of the physical dimensions of the grain cart to maintain nearly square cells. The actual width of each cell was 59 cm (Figure 14).

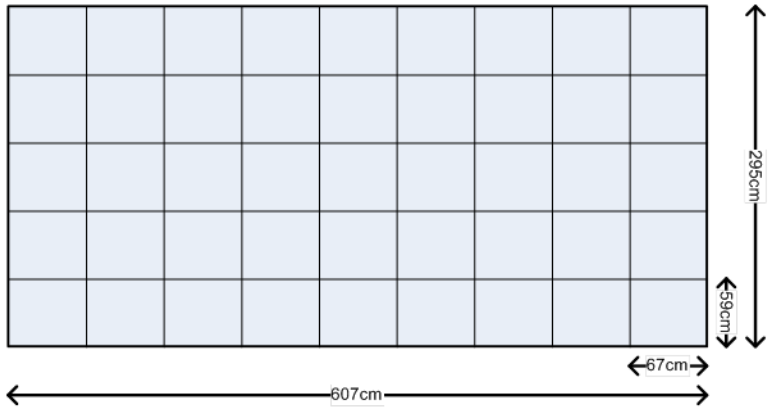

Figure 14: Fill grid five rows long and nine columns wide with each cell having dimensions of 67 cm wide by 59 cm deep

Ultrasonic sensor mounting locations on the cart were affected by two main factors: interference with other important functions on the cart and the physical limitations of ultrasonic sensors. The ideal mounting height above the cart opening to avoid breaching the minimum sensing threshold was 30 cm. A 30 cm mounting height would have severely occluded the view of the stereovision camera being developed simultaneously that was mounted at the end of the combine auger. Sensors mounted at a high enough elevation to avoid blocking the camera would be in the swinging path of the unloading auger as it moved back and forth over the cart. Sensors mounted close to the cart opening would be limited by their minimum sensing range. It was decided the best solution was to mount the sensors close to the cart opening, knowing the sensors will reach their minimum sensing limits before the cart is full. This was not an issue for this research because the system fulfilled the objective of providing data to generate fill grids. The generated fill grids just never reached the maximum capacity of the cart they were installed on.

Ideally, one sensor would be placed at all 45 cells of the five-by-nine fill grid; however, due to multiple issues, some sensors were eliminated. Although the sensors were mounted to minimize obstructing the stereovision camera's view, the mounting hardware for all sensors would have severely reduced camera performance; removing two rows of sensors significantly reduce blockage of the camera. Sensors were also removed from the first and last columns of the fill grid to reduce view obstruction at the front and rear edges. Grain height information at the front and rear was not important because using an autonomous system to deliver grain that close to an edge has a high risk of spilling grain during sudden changes in vehicle speed. After removing sensors from the fill grid,

the number of cells that had a dedicated sensor was reduced from 45 to 21. Figure 15 shows the remaining cells that still had sensors.

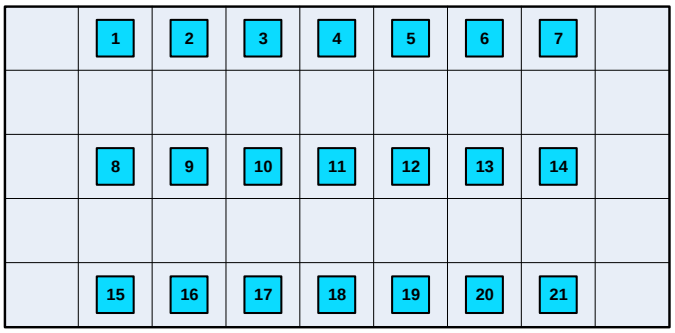

Figure 15: Fill grid with cells that have a dedicated sensor to measure the height

Significant effort was required to prevent the sound waves, emitted from the ultrasonic sensors, from bouncing off structures inside the grain cart and interfering with other measurement signals. The manufacturer's guidelines for installation recommended the surface being measured be perpendicular to the signal's direction of travel in order to utilize the full operating range. A perpendicular surface is recommended because it becomes more difficult for the emitted wave to return to the sensor as the reflecting object moves farther away. If the signal was reflected off a surface oriented 45 degrees from perpendicular, it would have a much lower probability of returning to the sensor.

Each sensor mounting configuration also required a unique function to convert its measured distance into a grain height referenced from the opening of the cart. The extra equation was required because several sensors were not mounted on the same vertical plane as the opening, and several sensors were not pointed straight down (Figure 16) so the raw measured distance was not equal to the grain height.

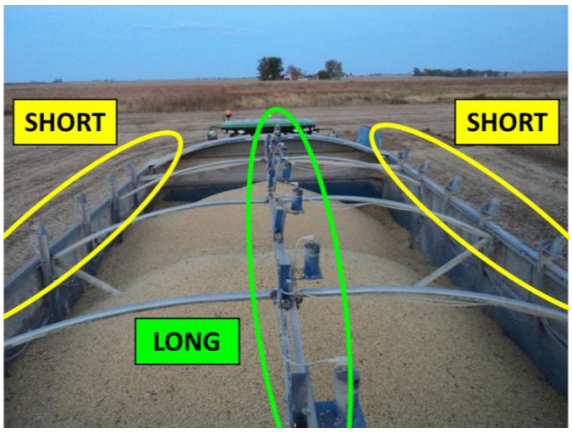

Figure 16: Mounting locations of short-range and long-range ultrasonic sensors on the grain cart

The long-range sensors were mounted higher than the cart opening so they could be anchored to existing hoop structures on the cart. They were pointed straight downward so an offset equal to the difference in elevation between the sensor head and the cart opening was the only modification done to the signal (Equation 5); this distance was 36 cm. The resolution of these sensors was calculated to be just over 1 cm/bit using Equation 6. This was well below the required resolution of 5 cm/bit and provided adequate resolution of the grain height. The maximum height measurement that could be achieved with this sensor was 6 cm above the plane of the cart opening (Equation 7). This height was above the required level of 0 cm.

$$h_{MID} = -(d_{30} - 36) \tag{5}$$

where d_{30} = distance from sensor head to object, cm

h_{MID} = height of grain with respect to cart opening, cm

$$Resolution = \frac{Range_{MAX} - Range_{MIN}}{2^n} = \frac{300 - 30}{2^8} = 1.05\ cm/bit \tag{6}$$

where $Range_{MAX}$ = maximum sensing distance for 30mm model ultrasonic sensor, cm

$Range_{MIN}$ = minimum sensing distance for 30mm model ultrasonic sensor, cm

n = bits of analog-digital resolution

$$Height_{MAX} = -(Distance_{MIN} + 36) = -(30 - 36) = +6cm \tag{7}$$

where $Distance_{MIN}$ = minimum sensing distance for 30mm model ultrasonic sensor, cm

Short-range sensors mounted along the near and far edges were angled inward so the measured distances needed a function to be converted to grain height. The equation used was developed by constraining the sensor mounting angle and mounting position as well as making

geometric assumptions about the angle of repose of the grain pile. Specifically, the sensor had to be mounted perpendicular to the angle of repose and in the same plane as the side walls of the grain cart (Figure 17).

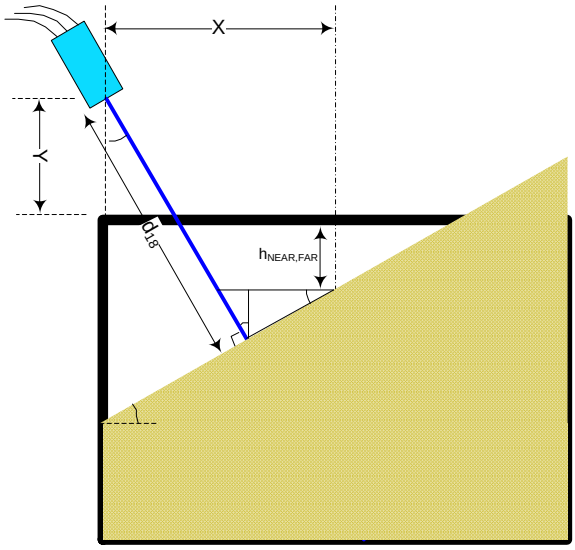

Figure 17: Geometric model used to derive the conversion equation for sensors along the near and far edges

With these constraints and assumptions, trigonometry was used to derive the expression that converted the measured distance to the actual grain height in the middle of that cell (Equation 8).

$$h_{NEAR,FAR} = -\left(\frac{d_{18} - X \sin\theta}{\cos\theta} - Y\right) \tag{8}$$

where d_{18} = distance from sensor head to object, cm

X = half the depth of a fill grid cell, cm

Y = height sensor head is mounted above the opening of the grain cart, cm

Θ = grain angle of repose and sensor mounting angle, deg

$h_{NEAR,FAR}$ = height of grain with respect to cart opening, cm

The resolution of these sensors was 0.75 cm/bit (Equation 9), which was also well below the maximum allowable resolution.

$$Resolution = \frac{Range_{MAX} - Range_{MIN}}{\cos\theta \cdot 2^n} = \frac{200 - 20}{\cos 20° \cdot 2^8} = 0.75\ cm/bit \tag{9}$$

where $Range_{MAX}$ = maximum sensing distance for 30mm model ultrasonic sensor, cm

$Range_{MIN}$ = minimum sensing distance for 30mm model ultrasonic sensor, cm

Θ = angle of repose of grain, deg

n = bits of analog-digital resolution

Sensors along the near and far edges were mounted even with the cart opening to limit potential interference with stereovision camera development. Table 3 lists the parameters associated the mounting location of these sensors (Equation 10).

Table 3: Parameters that define the mounting location of ultrasonic sensors mounted on the near and far edges of the grain cart

Parameter	Symbol	Value	Units
Half the depth of a grid cell	X	29.5	cm
Height of sensor head above the cart opening	Y	0	cm
Grain angle of repose	Θ	20	deg

$$Height_{MAX} = -\left(\frac{Distance_{MIN} - X\sin\theta}{\cos\theta} - Y\right) = -\left(\frac{20.8 - 34\sin 20}{\cos 20} - 0\right) = -14cm \qquad (10)$$

where $Distance_{MIN}$ = minimum sensing distance for 30mm model ultrasonic sensor, cm
X = half the depth of a fill grid cell, cm
Y = height sensor head is mounted above the opening of the grain cart, cm
Θ = grain angle of repose and sensor mounting angle, deg

The calculation shows the maximum height that can be detected by the sensors along the near and far edges was 14 cm below the opening, leaving significant volume left in the grain cart after the minimum sensing point has been reached along the edges. This sensing range limitation did not render the system useless, but it caused the usable range of the system to be lower than grain carts are typically filled. The data acquisition system was still able to provide an adequate data set to use for building and evaluating grain height estimation models.

4.2.4 Distributed data acquisition and communication

Embedded microcontrollers were used extensively for several functions on the grain cart and combine. Altogether, three custom electronic control units (ECUs) were designed and programmed to handle data transfer, and two more controllers were purchased to log data on the combine Controller Area Network (CAN) bus. The first controller on the grain cart read the 21 analog signals from the ultrasonic sensors. It used an 8-bit A/D converter and a 0-5VDC reference voltage. The sensor output signals were wired to a multiplexing chip and then routed to the microcontroller since the microcontroller did not have 21 analog channels.

Because the combine housed the data acquisition system and decision support system, sensor data needed to be transmitted from the grain cart to the combine. Wireless radios were

used to communicate between the grain cart and the combine. Each radio communicated locally with a wired serial bus and transmitted data wirelessly to the other radio. The radio on the receiving end transmitted data on its own serial bus, where data was received by the custom ECU on the combine.

After all sensor signals had been read on the grain cart, their values were transmitted on a local CAN bus. Three CAN messages were specified to hold the sensor signals (Table 4). The identification field used a 29-bit identifier and followed CAN 2.0b protocol. Since an 8-bit A/D converter was used, it was simple to incrementally place each sensor value in a separate data byte of the CAN message. When the data field of one message was filled, the next ID was filled with data. The three messages were transmitted on the CAN bus as a packet of three messages at 16Hz.

Table 4: CAN message information for messages transmitted onto the grain cart CAN bus

	Data Field							
ID Field	D0	D1	D2	D3	D4	D5	D6	D7
0x18FFFCCB	Sensor 17	Sensor 18	Sensor 19	Sensor 20	Sensor 21	-	-	-
0x18FFFDCB	Sensor 9	Sensor 10	Sensor 11	Sensor 12	Sensor 13	Sensor 14	Sensor 15	Sensor 16
0x18FFFECB	Sensor 1	Sensor 2	Sensor 3	Sensor 4	Sensor 5	Sensor 6	Sensor 7	Sensor 8

The second custom ECU on the grain cart performed multiple transmission and receiving functions using two serial channels and one CAN channel. One serial channel received weight data from the scale head while the other serial channel was connected to the wireless radio mounted in the tractor. The serial communication output option was enabled in the scale head so the weight could be combined with signals from the ultrasonic sensors and transmitted simultaneously to the data acquisition system on the combine. The interface on the scale head allowed the serial communication parameters to be adjusted to the desired settings. Table 5 lists the communication protocol that was used.

Table 5: Serial communication parameters for serial port in scale head

Parameter	Setting
Baudrate	19200
Parity	None
Data Bits	8
Flow Control	None
Stop Bits	1

Data from the scale head was transmitted one byte at a time as ASCII characters so the ECU software used a built in ASCII-to-decimal converter. Table 6 shows the order in which data was transmitted and an example output for a scale weight of 54,321lb.

Table 6: Byte-by-byte serial output from weighing system scale head

Order	Description	Example
1	Weight Digit 1	0
2	Weight Digit 2	5
3	Weight Digit 3	4
4	Comma	,
5	Weight Digit 4	3
6	Weight Digit 5	2
7	Weight Digit 6	1
8	Space	
9	Weight Units 1	l
10	Weight Units 2	b
11	Carriage Return	Cr
12	Line Feed	Lf

Information in the table was transmitted in packets at 1 Hz from the scale head. Since the weight updated much more slowly than the sensor values on CAN, the previous weight was stored between updates and transmitted to the wireless radio with the updated sensor values. This way the same size data package was sent to the radio, regardless of whether the scale had updated. As a diagnostic tool, the scale weight was also transmitted on the local CAN bus using a fourth message (Table 7).

Table 7: CAN message information for fourth message on grain cart CAN bus; contains scale weight output read by a custom ECU before tranmitting the information to the combine through a wireless radio

	Data Field							
ID Field	D0	D1	D2	D3	D4	D5	D6	D7
0x18FFFA64	Wt. L-byte	Wt. H-byte	-	-	-	-	-	-

Electrical hardware and ECUs to process the sensor data was mounted in an enclosed electrical panel at the front of the grain cart (Figure 18). By mounting all the data acquisition components on the grain cart, the system was not tied to a specific tractor in the event that tractor was not available when tests were conducted.

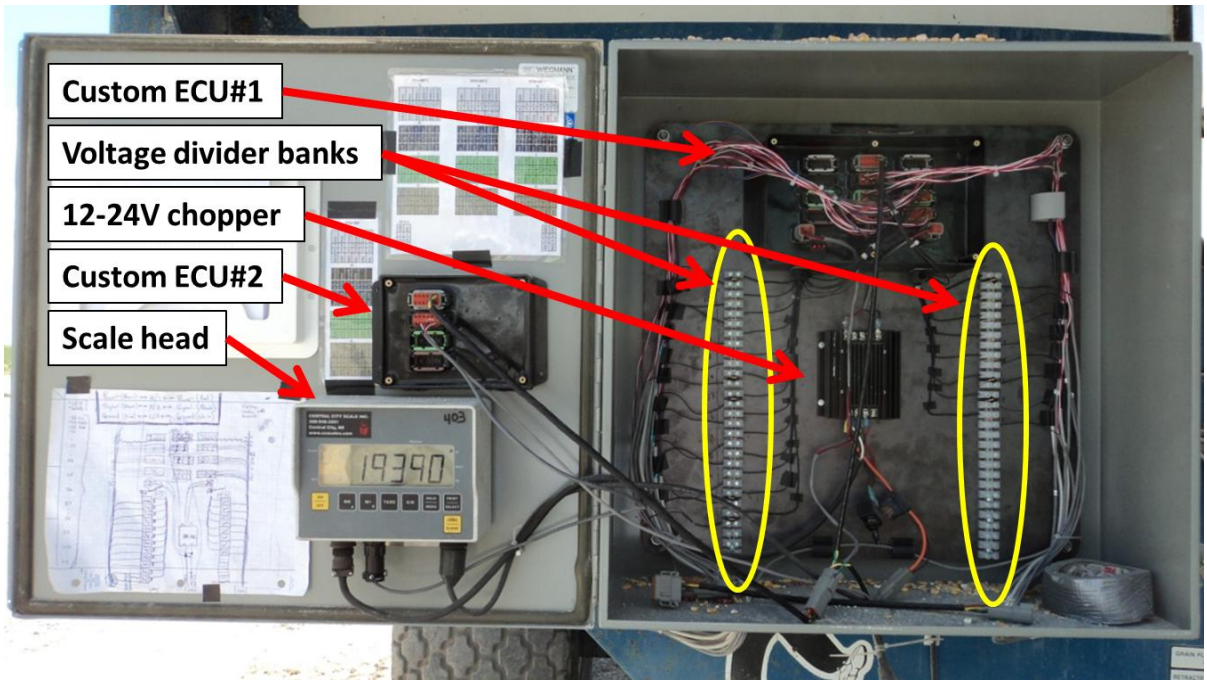

Figure 18: Electrical enclosure mounted on the grain cart to hold all electronics and data acquisition hardware

A custom ECU on the combine was used to read serial data from the wireless radio and rebroadcast it on the combine CAN bus. Because this information was on the same CAN bus used by all the other ECUs on the combine, it was important not to transmit a message with a conflicting ID field. A CAN message ID specifically for developing controllers was found in the John Deere database for 9x60 series combines. Table 8 shows the content of the broadcasted CAN messages.

Table 8: CAN messages transmitted by custom ECU onto the combine CAN bus that contain ultrasonic sensor data and cart scale data

	Data Field							
ID Field	D0	D1	D2	D3	D4	D5	D6	D7
0x1CEBFFCB	0x01	0xDF	Sensor 1	Sensor 2	Sensor 3	Sensor 4	Sensor 5	Sensor 6
0x1CEBFFCB	0x02	Sensor 7	Sensor 8	Sensor 9	Sensor 10	Sensor 11	Sensor 12	Sensor 13
0x1CEBFFCB	0x03	Sensor 14	Sensor 15	Sensor 16	Sensor 17	Sensor 18	Sensor 19	Sensor 20
0x1CEBFFCB	0x04	Sensor 21	Wt. L-byte	Wt. H-byte	Counter	-	-	-

The first data byte of each message was a sequencer to distinguish messages from one another since only one identifier was used. The second data byte of the first message was hard-coded to 0xDF and functioned as a software filter for other ECUs on the bus. The remaining data bytes were free to populate with information from the custom ECU.

Two commercial hardware products were used to collect data during tests: a Vector CANcaseXL and a dSPACE MicroAutoBox (Figure 19). Each product included a software package to control the hardware; the CANcaseXL used CANalyzer and the MicroAutoBox used ControlDesk. Both software packages were designed for use on personal computers.

Figure 19: dSPACE, Inc. MicroAutoBox used for signal logging in ControlDesk and running the decision support system in the background without controlling auger actuations

The CANcaseXL was connected to the combine CAN bus at the diagnostic port and only used to log CAN messages off the bus. The logger was connected to a PC during operation so signal values could also be viewed in real-time with CANalyzer. A filter was setup in the logging software to block all messages not listed in Table 8. Implementing a filter was necessary to manage data file size. Messages that passed through the filter were logged in text format using the logging software included with CANalyzer. Several pieces of information were automatically logged for every message, including a timestamp, the identifier for every message, and the data bytes. Other information was captured in text files, including the CAN channel used on the CANcaseXL and data length code.

The MicroAutoBox was also used to capture sensor data on the CAN bus; CANalyzer logs were a secondary data source in the event of a failure in the ControlDesk data acquisition software. Its functionality included CAN transmit and receive, serial transmit and receive, and analog and digital input/output. The inputs, outputs, and all internal variables of the data acquisition system were loaded to the MicroAutoBox and could be viewed in real-time with ControlDesk. For the experiment, each sensor signal was captured and logged as a structure that included a timestamp, signal value, data type, and other information. Since all captured signals shared the same time stamp, they could easily be spliced together for analysis. Each repetition generated a unique .mat file that contained the logged signals.

The MicroAutoBox also functioned as a programmable real-time target ECU for models built using Simulink. The decision support system model ran in real-time on the MicroAutoBox, but the rate which the model could be called was limited only by the processing power of the internal computer. Similarly, the data acquisition system could log variables at any desired rate the computer could handle. It was decided to leave the decision support system task period unchanged from its intended run rate of 5Hz for the decision support model. Sensor signals were logged at 10Hz so data points could accumulate during each period of time between active unloading events. Logged signals were polled by the data acquisition software before being sent to the decision support model so the time between logging signals was not reduced to 5Hz in the data acquisition system. An acceptable level of noise was observed by logging at 10Hz so the capture rate was not increased, but the system had the potential to run as fast as 1000Hz.

4.3 Results

Figure 20 shows a trace of the output signal measured with an 8-bit analog-digital converter during three periods of time between unloading events. The first two periods of time between unloading events showed noise levels around ±3-4 bits; however, the last period of time between unloading events had noise that was nearly twice the magnitude causing more than 6 cm of error in the grain height measurement. By averaging over the time between unloading events, the effect of the noise was removed (Figure 21).

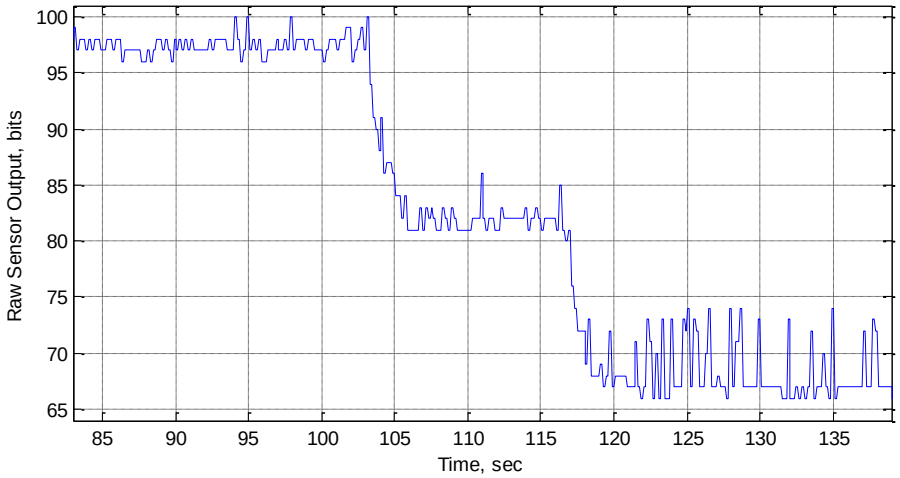

Figure 20: Raw output of Sensor 18 during three periods of time between unloading events where unloading stopped for a period of time so sensor data could be collected and averaged

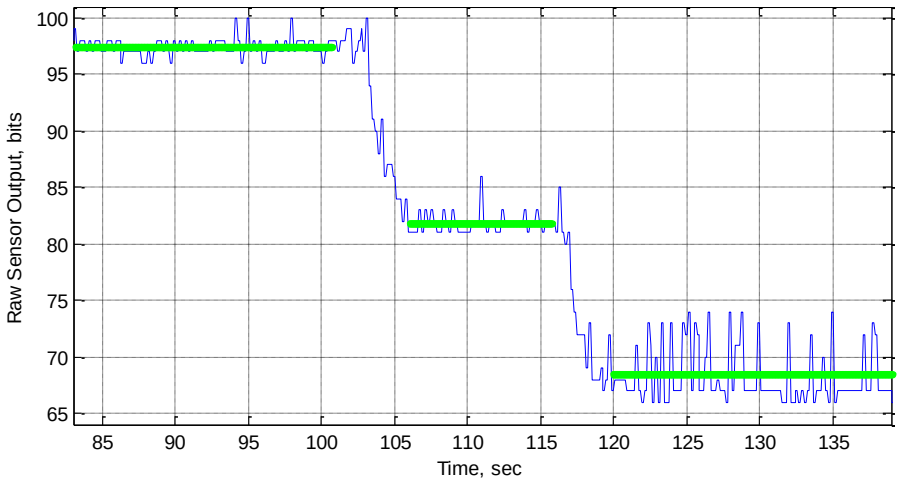

Figure 21: Same plot as in Figure 20 but with the average sensor output for each period of time between unloading events overlaid

It was critical for the system to be static when averaging the sensor output to obtain the actual distance. If averaging was done while grain continued being delivered to the cart, the average would be skewed to reflect an artificially higher level. This bias was removed by adding grain to the cart for a short period of time, around five seconds, and then stopping to collect static data for at least five seconds before reengaging the unloading auger. Tests conducted with this method produced sensor signal logs similar to Figure 22.

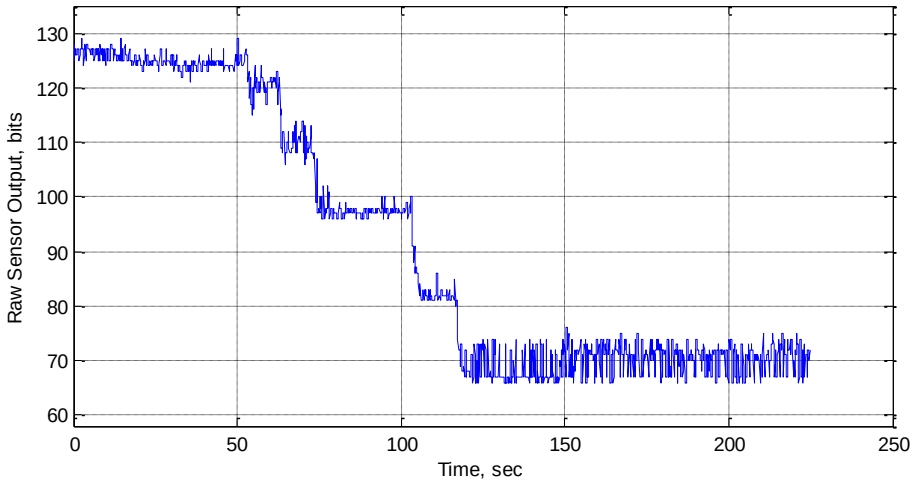

Figure 22: Plot of Sensor 18 during full repetition showing small changes in the output voltage during the beginning and end of the log but large changes in the middle of the log

By stopping the unloading auger for short periods of time during tests, measurements from the ultrasonic sensors could be captured effectively; however, it was still difficult to determine

exactly when to start and stop averaging the sensor value. Start-stop operation of the auger was conducted during the data collection process to obtain sensor values closest to the actual distance. Using the ultrasonic sensors to automate unloading on-the-go sacrificed sensor accuracy to obtain continuous operation.

With the weight being transmitted in the same messages as ultrasonic sensors, both pieces of data were logged with the same time stamp in the data acquisition system. Figure 23 shows a plot of scale weight during a preliminary test run. The periods of time when the weight was not changing were used as the intervals to average the data from the ultrasonic sensors. Figure 23 shows ten periods of time between unloading events that were recorded.

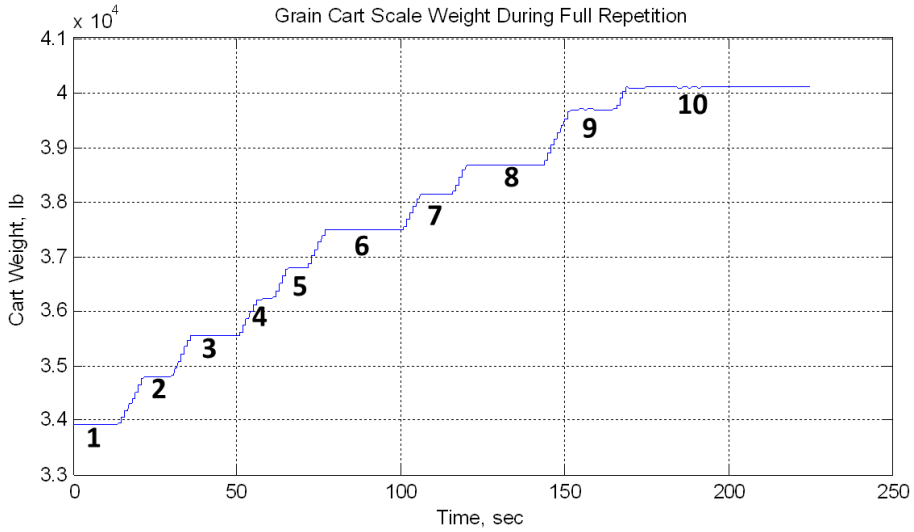

Figure 23: Scale weight measured with cart load-cell system showing time intervals when grain was unloaded into the cart characterized by a positive slope and intervals when unloading stopped to collect data characterized by zero slope

MATLAB scripts processed the raw data because significant handling of matrices was required. The format data captured with ControlDesk was also already referenced to a common time stamp that was setup in the data acquisition software making it simple to identify all signals collected at any moment in time. The script processed data in four main steps:

1. Load the .mat file containing the captured data. Each repetition had a unique file.
2. Plot weight over time and manually enter start/stop times for each period of time between unloading events. Rounding to the nearest whole second was acceptable since each time period contained approximately 50-70 data points, which was sufficient to calculate an average sensor value.

3. Plot raw sensor signal with average overlaid during each time interval to visually check for intervals that needed adjusted (Figure 24).
4. Export average values to Excel for graphical validation

It was common for sensor values to change after the weight had reached steady state or before the weight began to change. This typically occurred when sensors approached their minimum measurement distance and would momentarily output erroneous data (Figure 25).

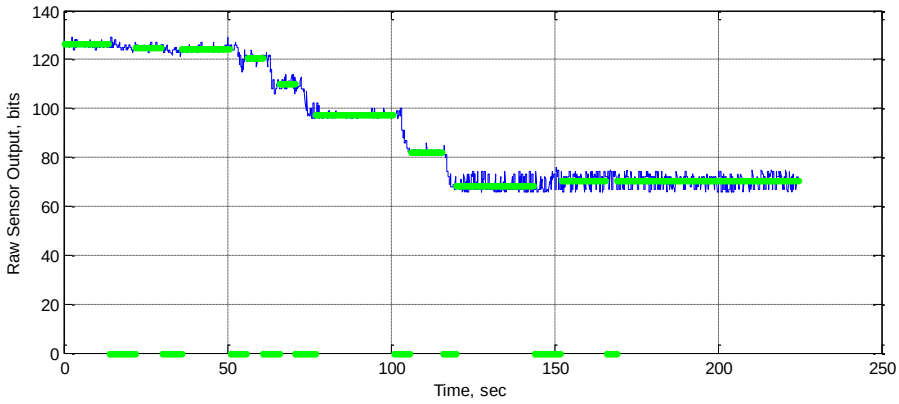

Figure 24: Output of Sensor 18 while performing a test; all calculated averages (green lines) accurately represent average values so the interval did not need adjusted

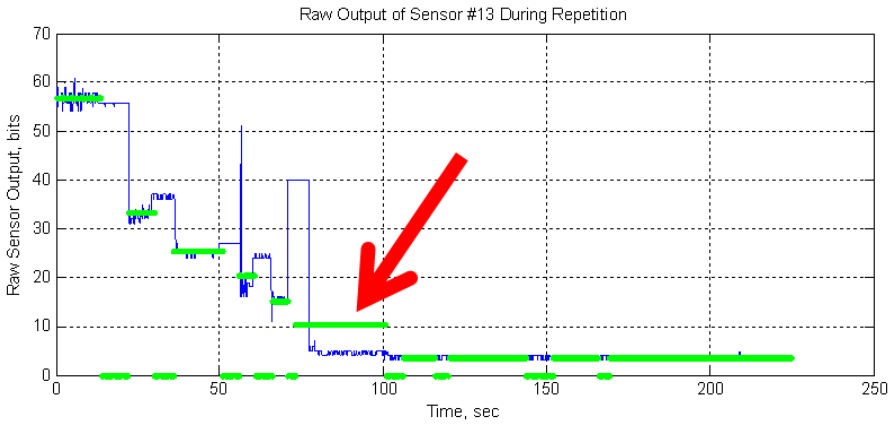

Figure 25: Output of Sensor 13 while performing a test; green lines accurately reflect interval averages except for the interval at 70-100sec

For the case in Figure 25, the interval start time was adjusted forward to remove the erroneous output from being included in the calculated average. After the interval was adjusted, the green line more accurately represented the true average of that interval (Figure 26). After the intervals were adjusted manually to remove bad data points, the final step in MATLAB packed each average into an array and exported the data to Excel for further analysis.

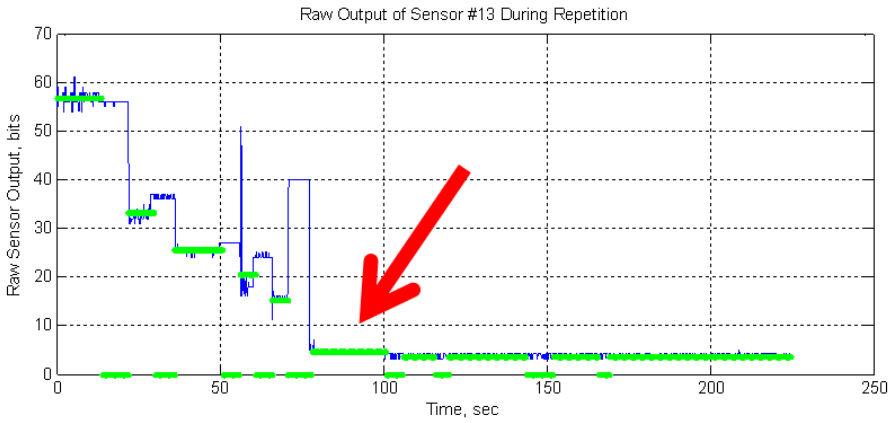

Figure 26: Interval corrected to match the true average output of Sensor 13

4.4 Conclusions

The data acquisition system installed on the grain cart and combine had the ability to capture fill grids generated by ultrasonic sensors in real-time. The middle row of sensors was able to detect grain up to a height 6 cm above the cart opening. Sensors along the near and far edges were able to detect grain up to 14 cm below the cart opening also to accommodate stereovision software development. This resulted in the inability to collect valid fill grids when the grain cart was completely full. When the measured grain heights were within the valid sensing range, the heights could be measured with 0.75 cm and 1.05 cm of resolution for the short- and long-range sensor models, respectively. Data was recorded by the MicroAutoBox at 10Hz with the weight only updating at 1Hz.

Error-checking opportunities were available in MATLAB and Excel to verify the sensors were representing the actual grain heights in the fill grids. This system provided an adequate platform for collecting data to build and evaluate grain height estimation models and to develop a decision support system.

Chapter 5 Grain Height Modeling

5.1 Introduction

The goal of this phase of the research was to identify a modeling technique to accurately estimate the grain height at locations in the cart where sensor data was missing or highly variable. Based on a review of literature on spatial modeling, it appeared the inverse distance weighting method would be the most accurate and robust modeling technique for this application. This method was chosen over kriging because several studies indicated the extra complexity was not justified by better accuracy (Han et al., 1993) (Han et al., 2004).

5.2 Experiment Design

5.2.1 Evaluation of the Inverse Distance Weighting Method

The inverse distance weighting method was used to estimate points in a fill grid susceptible to becoming immeasurable with any type of height measurement device. Two unloading scenarios were identified to represent the most common data loss scenarios:

Scenario 1: Loss of data from sensors near the grain delivery location when grain was flowing;

Scenario 2: Loss of data due to occlusion of the far side of the cart by piles of grain in the middle.

Each scenario was divided into two specific modeling situations that were used to qualitatively evaluate the inverse distance weighting method. Scenario 1 was divided into Situations 1 and 2, and Scenario 2 was divided into Situations 3 and 4.

Situation 1: Single height measurement directly beneath the end of the unloading auger in the grain delivery area. When grain poured from the end of the auger, it was impossible to detect the grain height directly where grain was delivered (Figure 27).

Figure 27: Grain being delivered directly onto an ultrasonic sensor causing an erroneous output for the distance measurement (Situation 1)

Situation 2: Single height measurement along the far edge of the cart. Peaks often formed in the center of grain carts blocking the view of a vision sensor mounted on the auger. Relative movement of the combine and grain cart typically allowed the sensor to view grain behind the peak so only small areas could not be measured.

Situation 3: Three adjacent measurements along the far edge of the cart and one measurement in the grain delivery area directly beneath the end of the unloading auger (Figure 28). This situation was similar to the previous situation but occurred when both machines remained static so the view of the grain cart never changed to gain a different perspective of the grain on the far side of the cart.

Figure 28: Grain being delivered to a grain cart with heavy dust conditions blocking the view of the grain pile by a stereovision camera mounted on the auger of the combine (Situation 3)

Situation 4: All measurements along the far edge of the cart. No information along the far edge would be available when a peak was already formed along the center of the cart from a previous unload on-the-go (Figure 29).

Figure 29: View from an auger-mounted stereovision camera of the grain height on the far half of the cart obstructed by a peak in the center (Situation 4)

The impact of the inverse distance weighting exponent (*p* in Equation 3) on the error of the estimated grain height was tested. Treatment levels of the distance weighting exponent ranged from 0-10 with whole number increments. When estimating unknown grain heights, sensor values were removed from the fill grid for the corresponding situation, and the remaining sensor values were used by the inverse distance weighting method governing equation (Equation 3) to estimate the removed point(s). The true sensor values were subtracted from the estimated value to calculate the error in each estimated value. Positive errors indicated the true height was overestimated, and negative errors indicated the true height was underestimated.

The first modeling situation was tested at each sensor location in the middle row of the grain cart. Tests were conducted by removing a single point and using the 20 remaining sensors to estimate the removed point (Figure 30). The removed point is denoted by a gray cell in Figure 30, and the colored cells represent the known heights in units of centimeters. White cells were not included in the inverse distance weighting equation. The example in Figure 30 shows the estimations of MID_2, MID_3, and MID_4.

	-44	-42	-49	-45	-62	-50	-71
	???	-16	-16	-11	-21	-14	-46
	-50	-45	-48	-38	-45	-45	-59

,

	-44	-42	-49	-45	-62	-50	-71
	-29	???	-16	-11	-21	-14	-46
	-50	-45	-48	-38	-45	-45	-59

,

	-44	-42	-49	-45	-62	-50	-71
	-29	-16	???	-11	-21	-14	-46
	-50	-45	-48	-38	-45	-45	-59

, ...

Figure 30: Known and unknown points for Situation 1 when estimating MID_2 (left), MID_3 (center), and MID_4 (right); colored cells are the known heights in units of centimeters. The gray cell is the point being estimated, and white cells were not included in the estimation model.

The second modeling situation was tested at each sensor location along the far edge of the grain cart in the same manner as the previous instance (FAR_2, FAR_3, FAR_4, etc.). One point was removed and the 20 remaining points were used to estimate the removed point (Figure 31).

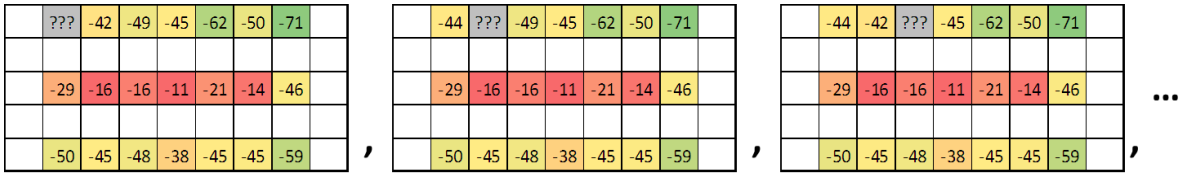

Figure 31: Known and unknown points for Situation 2 when estimating FAR_2 (left), FAR_3 (center), and FAR_4 (right); colored cells are the known heights in units of centimeters. The gray cell is the point being estimated, and white cells were not included in the estimation model.

The third modeling situation was only tested in the center column of the cart. Figure 32 shows the triangular group of points that were removed (MID_5, FAR_4, FAR_5, and FAR_6). Analysis was not necessary at every location in the cart because trends in the model that were column-dependent were observed in Situations 1 and 2.

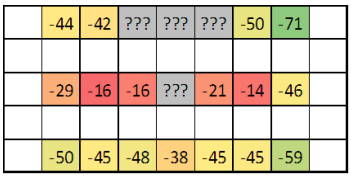

Figure 32: Known and unknown points for Situation 3 when estimating MID_5, FAR_4, FAR_5, and FAR_6; colored cells are the known heights in units of centimeters. Gray cells are the points being estimated, and white cells were not included in the estimation model.

The last modeling situation was tested at each sensor location along the far edge of the grain cart except the other points along the far edge were made unavailable to use by the model (Figure 33).

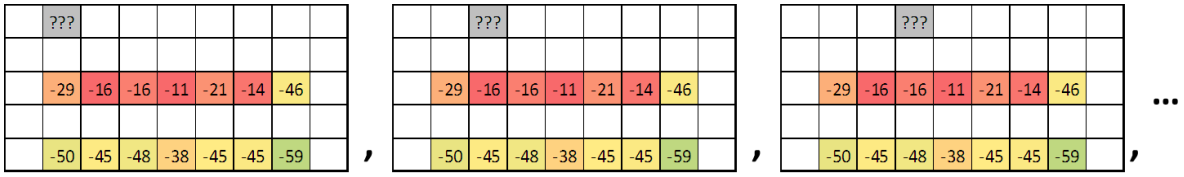

Figure 33: Known and unknown points for Situation 4 when estimating FAR_2 (left), FAR_3 (center), and FAR_4 (right); colored cells are the known heights in units of centimeters. The gray cell is the point being estimated, and white cells were not included in the estimation model.

The distance, in cells, from one point to another was used to assign weights to each known point in all estimation models. For example, the distance from FAR_2 to FAR_3 was 1 cell, and the distance from FAR_2 to $NEAR_2$ was 4 cells.

5.2.2 Grain Delivery Conditions

Data to evaluate the inverse distance weighting method was collected under diverse grain delivery conditions. It was critical to test the inverse distance weighting method with a diverse data set to assure the model could perform robustly in the field and avoid limiting the model to specific conditions. Four specific treatment factors of the delivery conditions were identified:

1. Fullness level of the grain cart
2. Lateral distance between the combine and grain cart
3. Order in which the zones of the grain cart were filled
4. Number of discrete fill zones the grain cart was divided

The treatment factor for the fullness of the grain cart was measured by the average grain height in the fill column of each zone. It had three levels: -40 cm, -25 cm, and -10 cm (Figure 34). The average of the third, fifth, and seventh columns of the fill grid determined when a zone was considered full in a 3-zone test. The average of second through eighth columns of the fill grid determined when a zone was considered full in a 7-zone test. Figure 35 shows the sequence of fullness states that were achieved before the grain delivery location was changed to the next zone for a -40 cm desired fullness level.

Figure 34: Grain carts filled with three fill zones to an average height of -40 cm (left), -25 cm (center), and -10 cm (right), as determined by the average height measured in Columns 3, 5, and 7 of the fill grid; Columns 3, 5, and 7 were at the center of the three fill zones

-121	-111	-96	-93	-75	-48	**-37**	-51	-61
-114	-109	-100	-79	-60	-38	**-30**	-43	-48
-109	-99	-90	-69	-50	-28	**-20**	-33	-43
-114	-109	-100	-79	-60	-38	**-30**	-43	-48
-156	-146	-123	-116	-87	-75	**-80**	-83	-93
-123	-115	-101	-88	-66	-45	**-40**	-51	-59

-119	-109	-93	-58	**-43**	-48	-37	-51	-61
-114	-109	-84	-56	**-29**	-38	-30	-43	-48
-109	-99	-74	-46	**-19**	-28	-20	-33	-43
-114	-109	-84	-56	**-29**	-38	-30	-43	-48
-156	-146	-119	-86	**-79**	-75	-80	-83	-93
-122	-114	-91	-60	**-40**	-45	-40	-51	-59

-57	-47	**-40**	-55	-43	-48	-37	-51	-61
-46	-41	**-29**	-37	-29	-38	-30	-43	-48
-41	-31	**-19**	-27	-19	-28	-20	-33	-43
-46	-41	**-29**	-37	-29	-38	-30	-43	-48
-98	-88	**-82**	-86	-79	-75	-80	-83	-93
-58	-50	**-40**	-49	-40	-45	-40	-51	-59

Figure 35: Fill grids for a -40 cm desired fullness level before the grain delivery location can change to the next fill zone backward in a test using three fill zones and a Front-Middle-Back filling order; values are grain heights in centimeters, and the bottom row is the average grain height in each column

The treatment factor for the lateral distance between the combine and the grain cart had two levels: 590 cm and 520 cm (Figure 36). In row crops such as corn and soybeans, it is easier to maintain a consistent distance because existing crop residue is visible for the tractor operator to follow while in other crops, such as rice where no clear marks are visible, this offset distance can have a much higher variation (Figure 37).

Figure 36: Lateral distance between a combine and grain cart

Figure 37: Corn field residue remaining after harvest (left) used by tractor operators to maintain more consistent offset distances from the combine versus a rice field (right) where no natural lines exist after the grain has been harvested

A distance of 590 cm between the machines placed the peak of the grain pile in the lateral center of the cart. Human error during tests often caused the peak to vary several centimeters from the center. The actual distance between machines was not recorded during tests. At a distance of 520 cm, the peak of the grain pile was placed between the far- and middle-thirds of the grain cart (Figure 38). This distance was used as the other level of the lateral offset distance treatment factor.

Figure 38: Grain cart filled with a lateral distance between the combine and grain cart of 590 cm (left), placing the peak directly below the middle row of sensors, and 520 cm (right), placing the center of the peak closer to the far edge

The treatment factor for the zone filling order had a Front-Middle-Back level and a Middle-Front-Back level (Figure 39). For a Front-Middle-Back treatment level, grain was delivered to the front of the grain cart first and incrementally moved toward the rear. The Middle-Front-Back treatment level started in the middle, moved forward, and finished in the back. A Middle-Front-Back filling order was chosen to test a model's unintentional reliance on prior knowledge of the grain surface profile. If all tests were conducted filling Front-Middle-Back, a model could inadvertently rely on having greater grain heights on the forward side and lesser grain heights on the rearward side of the point being estimated.

Figure 39: Numbered order in which grain was delivered to discrete fill zones of the grain cart; Front-Middle-Back (left) and Middle-Front-Back (right)

The number of fill zones treatment factor had treatment levels of three zones and seven zones (Figure 40). With three fill zones, grain was delivered to points MID_3, MID_5, and MID_7 of the fill grid. When seven zones were used, grain was delivered to all points in the middle row of the fill grid except the first and last points (MID_2, MID_3, MID_4, MID_5, MID_6, MID_7, and MID_8). Seven fill zones were chosen to provide the highest probability of demonstrating a significant difference caused by the number of fill zones. In the field the relative position of the combine and grain cart constantly change with variable crop conditions and terrain. A test with a high number of fill zones was

intended to be representative of an unloading on-the-go cycle with substantial relative machine movement.

Figure 40: Grain cart filled using three fill zones (left) and seven fill zones (right) in a Front-Middle-Back zone filling order

5.2.3 Test matrix

All treatment factors and treatment levels were compiled into a test matrix (Figure 41). Each test ID included 0 to 68 instances when the unloading auger was disengaged to allow the distance measurements and scale weight to be logged. Some test IDs did not have fill grids because invalid sensor readings were reported, and the fill grid samples had to be removed. Tests began with the grain height of entire cart below -40 cm. All zones were filled to -40 cm before filling all zones to -25 cm and -10 cm, sequentially. When all zones reached -10 cm, a single repetition had been collected for Test IDs 1-3, 4-6, 7-10, or 10-12, depending on the other delivery conditions. Four repetitions were conducted for each set of three tests. The number of fill grids collected for each test ID was not the same because the starting condition of the cart and the amount of grain delivered between auger disengagements varied.

Test ID	Repetitions	Number of Fill Grid Samples	Fill Level			Lateral Distance Between Vehicles		Filling Order		Number of Zones	
			-40cm (80%)	-25cm (90%)	-10cm (100%)	590cm	520cm	Front-Middle-Back	Middle-Front-Back	3 Zones	7 Zones
1	4	68	X			X		X		X	
2	4	19		X		X		X		X	
3	4	19			X	X		X		X	
4	4	59	X				X	X		X	
5	4	18		X			X	X		X	
6	4	0			X		X	X		X	
7	4	63	X			X			X	X	
8	4	16		X		X			X	X	
9	4	0			X	X			X	X	
10	4	54	X			X		X			X
11	4	17		X		X		X			X
12	4	0			X	X		X			X

Figure 41: Test matrix for the grain delivery conditions that were used to collect data to evaluate the point estimation model; the total number of fill grids collected was 333.

Each set of tests was conducted to collect data for a specific delivery condition. Test IDs 1-3 collected 106 fill grid samples for the baseline conditions of the lateral distance between vehicles, filling order, and number of fill zones. Test IDs 4-6 tested the lateral distance between vehicles and used 77 fill grids, and Test IDs 7-9 tested the filling order using 79 fill grids. The last set of IDs used 71 fill grid samples and tested the number of fill zones. The total number of fill grid samples collected was 333.

5.3 Results

5.3.1 Situation 1 Modeling

Situation 1 was included in the modeling tests to analyze the ability of the inverse distance weighting method to estimate a single point at the grain delivery location. Analysis was conducted individually for each point in the middle row of the fill grid with the intent to find column-by-column trends in the error of estimated points. A comparison of different values for the distance weighting exponent was conducted using the full data set of 333 total fill grids. The data in Table 9 was produced using the combined delivery conditions of the four data subsets.

Table 9: Mean errors and standard deviations (in parentheses) of the estimated grain heights in Sitution 1 at each point of the fill grid for the range of distance exponents tested; the lowest magnitude mean errors for each point are highlighted blue.

	Cart Location						
Distance Weighting Exponent	MID_2 $\dot{\epsilon_2}(\sigma_{\epsilon_2})$ (cm)	MID_3 $\dot{\epsilon_3}(\sigma_{\epsilon_2})$ (cm)	MID_4 $\dot{\epsilon_4}(\sigma_{\epsilon_4})$ (cm)	MID_5 $\dot{\epsilon_5}(\sigma_{\epsilon_5})$ (cm)	MID_6 $\dot{\epsilon_6}(\sigma_{\epsilon_6})$ (cm)	MID_7 $\dot{\epsilon_7}(\sigma_{\epsilon_7})$ (cm)	MID_8 $\dot{\epsilon_8}(\sigma_{\epsilon_8})$ (cm)
0	-16 (16) A	-32 (14) A	-31 (10) A	-44 (12) A	-41 (9) A	-46 (10) A	-33 (15) A
1	-14 (14) A	-29 (12) A	-26 (8) A	-38 (11) AB	-34 (8) AB	-39 (8) AB	-28 (13) A
2	-9 (12) AB	-24 (10) AB	-18 (7) AB	-29 (10) AB	-23 (7) B	-30 (7) AB	-19 (12) AB
3	-2 (11) AB	-18 (9) AB	-9 (6) AB	-21 (9) B	-13 (7) BC	-21 (7) B	-8 (11) AB
4	5 (11) AB	-13 (8) AB	-2 (6) AB	-15 (9) B	-5 (7) C	-15 (7) B	1 (11) B
5	10 (11) AB	-10 (8) AB	2 (6) AB	-11 (9) B	-1 (7) C	-12 (7) B	6 (11) B
6	13 (11) B	-9 (8) B	4 (6) B	-9 (9) B	1 (7) C	-10 (8) B	9 (11) B
7	14 (11) B	-8 (9) B	5 (6) B	-8 (9) B	3 (8) C	-9 (8) B	11 (11) B
8	15 (11) B	-8 (9) B	6 (6) B	-8 (9) B	3 (8) C	-9 (8) B	12 (11) B
9	15 (11) B	-8 (9) B	6 (6) B	-8 (9) B	3 (8) C	-9 (8) B	12 (11) B
10	15 (11) B	-8 (9) B	6 (6) B	-7 (9) B	3 (8) C	-8 (8) B	12 (11) B

All locations experienced increased error, but not necessarily an increase in magnitude, as the distance exponent increased. MID_5 and MID_7 were very negative (highly underestimated) at low distance exponent values and moved to slightly negative (slightly underestimated) for higher values of the distance exponent. This was due to points along the edges given more weight at first, bringing down the estimated value. At high exponents, almost all the weight was assigned to points in the same row, fortifying the hypothesis that the closest points were the best to use in this application when estimating unknown points. Even points, which did not receive grain, started with large negative errors and eventually became overestimated. High exponents placed all the weight on the closest points, which were peaks so overestimation was caused by not knowing the even point numbers were valleys. Even points experienced the lowest mean error at an exponent value of three to five. Higher exponents shifted too much weight to the closest points, which were peaks, and caused overestimation. Exponent values in the 3-5 range placed enough weight on the near and far edge points to bring estimate down. The optimum exponent for locations not receiving grain was likely dependent on the data set the model was used with. The optimum distance exponent at locations not receiving grain could have been higher or lower than 3-5 for data collected with a different angle of repose or while traveling through the field. The optimum mean error for each column was highlighted blue in Table 9.

Odd points, which were the three locations that received grain, started with large negative errors and moved to less negative errors. These locations were always peaks. The inverse distance

weighting equation is unable to produce estimates larger than the known population of points so it was expected the error will always remain underestimated. That was also why an exponent nearing infinity produced the smallest error.

The highest variation in the error occurred for all points when the distance exponent was zero. This happened because equal weight in the estimate was placed in all points of the known population. This meant an increased grain height at the front-far corner would raise the estimated unknown point at the rear-near corner, where intuitively there should have been no relationship. Changes in the mean error were insignificant past a distance exponent value of three for all points; however, the mean error at MID_3, MID_5, and MID_7 continued experiencing a decreasing trend. After the distance reached a cubic relationship in the inverse distance equation, the weight transfer was negligible. If a very high exponent was the selected estimation method, a value of three could have been used instead of ten to reduce computation time on a low-level controller. This claim was supported by the variation experiencing minimal change for distance exponent values greater than three. The significance intervals transitioned around a value of three for the distance exponent in all points. The transition occurred at this value because the variation decreased while the error improved, indicating the estimated value began nearing the true value of the missing points.

The accuracy goal for the mean error of the model was -15 cm to +25 cm (15 cm underestimation to 25 cm overestimation). The acceptance range was smaller on the negative side because the consequences were worse if the grain height was underestimated versus overestimated. The test showed all locations met or exceeded this goal using the inverse distance weighting method for distance exponents greater than three (Table 10). Lower distance exponent values underestimated the height because the weight assigned to lower points along the near and far edges decreased the estimation. Overestimation error increased in the even points, but the mean error remained within the acceptable range because of the higher allowable overestimation error. For all tables included in this chapter, results highlighted red indicate the mean error was outside the acceptable range, results highlighted yellow produced a mean inside the acceptable range but ±1 standard deviation reached beyond, and results highlighted green indicate the mean ±1 standard deviation was completely located within the acceptable range. Results highlighted red did not meet the accuracy goal. Green and yellow values met the specified goal, but green values exceeded the performance expectations of the model. A distance weighting exponent of four or ten

produced the most accurate results based on the mean errors averaged across the length of the cart for at least two of the modeled points. Further investigation was conducted into the performance of both exponents under diverse grain delivery conditions.

Table 10: Mean errors and standard deviations (in parentheses) of the estimated grain heights in Situation 1 at each point in the grain delivery area for the range of distance exponents tested; red cells indicate the mean error was outside the desired accuracy range, yellow cells indicate the mean was inside the desired range but ±1 standard deviation extended beyond the range, and green cells indicate the mean error ±1 standard deviation was completely contained by the desired accuracy range.

	Cart Location						
Distance Weighting Exponent	MID_2 $\dot{\epsilon}_2\ (\sigma_{\epsilon_2})$ (cm)	MID_3 $\dot{\epsilon}_3\ (\sigma_{\epsilon_3})$ (cm)	MID_4 $\dot{\epsilon}_4\ (\sigma_{\epsilon_4})$ (cm)	MID_5 $\dot{\epsilon}_5\ (\sigma_{\epsilon_5})$ (cm)	MID_6 $\dot{\epsilon}_6\ (\sigma_{\epsilon_6})$ (cm)	MID_7 $\dot{\epsilon}_7\ (\sigma_{\epsilon_7})$ (cm)	MID_8 $\dot{\epsilon}_8\ (\sigma_{\epsilon_8})$ (cm)
0	-16 (16) A	-32 (14) A	-31 (10) A	-44 (12) A	-41 (9) A	-46 (10) A	-33 (15) A
1	-14 (14) A	-29 (12) A	-26 (8) A	-38 (11) AB	-34 (8) AB	-39 (8) AB	-28 (13) A
2	-9 (12) AB	-24 (10) AB	-18 (7) AB	-29 (10) AB	-23 (7) B	-30 (7) AB	-19 (12) AB
3	-2 (11) AB	-18 (9) AB	-9 (6) AB	-21 (9) B	-13 (7) BC	-21 (7) B	-8 (11) AB
4	5 (11) AB	-13 (8) AB	-2 (6) AB	-15 (9) B	-5 (7) C	-15 (7) B	1 (11) B
5	10 (11) AB	-10 (8) AB	2 (6) AB	-11 (9) B	-1 (7) C	-12 (7) B	6 (11) B
6	13 (11) B	-9 (8) B	4 (6) B	-9 (9) B	1 (7) C	-10 (8) B	9 (11) B
7	14 (11) B	-8 (9) B	5 (6) B	-8 (9) B	3 (8) C	-9 (8) B	11 (11) B
8	15 (11) B	-8 (9) B	6 (6) B	-8 (9) B	3 (8) C	-9 (8) B	12 (11) B
9	15 (11) B	-8 (9) B	6 (6) B	-8 (9) B	3 (8) C	-9 (8) B	12 (11) B
10	15 (11) B	-8 (9) B	6 (6) B	-7 (9) B	3 (8) C	-8 (8) B	12 (11) B

5.3.1.1 520 cm Lateral Distance between Vehicles

It was desirable for the model to have no significant impact on the error of the estimated points from the lateral vehicle offset distance. Changing the lateral distance from 590 cm to 520 cm showed no significant differences in the error of the estimated points at all seven points in the grain delivery area (Table 11). No significant impact was expected because delivering grain to locations offset from center did not visually change the shape of the grain profile along the middle row of the cart. Three distinct peaks were created at the delivery locations with valleys between them. MID_4 changed from being underestimated by 2 cm in the control subset to being overestimated by 2 cm in the 520 cm subset, and MID_6 increased from being underestimated by 7 cm to being underestimated by 1 cm. The changes in the mean error of the estimates were not significant to further investigate. This indicated an inverse distance weighting model with a distance exponent of four could be used to estimate unknown grain heights in the grain delivery area without influence from the lateral distance between the combine and grain cart.

Table 11: Comparison of the effect of the lateral distance between vehicles of 590 cm and 520 cm on the mean errors and standard deviations (in parentheses) of the estimated grain heights in the delivery area in Situation 1 with a distance exponent of four; red cells indicate the mean error was outside the desired accuracy range, yellow cells

indicate the mean was inside the desired range but ±1 standard deviation extended beyond the range, and green cells indicate the mean error ±1 standard deviation was completely contained by the desired accuracy range.

Grain Delivery Conditions			Cart Location						
Lateral Distance Between Vehicles	Filling Order	Number of Fill Zones	MID_2 $\dot{\epsilon}_2\ (\sigma_{\epsilon_2})$ (cm)	MID_3 $\dot{\epsilon}_3\ (\sigma_{\epsilon_2})$ (cm)	MID_4 $\dot{\epsilon}_4(\sigma_{\epsilon_4})$ (cm)	MID_5 $\dot{\epsilon}_5\ (\sigma_{\epsilon_5})$ (cm)	MID_6 $\dot{\epsilon}_6(\sigma_{\epsilon_6})$ (cm)	MID_7 $\dot{\epsilon}_7(\sigma_{\epsilon_7})$ (cm)	MID_8 $\dot{\epsilon}_8(\sigma_{\epsilon_8})$ (cm)
590cm	F - M - B	3	9 (6) A	-13 (9) A	-2 (5) A	-12 (11) A	-7 (8) A	-18 (7) A	4 (7) A
520cm	F - M - B	3	8 (5) A	-13 (4) A	2 (4) A	-16 (5) A	-1 (4) A	-14 (5) A	2 (6) A

The mean error at even points exceeded the accuracy goal for the control group and 520 cm offset group. Even points were expected to be within the acceptable range because they tended to be overestimated. For the control sample, MID_7 was underestimated beyond the acceptable level by 3 cm while the other points located at peaks were underestimated but within the target range. The 520 cm offset group showed similar accuracy results, but MID_5 was underestimated by an additional 4 cm and MID_7 was underestimated by 4 cm less. Although these changes in error were large enough to move these points in and out of the acceptable range, 4 cm was not significant relative to the size of the grain cart.

A test of the lateral offset between vehicles of 590 cm was repeated with a distance exponent of ten (Table 12). In the control sample, the mean error along the length of the cart developed a saw-tooth pattern from the delivery points being underestimated and the other points being overestimated (Figure 42). The number of sensors in a row limited the model's capability to recognize peaks and valleys and compensate the value of the estimated point. Changing the lateral distance from 590 cm to 520 cm showed no significant changes in the error of the estimated points at all seven locations in the grain delivery area. No significant impact was expected because delivering grain to locations offset from center did not visually change the shape of the grain profile along the middle row of the cart. This indicated an inverse distance weighting model with a distance exponent of ten could be also used to estimate unknown grain heights in the grain delivery area without influence from the lateral distance between the combine and grain cart.

Table 12: Comparison of the effect of the lateral distance between vehicles of 590 cm and 520 cm on the mean errors and standard deviations (in parentheses) of the estimated grain heights in the delivery area in Situation 1 with a distance exponent of ten; yellow cells indicate the mean was inside the desired range but ±1 standard deviation extended beyond the range and green cells indicate the mean error ±1 standard deviation was completely contained by the desired accuracy range.

Grain Delivery Conditions			Cart Location						
Lateral Distance Between Vehicles	Filling Order	Number of Fill Zones	MID_2 $\hat{\epsilon}_2(\sigma_{\epsilon_2})$ (cm)	MID_3 $\hat{\epsilon}_3(\sigma_{\epsilon_2})$ (cm)	MID_4 $\hat{\epsilon}_4(\sigma_{\epsilon_4})$ (cm)	MID_5 $\hat{\epsilon}_5(\sigma_{\epsilon_5})$ (cm)	MID_6 $\hat{\epsilon}_6(\sigma_{\epsilon_6})$ (cm)	MID_7 $\hat{\epsilon}_7(\sigma_{\epsilon_7})$ (cm)	MID_8 $\hat{\epsilon}_8(\sigma_{\epsilon_8})$ (cm)
590cm	F - M - B	3	18 (7) A	-9 (8) A	6 (6) A	-5 (11) A	2 (9) A	-12 (7) A	16 (8) A
520cm	F - M - B	3	15 (5) A	-9 (4) A	8 (4) A	-10 (6) A	6 (5) A	-9 (5) A	12 (7) A

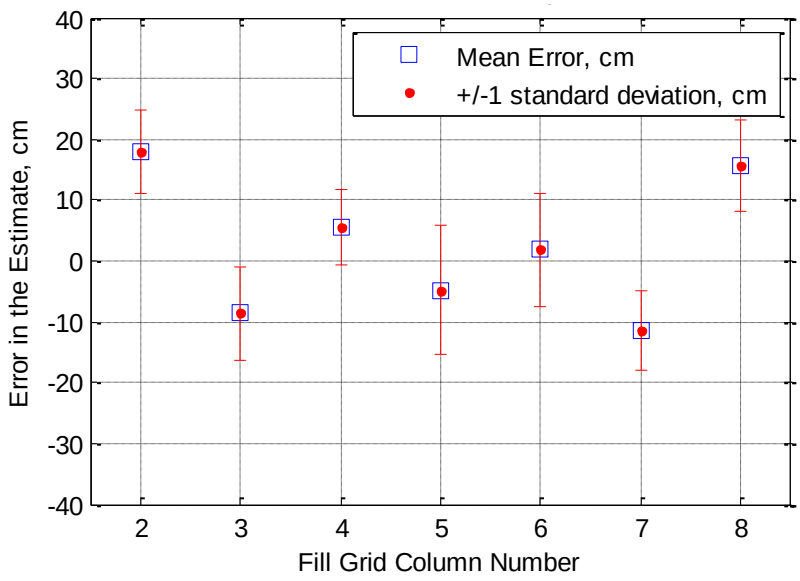

Figure 42: Mean error of the estimated points in the grain delivery area using the inverse distance weighting method with a distance exponent of ten showing a saw-tooth pattern; error bars are one standard error from the mean

The estimation model exceeded the performance goal at points that did not directly receive grain (Table 12) and met the goal at points that did receive grain with the control sample. This was expected based on the mean error results across all delivery conditions in Table 9 which showed higher exponents produced more favorable error at the points directly receiving grain. The group with a smaller lateral offset also exceeded the performance goal at points that did not receive grain. This group exceeded the goal at MID_3 and MID_7 due mostly to a smaller standard deviation compared to the control group. The mean error at MID_5 met the accuracy goal, but it was expected to exceed the goal as MID_3 and MID_7 did. This was likely caused by more grain flowing toward the far edge and creating low measurements in the delivery area. Although accuracy differences were

observed with a shorter (520 cm) lateral offset, the changes did not demonstrate degradation or improvement in model performance.

5.3.1.2 Middle-Front-Back Filling Order

A test was conducted that changed the filling order of three fill zones from the control level of Front-Middle-Back to the Middle-Front-Back fill order, while maintaining a distance exponent value of four (Table 13). It was desirable for a model to have no significant impact from the filling order on the error of the estimated points. Changing the filling order to Middle-Front-Back showed no significant differences in the error of the estimated points at all seven points in the grain delivery area. The largest differences in the mean error were in MID_3 and MID_5 at 7 cm and 9 cm, respectively. These differences were small enough to show this estimation model was not impacted by filling the grain cart in a different filling order. The changes in the mean error of the estimates that were observed were probably due to the grain peak being located closer to the exact sensing point when data with a Middle-Front-Back filling order was collected. This caused the sensor measurement to detect the exact highest point, and the estimation model showed a larger underestimation error.

Table 13: Comparison of the effect of the filling order on the mean errors and standard deviations (in parentheses) of the estimated grain heights in the delivery area in Situation 1 with a distance exponent of four; red cells indicate the mean error was outside the desired accuracy range, yellow cells indicate the mean was inside the desired range but ±1 standard deviation extended beyond the range, and green cells indicate the mean error ±1 standard deviation was completely contained by the desired accuracy range.

Grain Delivery Conditions			Cart Location						
Lateral Distance Between Vehicles	Filling Order	Number of Fill Zones	MID_2 $\dot{\epsilon}_2(\sigma_{\epsilon_2})$ (cm)	MID_3 $\dot{\epsilon}_3(\sigma_{\epsilon_2})$ (cm)	MID_4 $\dot{\epsilon}_4(\sigma_{\epsilon_4})$ (cm)	MID_5 $\dot{\epsilon}_5(\sigma_{\epsilon_5})$ (cm)	MID_6 $\dot{\epsilon}_6(\sigma_{\epsilon_6})$ (cm)	MID_7 $\dot{\epsilon}_7(\sigma_{\epsilon_7})$ (cm)	MID_8 $\dot{\epsilon}_8(\sigma_{\epsilon_8})$ (cm)
590cm	F - M - B	3	9 (6) A	-13 (9) A	-2 (5) A	-12 (11) A	-7 (8) A	-18 (7) A	4 (7) A
590cm	M - F - B	3	12 (5) A	-20 (5) A	0 (4) A	-21 (5) A	-3 (5) A	-19 (5) A	9 (6) A

The mean error of the Middle-Front-Back group was unacceptable at points that directly received grain but exceeded the accuracy goal at points that did not receive grain. This reinforced the hypothesis that the three peaks of grain in this group were located nearly exactly beneath the sensing points causing greater magnitude changes of the grain profile along the length of the delivery area. Even points were substantially overestimated as a result of high peaks at MID_3, MID_5, and MID_7, but the weight assigned to points along the near and far edges in this model decreased the overestimation to bring the mean error well within the acceptable error range. If filling were to

occur while traveling over rough terrain in the field, the grain will distribute more evenly across the surface of the cart. It was expected a smaller distance exponent would produce similar accuracy results at MID_3, MID_5, and MID_7 with rough terrain because the difference in grain height between the delivery area and the edges would be smaller so more weight would need shifted to the edge points. The mean errors at points directly receiving grain were outside the acceptable range by 4-6 cm. This extra error was not enough to eliminate using four as a viable distance exponent, but it decreased confidence in the model since estimations in **Error! Reference source not found.** also howed points close to and beyond the acceptable range.

A test of the Middle-Front-Back filling order was repeated with a distance exponent of ten (Table 14). Changing the filling order to Middle-Front-Back showed no significant changes in the error of the estimated points at all seven locations in the grain delivery area. The data did show the magnitudes of the errors at all points increased. The errors at MID_2, MID_4, MID_6, and MID_8 showed a larger overestimation, and the errors at MID_3, MID_5, and MID_7 showed a larger overestimation. This observation probably occurred because the peak of grain was more directly centered where the grain height measurement was taken. This was likely not due to an effect of the filling order on the estimation model. The results indicated changing the filling order to Middle-Front-Back showed did not impact the model's error of the estimated points in the grain delivery area.

Table 14: Comparison of the effect of the filling order on the mean errors and standard deviations (in parentheses) of the estimated grain heights in the delivery area in Situation 1 with a distance exponent of ten; yellow cells indicate the mean was inside the desired range but ±1 standard deviation extended beyond the range and green cells indicate the mean error ±1 standard deviation was completely contained by the desired accuracy range.

Grain Delivery Conditions			Cart Location						
Lateral Distance Between Vehicles	Filling Order	Number of Fill Zones	MID_2 $\dot{\epsilon}_2\ (\sigma_{\epsilon_2})$ (cm)	MID_3 $\dot{\epsilon}_3\ (\sigma_{\epsilon_2})$ (cm)	MID_4 $\dot{\epsilon}_4(\sigma_{\epsilon_4})$ (cm)	MID_5 $\dot{\epsilon}_5\ (\sigma_{\epsilon_5})$ (cm)	MID_6 $\dot{\epsilon}_6(\sigma_{\epsilon_6})$ (cm)	MID_7 $\dot{\epsilon}_7(\sigma_{\epsilon_7})$ (cm)	MID_8 $\dot{\epsilon}_8(\sigma_{\epsilon_8})$ (cm)
590cm	F - M - B	3	18 (7) A	-9 (8) A	6 (6) A	-5 (11) A	2 (9) A	-12 (7) A	16 (8) A
590cm	M - F - B	3	24 (6) A	-15 (5) A	10 (5) A	-13 (5) A	7 (5) A	-13 (5) A	21 (5) A

The accuracy at MID_2 and MID_8 changed from a green status to yellow status because the mean error at these points was overestimated more than the control (Table 14). The zone filling order was not expected to cause the error to change at these points. This was likely caused by steeper peaks in the grain during these tests, which was not intended to occur when the experiment was performed. Unloading on-the-go in real harvesting conditions is not expected to create steeper peaks a Middle-Front-Back filling order is used instead of a Front-Middle-Back order.

Overestimation of the mean error at MID_2 and MID_8 increased by 6 cm and 5 cm, respectively, but these changes were not significant for the application of the model. MID_5 experienced the largest change in error (underestimated extra 8 cm), but this was also insignificant.

5.3.1.3 Seven Fill Zones

A test was conducted that changed the number of fill zones the cart was divided into from the control level of three zones to seven zones using a distance exponent of four. Changing the number of fill zones from three to seven showed a significant impact in the error of the estimated points in the front-most and rear-most points of the grain cart: MID_2 and MID_8(Table 15).

Table 15: Comparison of the effect of 3 fill zones and 7 fill zones on the mean errors and standard deviations (in parentheses) of the estimated grain heights in the delivery area in Situation 1 with a distance exponent of ten; red cells indicate the mean error was outside the desired accuracy range, yellow cells indicate the mean was inside the desired range but ±1 standard deviation extended beyond the range, and green cells indicate the mean error ±1 standard deviation was completely contained by the desired accuracy range.

Grain Delivery Conditions			Cart Location						
Lateral Distance Between Vehicles	Filling Order	Number of Fill Zones	MID_2 $\dot{\epsilon}_2\ (\sigma_{\epsilon_2})$ (cm)	MID_3 $\dot{\epsilon}_3\ (\sigma_{\epsilon_2})$ (cm)	MID_4 $\dot{\epsilon}_4(\sigma_{\epsilon_4})$ (cm)	MID_5 $\dot{\epsilon}_5\ (\sigma_{\epsilon_5})$ (cm)	MID_6 $\dot{\epsilon}_6(\sigma_{\epsilon_6})$ (cm)	MID_7 $\dot{\epsilon}_7(\sigma_{\epsilon_7})$ (cm)	MID_8 $\dot{\epsilon}_8(\sigma_{\epsilon_8})$ (cm)
590cm	F - M - B	3	9 (6) A	-13 (9) A	-2 (5) A	-12 (11) A	-7 (8) A	-18 (7) A	4 (7) A
590cm	F - M - B	7	-11 (10) B	-6 (7) A	-8 (6) A	-11 (7) A	-10 (7) A	-8 (6) A	-16 (7) B

When seven fill zones were used, the grain height at these two locations was significantly underestimated compared to the control subset. This was because MID_2 and MID_8 were not grain delivery points in the control subset. When these points became delivery points, the height was underestimated by the model, just like the three delivery points (MID_3, MID_5, and MID_7) were consistently underestimated in the control subset. The other points that did not receive grain with three fill zones but did receive grain with seven fill zones (MID_4 and MID_6) showed the estimated points were underestimated more with seven fill zones. This was expected because a distance exponent of four placed enough weight on the points along the near and far edges to lower the estimated point in the middle of the cart. This effect decreased the estimate, which improved the error when the unknown point was in a valley by countering the nearby peaks. With seven zones, that point was no longer in a valley so the weight placed on points along the near and far edges had a negative effect. This indicated the best distance exponent could be very high when filling with seven zones. The mean errors in the estimates at the points that received grain with three fill zones (MID_3, MID_5, and MID_7) were closer to zero when seven fill zones were used. These locations were

highly underestimated with three fill zones. The error improved with seven zones because the neighboring points that had the most weight in calculating the estimate were also peaks. The error at these points was expected to improve for higher values of the distance exponent. With seven fill zones the mean errors of the estimates across all locations were underestimated by 6-16 cm (10 cm range). Three fill zones saw the mean error of the estimates range from an underestimation of 18 cm to an overestimation of 9 cm (27 cm range). The tighter grouping of the mean errors with seven zones was expected because all estimated points eventually reached the same height so a very large distance exponent reduced the weight placed on the points along the near and far edges and increased the weight on the known points in the middle row that were filled to the same level. For these reasons a distance exponent of ten was expected to have better results.

The accuracy of the estimation model when seven fill zones were used included mean errors that fell under all three categories used to describe the accuracy and did not display any trends relating the position of each point. MID_3, MID_4, and MID_7 exceeded the expected accuracy, MID_2, MID_5, and MID_6 met the accuracy goal, and MID_8 fell outside the desired accuracy (Table 15). The randomness of the data was caused by all the mean errors having values near the -15 cm underestimation limit. Small changes in the mean error caused points to move into a different category. The poorest accuracy occurred at the front and rear of the cart instead of the three peaks of grain. The accuracy at the three peaks was expected to improve because there were no sensors in the valleys between large peaks of grain when seven fill zones were used. The error at the front and rear was not large enough to distinguish it from the other points.

A test with seven fill zones was repeated with a distance exponent of ten (Table 16). Changing the number of fill zones from three to seven showed a significant impact in the error of the estimated points in the front-most and rear-most columns of the grain cart: MID_2 MID_8. When seven fill zones were used, the grain height at these two points was significantly underestimated compared to the control subset. The cause of this was the same as the previous test when a distance exponent of four was used. MID_2 and MID_8 were not grain delivery locations in the control subset. When these points became grain delivery locations, the height was underestimated by the model, just like the three delivery locations (MID_3, MID_5, and MID_7) were underestimated in the control subset.

Table 16: Comparison of the effect of 3 fill zones and 7 fill zones on the mean errors and standard deviations (in parentheses) of the estimated grain heights in the delivery area in Situation 1 with a distance exponent of ten; yellow cells indicate the mean was inside the desired range but ±1 standard deviation extended beyond the range and green cells indicate the mean error ±1 standard deviation was completely contained by the desired accuracy range.

Grain Delivery Conditions			Cart Location						
Lateral Distance Between Vehicles	Filling Order	Number of Fill Zones	MID_2 $\dot{\epsilon}_2(\sigma_{\epsilon_2})$ (cm)	MID_3 $\dot{\epsilon}_3(\sigma_{\epsilon_2})$ (cm)	MID_4 $\dot{\epsilon}_4(\sigma_{\epsilon_4})$ (cm)	MID_5 $\dot{\epsilon}_5(\sigma_{\epsilon_5})$ (cm)	MID_6 $\dot{\epsilon}_6(\sigma_{\epsilon_6})$ (cm)	MID_7 $\dot{\epsilon}_7(\sigma_{\epsilon_7})$ (cm)	MID_8 $\dot{\epsilon}_8(\sigma_{\epsilon_8})$ (cm)
590cm	F - M - B	3	18 (7) A	-9 (8) A	6 (6) A	-5 (11) A	2 (9) A	-12 (7) A	16 (8) A
590cm	F - M - B	7	0 (10) B	2 (7) A	0 (7) A	-2 (7) A	-1 (7) A	1 (6) A	-4 (7) B

The mean errors of the grain height estimates were closer to zero with seven fill zones at all locations and clearly lacked the saw-tooth effect experienced with three zones (Figure 43). When seven fill zones were used, the overestimation errors observed in the valleys of the fill grid were removed because these locations also directly received grain with seven zones. The error at the points directly receiving grain was closer to zero because the closest known points were also peaks of grain as opposed to valleys. This indicated the inverse distance weighting model with a very high distance exponent was best suited to model unknown points in the grain delivery area when the grain cart was filled under these conditions.

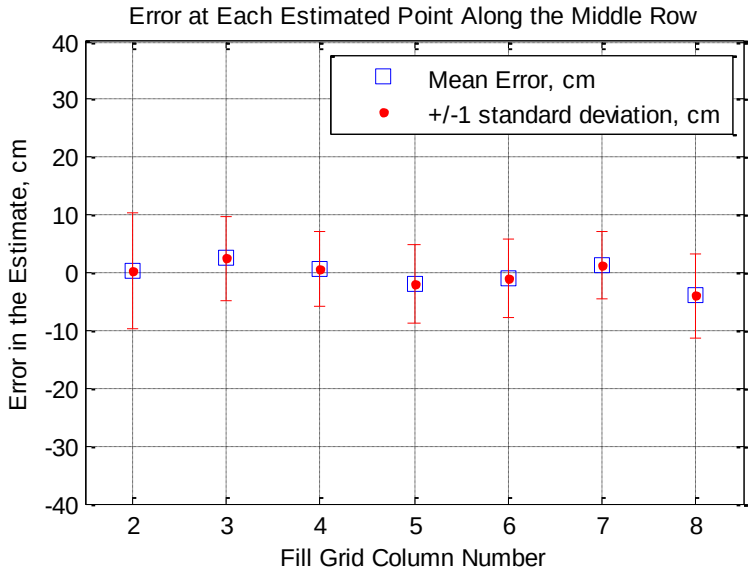

Figure 43: Mean error of the estimated points in the grain delivery area using seven fill zones; error bars are one standard error from the mean

The mean error ±1 standard deviation was located within the accuracy goal at all points in the grain delivery area. The modeling results were the best under these delivery conditions than

any other condition tested. The errors were expected to be the lowest with this test because the highest distance exponent was used and the closest known points were filled to the same height. MID_3, MID_5, and MID_7 changed to a green status because they had peaks on both sides instead of valleys. MID_8 experienced the most error, being underestimated by 4 cm, but this was well within the expectations of this model. This was the only test where zero mean error was within one standard deviation of the mean error at all points. This estimation model is expected to perform extremely well if similar delivery conditions are experienced in the field.

5.3.2 Situation 2 Modeling

A comparison of different values for the distance weighting exponent was conducted using the same data set as the previous situation. The data in Table 17 was produced using the combined delivery conditions of the four data subsets.

Table 17: Mean errors and standard deviations (in parentheses) of the estimated grain heights in Situation 2 at each point along the far edge for the range of distance exponents tested; the lowest magnitude mean errors for each column are highlighted in blue.

	Cart Location						
Distance Weighting Exponent	FAR_2 $\bar{\epsilon}_2$ (σ_{ϵ_2}) (cm)	FAR_3 $\bar{\epsilon}_3$ (σ_{ϵ_2}) (cm)	FAR_4 $\bar{\epsilon}_4$(σ_{ϵ_4}) (cm)	FAR_5 $\bar{\epsilon}_5$ (σ_{ϵ_5}) (cm)	FAR_6 $\bar{\epsilon}_6$(σ_{ϵ_6}) (cm)	FAR_7 $\bar{\epsilon}_7$(σ_{ϵ_7}) (cm)	FAR_8 $\bar{\epsilon}_8$(σ_{ϵ_8}) (cm)
0	12 (19) A	6 (21) A	8 (16) A	1 (17) A	2 (15) A	-4 (18) A	8 (17) A
1	13 (15) A	7 (18) A	11 (12) A	4 (14) A	7 (12) A	1 (15) A	13 (14) A
2	13 (11) A	5 (13) A	11 (8) A	4 (10) A	9 (8) A	0 (11) A	16 (10) A
3	11 (8) A	2 (10) A	9 (6) A	2 (8) A	7 (7) A	-2 (8) A	15 (9) A
4	8 (8) A	-1 (9) A	7 (6) A	-1 (7) A	6 (6) A	-5 (7) A	14 (9) A
5	7 (9) A	-3 (8) A	6 (6) A	-3 (7) A	5 (6) A	-7 (7) A	12 (9) A
6	6 (9) A	-3 (8) A	5 (6) A	-3 (7) A	4 (6) A	-8 (7) A	12 (10) A
7	6 (9) A	-4 (8) A	5 (6) A	-4 (7) A	4 (6) A	-8 (7) A	11 (10) A
8	6 (9) A	-4 (8) A	5 (6) A	-4 (7) A	4 (6) A	-8 (7) A	11 (10) A
9	6 (9) A	-4 (8) A	5 (6) A	-4 (7) A	4 (6) A	-8 (7) A	11 (10) A
10	6 (9) A	-4 (8) A	5 (6) A	-4 (7) A	4 (6) A	-8 (7) A	11 (10) A

Slight dips in the magnitude of the estimation error occurred at most points when the distance exponent was zero. The smallest magnitude of error at FAR_6 and FAR_8 was recorded when the distance exponent was zero. These were considered anomalies of the collected data set because it was not logical for the average of all known points in the cart to be the best predictor of the height at a single point. The highest variation in the estimation error was also observed at this level of the distance exponent because the estimate was dependent on the value of all other points in the fill grid. The overestimation FAR_2, FAR_4, FAR_6, and FAR_8 moved closer to zero as the distance exponent increased because the weight in the estimated value shifted off the known points in the

middle row. The same trend occurred FAR_3, FAR_5, and FAR_7 except the overestimation passed zero to become an underestimation. FAR_2, FAR_4, FAR_6, and FAR_8 had the lowest magnitude of error when the distance exponent was very high because lower values of the exponent shifted weight in the estimated value to the middle row, which was almost always higher than points along the far edge. This increased the model's estimated value above the actual value. FAR_3, FAR_5, and FAR_7 had the lowest error magnitudes for exponent values from 2-4 because these points were at the peaks of grain. A high distance exponent underestimated these points because the closest known points were valleys. As the exponent increased, more weight of the estimated value was transferred from the middle row of points to far edge points, which were lower than the peak. Points that received grain (FAR_3, FAR_5, and FAR_7) had the lowest error magnitude when the distance exponent was 2-4. Points that did not receive grain (FAR_2, FAR_4, FAR_6, and FAR_8) had the lowest error magnitude when the distance exponent was very high. The optimum mean error for each column was highlighted blue in Table 17. In general, these results were opposite of using the inverse distance weighting method in the delivery area. The same alternating pattern occurred because the points along the far edge experienced the same peaks and valleys as the delivery area. The optimum distance exponents were opposite because points along the far edge were influenced less by points greater in value (MID_n) as the distance exponent increased; whereas, points in the delivery area were influenced less by points lesser in value (FAR_n) as the distance exponent increased.

The same trend in the estimation of grain delivery points appeared in the estimation of far edge points. It was evident the optimum distance exponent was nearly the same for points that received grain, and the same distance exponent was optimal for points that did not receive grain. However, the optimum exponent was not the same value for both groups.

The estimation of single points along the far edge was generally more accurate than in the delivery area because grain delivered to the center of the cart flowed evenly toward the near and far edges. Peaks and valleys were still visually present along the edges. The data showed a saw-tooth pattern in the error, but the height difference from peak to valley was much lower (Figure 44) than the delivery area.

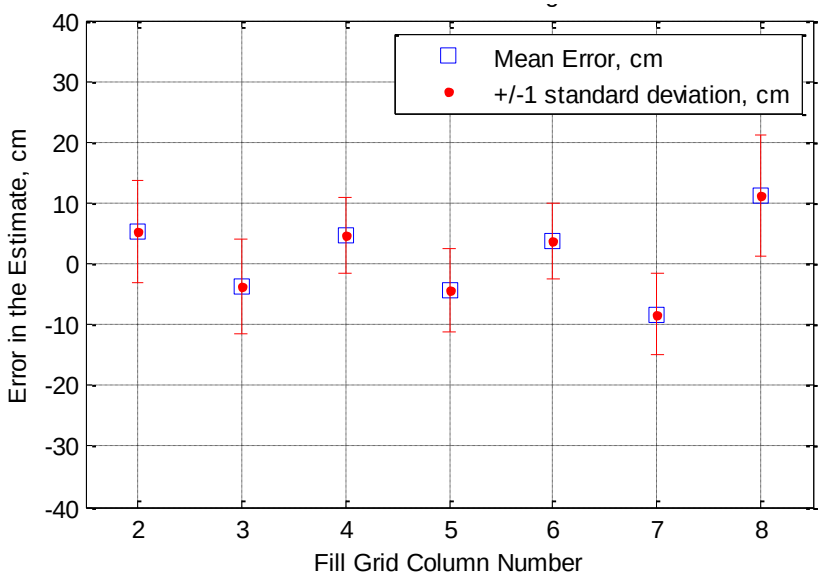

Figure 44: Mean error of the estimated points along the far edge using the inverse distance weighting method with a distance exponent of ten showing a saw-tooth pattern opposite the peaks and valleys in grain delivery area and with smaller magnitude errors; error bars are one standard error from the mean

The inverse distance weighting method produced no instances where the mean error at any point along the far edge was outside the desired accuracy range of -15 cm to +25 cm against distance exponent values ranging 0-10 (Table 18). Only five cases were found where the mean error ±1 standard deviation went beyond the accuracy range. All other estimations produced a mean error ±1 standard deviation that was contained entirely within the desired accuracy range. Two differences were attributed to better performance of the models. The first was that grain flowed to the far edge from the delivery point in the center of the cart, mitigating the creation of large peaks at the delivery points and valleys between the delivery points. The second was that the far edge was not the highest area in the fill grid, leaving points available in the delivery area to increase the value of the estimated points along the far edge. Because the lowest magnitude of error at several points along the far edge occurred at distance exponent values of four and ten, further investigation was conducted into both model's performance under diverse grain delivery conditions.

Table 18: Mean errors and standard deviations (in parentheses) of the estimated grain heights in Situation 2 at each point in along the far edge for the range of distance exponents tested; yellow cells indicate the mean was inside the desired range but ±1 standard deviation extended beyond the range and green cells indicate the mean error ±1 standard deviation was completely contained by the desired accuracy range.

	Cart Location						
Distance Weighting Exponent	FAR_2 $\bar{\epsilon}_2\ (\sigma_{\epsilon_2})$ (cm)	FAR_3 $\bar{\epsilon}_3\ (\sigma_{\epsilon_2})$ (cm)	FAR_4 $\bar{\epsilon}_4(\sigma_{\epsilon_4})$ (cm)	FAR_5 $\bar{\epsilon}_5\ (\sigma_{\epsilon_5})$ (cm)	FAR_6 $\bar{\epsilon}_6(\sigma_{\epsilon_6})$ (cm)	FAR_7 $\bar{\epsilon}_7(\sigma_{\epsilon_7})$ (cm)	FAR_8 $\bar{\epsilon}_8(\sigma_{\epsilon_8})$ (cm)
0	12 (19) A	6 (21) A	8 (16) A	1 (17) A	2 (15) A	-4 (18) A	8 (17) A
1	13 (15) A	7 (18) A	11 (12) A	4 (14) A	7 (12) A	1 (15) A	13 (14) A
2	13 (11) A	5 (13) A	11 (8) A	4 (10) A	9 (8) A	0 (11) A	16 (10) A
3	11 (8) A	2 (10) A	9 (6) A	2 (8) A	7 (7) A	-2 (8) A	15 (9) A
4	8 (8) A	-1 (9) A	7 (6) A	-1 (7) A	6 (6) A	-5 (7) A	14 (9) A
5	7 (9) A	-3 (8) A	6 (6) A	-3 (7) A	5 (6) A	-7 (7) A	12 (9) A
6	6 (9) A	-3 (8) A	5 (6) A	-3 (7) A	4 (6) A	-8 (7) A	12 (10) A
7	6 (9) A	-4 (8) A	5 (6) A	-4 (7) A	4 (6) A	-8 (7) A	11 (10) A
8	6 (9) A	-4 (8) A	5 (6) A	-4 (7) A	4 (6) A	-8 (7) A	11 (10) A
9	6 (9) A	-4 (8) A	5 (6) A	-4 (7) A	4 (6) A	-8 (7) A	11 (10) A
10	6 (9) A	-4 (8) A	5 (6) A	-4 (7) A	4 (6) A	-8 (7) A	11 (10) A

5.3.2.1 520 cm Lateral Distance between Vehicles

A test was conducted with the lateral distance between the combine and the grain cart decreased from 590 cm to 520 cm to determine if the offset distance impacted the errors of the estimated points. Changing the lateral distance from 590 cm to 520 cm showed no significant differences in the error of the estimated points at all seven locations along the far edge (Table 19). The Table 19errors of the estimates were expected to show further underestimation because the grain was delivered halfway between the sensors in the middle row and the sensors along the far edge. The heights at the far edge and in the middle were expected to be nearly the same, removing the effect from the middle row that would have normally caused the far edge estimates to be higher. The absence of this effect was observed at points that directly received grain. The mean error in the estimates decreased by 6 cm FAR_3, 6 cm at FAR_5, and 3 cm at MID_7; however, the change was not significant enough to separate the A-B intervals. The impact of the lateral offset distance was present, but the effect was not significant enough to eliminate this model as a viable estimation method.

Table 19: Comparison of the effect of the lateral distance between vehicles of 590 cm and 520 cm on the mean errors and standard deviations (in parentheses) of the estimated grain heights along the far edge in Situation 2 with a distance exponent of four; yellow cells indicate the mean was inside the desired range but ±1 standard deviation extended beyond the range and green cells indicate the mean error ±1 standard deviation was completely contained by the desired accuracy range.

Grain Delivery Conditions			Cart Location						
Lateral Distance Between Vehicles	Filling Order	Number of Fill Zones	FAR_2 $\dot{\epsilon}_2\ (\sigma_{\epsilon_2})$ (cm)	FAR_3 $\dot{\epsilon}_3\ (\sigma_{\epsilon_2})$ (cm)	FAR_4 $\dot{\epsilon}_4(\sigma_{\epsilon_4})$ (cm)	FAR_5 $\dot{\epsilon}_5\ (\sigma_{\epsilon_5})$ (cm)	FAR_6 $\dot{\epsilon}_6(\sigma_{\epsilon_6})$ (cm)	FAR_7 $\dot{\epsilon}_7(\sigma_{\epsilon_7})$ (cm)	FAR_8 $\dot{\epsilon}_8(\sigma_{\epsilon_8})$ (cm)
590cm	F - M - B	3	9 (6) A	-2 (7) A	6 (6) A	0 (8) A	5 (6) A	-7 (6) A	17 (7) A
520cm	F - M - B	3	8 (9) A	-8 (10) A	8 (5) A	-6 (6) A	5 (7) A	-10 (5) A	16 (4) A

The mean error ±1 standard deviation of the control sample was completely contained within the desired accuracy range at all points along the far edge (Table 19). This was expected because the grain was smoother along the far edge than in the delivery area. The largest mean error magnitude was 17 cm at FAR_8 with the second largest mean error magnitude at FAR_2 or 9 cm. These points were expected to have the highest magnitude of error based on results from previous tests that showed the highest error with three fill zones was at the very front and very back. When testing the 520 cm offset group, the accuracy of all points maintained a green status except FAR_3, which changed to a yellow status. This point was underestimated by 6 cm more when the offset distance changed to 520 cm. FAR_3 tied FAR_5 for the most change in accuracy at 6 cm. Although 6 cm changed the status of one point from green to yellow, it was not enough to demonstrate inadequate model performance.

A test of the lateral offset between vehicles of 590 cm was repeated with a distance exponent of ten (Table 20). Changing the lateral distance from 590 cm to 520 cm showed no significant changes in the error of the estimated points at all seven points along the far edge. The same effect was expected as with the previous model where all estimates were underestimated because the height of the middle row of known points was at the same level as the far edge. This model was expected to show less of an impact because the distance exponent was higher. The unknown point estimation showed almost no effects from the 520 cm subset FAR_2, FAR_4, FAR_6, and FAR_8.

FAR_3, FAR_5, and FAR_7 showed a larger underestimation of 5 cm, 4 cm, and 1 cm, respectively (Table 20). The differences were not significant and were less than the estimation model with an exponent of four. The overestimation error increased less than 5 cm at FAR_2, FAR_4, FAR_6, and FAR_8

when the lateral distance changed from 590 cm to 520 cm. These differences were negligible, and only FAR_3 experienced a status degrade by underestimating five more centimeters. Since the changes in the error of the unknown points were small at all locations when the lateral distance changed to 520 cm, this model remained a viable estimation method for unknown points along the far edge.

Table 20: Comparison of the effect of the lateral distance between vehicles of 590 cm and 520 cm on the mean errors and standard deviations (in parentheses) of the estimated grain heights along the far edge in Situation 2 with a distance exponent of ten; yellow cells indicate the mean was inside the desired range but ±1 standard deviation extended beyond the range and green cells indicate the mean error ±1 standard deviation was completely contained by the desired accuracy range.

Grain Delivery Conditions			Cart Location						
Lateral Distance Between Vehicles	Filling Order	Number of Fill Zones	FAR_2 $\dot{\epsilon}_2(\sigma_{\epsilon_2})$ (cm)	FAR_3 $\dot{\epsilon}_3(\sigma_{\epsilon_2})$ (cm)	FAR_4 $\dot{\epsilon}_4(\sigma_{\epsilon_4})$ (cm)	FAR_5 $\dot{\epsilon}_5(\sigma_{\epsilon_5})$ (cm)	FAR_6 $\dot{\epsilon}_6(\sigma_{\epsilon_6})$ (cm)	FAR_7 $\dot{\epsilon}_7(\sigma_{\epsilon_7})$ (cm)	FAR_8 $\dot{\epsilon}_8(\sigma_{\epsilon_8})$ (cm)
590cm	F - M - B	3	7 (7) A	-4 (6) A	4 (6) A	-3 (8) A	3 (7) A	-10 (6) A	15 (7) A
520cm	F - M - B	3	9 (10) A	-9 (10) A	9 (5) A	-7 (6) A	6 (7) A	-11 (4) A	17 (4) A

5.3.2.2 Middle-Front-Back Filling Order

A test was conducted that changed the filling order of three fill zones from the control level of Front-Middle-Back to a Middle-Front-Back fill order, while maintaining the same distance exponent value of four. Changing the filling order to Middle-Front-Back showed no significant differences in the error of the estimated points at all seven locations along the far edge.

Table 21: Comparison of the effect of the filling order on the mean errors and standard deviations (in parentheses) of the estimated grain heights along the far edge in Situation 2 with a distance exponent of four; green cells indicate the mean error ±1 standard deviation was completely contained within the desired accuracy range.

Grain Delivery Conditions			Cart Location						
Lateral Distance Between Vehicles	Filling Order	Number of Fill Zones	FAR_2 $\dot{\epsilon}_2(\sigma_{\epsilon_2})$ (cm)	FAR_3 $\dot{\epsilon}_3(\sigma_{\epsilon_2})$ (cm)	FAR_4 $\dot{\epsilon}_4(\sigma_{\epsilon_4})$ (cm)	FAR_5 $\dot{\epsilon}_5(\sigma_{\epsilon_5})$ (cm)	FAR_6 $\dot{\epsilon}_6(\sigma_{\epsilon_6})$ (cm)	FAR_7 $\dot{\epsilon}_7(\sigma_{\epsilon_7})$ (cm)	FAR_8 $\dot{\epsilon}_8(\sigma_{\epsilon_8})$ (cm)
590cm	F - M - B	3	9 (6) A	-2 (7) A	6 (6) A	0 (8) A	5 (6) A	-7 (6) A	17 (7) A
590cm	M - F - B	3	6 (4) A	3 (5) A	6 (5) A	-2 (5) A	8 (3) A	-4 (6) A	18 (5) A

The largest difference in the mean error when the filling order changed was in FAR_3 at 5 cm. All differences were small enough to show this estimation model was not impacted by filling the grain cart in a different filling order. The only anomaly noticed from this test was the height of FAR_3 changed from being underestimated in the control level to being overestimated with a Middle-Front-Back filling order. This was probably because the first grain peak was located at FAR_5 instead of FAR_7. The grain sloped backward causing FAR_4 to be higher than FAR_3 while the middle and front

zones were filled. The estimated height of FAR_3 was not offset by the measurement at FAR_2 because of grain already in the bottom of the cart prior to the start of the test. The grain cart was partially loaded with grain prior to the start of a test so the desired fullness level could be achieved with a single combine hopper of grain. The change from being underestimated to overestimated would not likely happen when a cart starts out empty. This would be highly likely in the field if a grain cart was partially loaded by one combine, and it traveled to another combine before emptying at the edge of the field. In either scenario, the error measured in the estimated point did not change enough to show this model performed differently when the filling order changed.

All points along the far edge produced a mean error ±1 standard deviation that was completely contained within the desired accuracy range (Table 21). The worst accuracy occurred at points that did not directly receive grain. These points were overestimated by 6-18 cm, while points that did receive grain had mean errors slightly above and slightly below zero (-4 cm to +3 cm). This indicated a distance exponent of four was probably tuned to estimate peak points best (FAR_3, FAR_5, and FAR_7), while the points at the valleys experienced overestimation due to points in the delivery area maintained a small influence on the estimated values.

A test of the Middle-Front-Back filling order was repeated with a distance exponent of ten. Changing the filling order to Middle-Front-Back showed no significant changes in the error of the estimated points at all seven locations in the grain delivery area. The same anomaly at FAR_3 was present as in the previous table but to a lesser degree. The unknown point at FAR_3 was underestimated in the control sample by 4 cm, but it reached a mean error of zero under the different filling order. The effect was probably present to a lesser degree because there was less weight placed on the known points in the delivery area where the height difference from point to point was greater. Since the error of the estimated points experienced small changes when the filling order switched to Middle-Front-Back, this model remained a viable estimation method for unknown points along the far edge.

Table 22: Comparison of the effect of the filling order on the mean errors and standard deviations (in parentheses) of the estimated grain heights along the far edge in Situation 2 with a distance exponent of ten; yellow cells indicate the mean was inside the desired range but ±1 standard deviation extended beyond the range and green cells indicate the mean error ±1 standard deviation was completely contained by the desired accuracy range.

Grain Delivery Conditions			Cart Location						
Lateral Distance Between Vehicles	Filling Order	Number of Fill Zones	FAR_2 $\dot{\epsilon_2}(\sigma_{\epsilon_2})$ (cm)	FAR_3 $\dot{\epsilon_3}(\sigma_{\epsilon_2})$ (cm)	FAR_4 $\dot{\epsilon_4}(\sigma_{\epsilon_4})$ (cm)	FAR_5 $\dot{\epsilon_5}(\sigma_{\epsilon_5})$ (cm)	FAR_6 $\dot{\epsilon_6}(\sigma_{\epsilon_6})$ (cm)	FAR_7 $\dot{\epsilon_7}(\sigma_{\epsilon_7})$ (cm)	FAR_8 $\dot{\epsilon_8}(\sigma_{\epsilon_8})$ (cm)
590cm	F - M - B	3	7 (7) A	-4 (6) A	4 (6) A	-3 (8) A	3 (7) A	-10 (6) A	15 (7) A
590cm	M - F - B	3	1 (4) A	0 (5) A	3 (5) A	-6 (5) A	5 (4) A	-8 (6) A	13 (7) A

The accuracy of FAR_7 was the only point that changed accuracy categories using the Middle-Front-Back filling order; it improved from a yellow status to a green status (Table 22). The mean error at this point improved by 2 cm, and the variation did not change. The accuracy of points along the far edge was not expected to improve when the filling order changed, and a 2 cm improvement was not significant enough to claim an improvement had occurred. The largest mean error was expected at the front or back of the fill grid, and FAR_8 was the least accurate with a mean overestimation of 13 cm. The error at this point met and exceeded the desired accuracy of the model so the higher magnitude of error at the front was not investigated further.

5.3.2.3 Seven Fill Zones

A test was conducted that changed the number of fill zones the cart was divided into from the control level of three zones to seven zones using four as the distance weighing exponent. Changing the number of fill zones from three to seven showed a significant impact in the error of the estimated unknown point FAR_8; no significant impact was detected in the other columns. FAR_8 showed a difference in the error because it was not a delivery location in the control subset with three fill zones. The estimate of FAR_8 was highly dependent on the measured height of FAR_7 in the control subset and the subset with seven zones. The subset with seven zones filled FAR_8 to the same height as FAR_7 so the overestimation was expected to be smaller. The reason a difference was not detected at FAR_2 was unknown because FAR_2 was expected to show the same results as FAR_8. The discrepancy could have been caused by the back being the last part to be filled, and the conditions of the cart at the start of some tests placed a peak under FAR_3. This would cause FAR_2 to be overestimated for fill grids collected before the back of the cart was filled. The model overestimated the grain height at every point along the far edge when seven fill zones were used. This was expected because every location was filled to the same level, but the distance exponent

was small enough to allow sufficient influence from the middle row of known points to increase the value of the model's estimates.

Table 23: Comparison of the effect of 3 fill zones and 7 fill zones on the mean errors and standard deviations (in parentheses) of the estimated grain heights along the far edge in Situation 2 with a distance exponent of ten; green cells indicate the mean error ±1 standard deviation was completely contained by the desired accuracy range.

Grain Delivery Conditions			Cart Location						
Lateral Distance Between Vehicles	Filling Order	Number of Fill Zones	FAR_2 $\dot{\epsilon}_2(\sigma_{\epsilon_2})$ (cm)	FAR_3 $\dot{\epsilon}_3(\sigma_{\epsilon_2})$ (cm)	FAR_4 $\dot{\epsilon}_4(\sigma_{\epsilon_4})$ (cm)	FAR_5 $\dot{\epsilon}_5(\sigma_{\epsilon_5})$ (cm)	FAR_6 $\dot{\epsilon}_6(\sigma_{\epsilon_6})$ (cm)	FAR_7 $\dot{\epsilon}_7(\sigma_{\epsilon_7})$ (cm)	FAR_8 $\dot{\epsilon}_8(\sigma_{\epsilon_8})$ (cm)
590cm	F - M - B	3	9 (6) A	-2 (7) A	6 (6) A	0 (8) A	5 (6) A	-7 (6) A	17 (7) A
590cm	F - M - B	7	9 (9) A	4 (7) A	8 (7) A	2 (6) A	6 (6) A	2 (7) A	2 (8) B

The mean error ±1 standard deviation fell within the desired accuracy range at all points along the far edge (Table 23). Model performance with seven fill zones was expected to be well within the desired range based on the analysis completed in the grain delivery area with seven fill zones. The largest magnitude mean error was FAR_2 at 9 cm, but this was not significant in the context of the filling a grain cart.

A test with seven fill zones was repeated with a distance exponent of ten. Changing the number of fill zones from three to seven showed a significant impact in the error of the estimating at FAR_8; no significant impact was detected in the other points. FAR_8 showed a difference in the error of the estimate for the same reason as the previous analysis. FAR_8 was not a delivery location in the control subset with three fill zones. The reason the same difference did not appear FAR_2 was unknown, but it could have been caused by the back being the last zone to be filled. The magnitude of the mean error at each location decreased or stayed the same compared to the control sample because each point received grain and was filled to the same level (Table 24). The estimation errors were positive and negative but did not show the alternating pattern present when three fill zones were used. The mean errors ±1 standard deviation of all points along the far edge were well within the acceptable accuracy limits. The mean error was -3 cm to +3 cm which was not significant in the context of the grain cart. The model's performance with seven fill zones appeared to be highly robust with standard deviations of 7-9 cm.

Table 24: Comparison of the effect of 3 fill zones and 7 fill zones on the mean errors and standard deviations (in parentheses) of the estimated grain heights along the far edge in Situation 2 with a distance exponent of ten; yellow cells indicate the mean was inside the desired range but ±1 standard deviation extended beyond the range and green cells indicate the mean error ±1 standard deviation was completely contained by the desired accuracy range.

Grain Delivery Conditions			Cart Location						
Lateral Distance Between Vehicles	Filling Order	Number of Fill Zones	FAR_2 $\bar{\epsilon}_2\ (\sigma_{\epsilon_2})$ (cm)	FAR_3 $\bar{\epsilon}_3\ (\sigma_{\epsilon_3})$ (cm)	FAR_4 $\bar{\epsilon}_4(\sigma_{\epsilon_4})$ (cm)	FAR_5 $\bar{\epsilon}_5\ (\sigma_{\epsilon_5})$ (cm)	FAR_6 $\bar{\epsilon}_6(\sigma_{\epsilon_6})$ (cm)	FAR_7 $\bar{\epsilon}_7(\sigma_{\epsilon_7})$ (cm)	FAR_8 $\bar{\epsilon}_8(\sigma_{\epsilon_8})$ (cm)
590cm	F - M - B	3	7 (7) A	-4 (6) A	4 (6) A	-3 (8) A	3 (7) A	-10 (6) A	15 (7) A
590cm	F - M - B	7	3 (9) A	-1 (7) A	3 (7) A	-3 (7) A	2 (7) A	-2 (7) A	-3 (8) B

5.3.3 Situation 3 Modeling

Situation 3 was included to analyze the ability to estimate points that would become occluded from the field of view of a vision sensor. The data in Table 25 was produced using the combined delivery conditions of the four data subsets. The unknown location in the delivery area (MID_5) was extremely underestimated when the distance exponent was zero, but the estimated value increased with the distance exponent to a satisfactory level. The standard deviation of the error of MID_5 decreased slightly as the distance exponent increased. A significant impact from the distance exponent was detected at a value of zero and one due to the estimates being grossly underestimated. This behavior was expected because the estimation of MID_5 was being influenced by known points along the near and far edge. When the distance exponent increased, MID_5 was nearly completely based on the two neighboring points in the delivery area. Since the mean error as the distance exponent got large was -7 cm. If the point in the delivery location chosen to analyze in this situation was a valley, the mean error would likely have been +7 cm.

Table 25: Mean errors and standard deviations (in parentheses) of the estimated grain heights at the four points tested in Situation 3 for the range of distance exponents tested; the lowest magnitude mean errors at each location are highlighted in blue.

	Cart Location				All Locations	
Distance Weighting Exponent	MID_5 $\bar{\epsilon}_{MID_5}\ (\sigma_{\epsilon_{MID_5}})$ (cm)	FAR_4 $\bar{\epsilon}_{FAR_4}\ (\sigma_{\epsilon_{FAR_4}})$ (cm)	FAR_5 $\bar{\epsilon}_{FAR_5}\ (\sigma_{\epsilon_{FAR_5}})$ (cm)	FAR_6 $\bar{\epsilon}_{FAR_6}\ (\sigma_{\epsilon_{FAR_6}})$ (cm)	$\overline{\lvert\bar{\epsilon}_{j,\dots}\rvert}$ (cm)	$\sigma_{\bar{\epsilon}_{j,\dots}}$ (cm)
0	-44 (11) A	6 (18) A	-1 (18) A	0 (16) A	13	16
1	-37 (10) A	9 (15) A	4 (17) A	6 (13) A	14	14
2	-27 (9) AB	10 (11) A	8 (15) A	10 (10) A	14	11
3	-18 (9) B	8 (9) A	11 (14) A	10 (7) A	12	10
4	-13 (9) B	6 (10) A	12 (13) A	9 (6) A	10	9
5	-10 (9) B	4 (10) A	12 (12) A	7 (7) A	8	9
6	-9 (9) B	3 (11) A	12 (11) A	6 (7) A	8	9
7	-8 (9) B	3 (11) A	11 (11) A	6 (7) A	7	9
8	-8 (9) B	2 (11) A	11 (11) A	6 (7) A	7	9
9	-7 (9) B	2 (11) A	10 (10) A	6 (7) A	6	9
10	-7 (9) B	2 (11) A	9 (10) A	6 (7) A	6	9

The estimation of three points along the far edge started highly accurate with mean errors within 6 cm of perfect, but their standard deviations were more than 15 cm. The high accuracy was a coincidence of the dataset, and not likely to occur with other datasets at this value of the distance exponent. The high variation occurred because equal weight was given to known points in the fill grid without regard from the distance to the point being estimated. As the distance exponent increased, the mean errors increased until local maxima were reached for all three points between the values of two and five for the distance exponent. Beyond a distance exponent of five, the magnitude of the error decreased to a suitable level. Although the standard deviation started high and continued decreasing as the distance exponent increased, the standard deviation remained high at these points because there were fewer known points close by in the fill grid to obtain a stable estimation. Ignoring the error when the distance exponent was zero or one, the lowest mean error was experienced at the highest distance exponent. Averaging the absolute values of the mean errors across all estimated points was used to determine the distance exponent that produced the most accurate general estimates (second column from the right in Table 25). The average absolute value of the mean error decreased as the distance exponent increased, reinforcing the conclusion that the most accurate model for estimating the delivery location and nearby points along the far edge was to use a large distance exponent.

The mean errors of MID_5 with a distance exponent greater than three were within the target accuracy range (Table 26). Within the range of distance exponents tested, the mean error ±1 standard deviation was never completely contained in the desired accuracy range. The mean errors of FAR_5 and FAR_6 were best when the distance exponent was zero, but the high variability of the error did not allow these estimates to fall under the best accuracy category.

Table 26: Mean errors and standard deviations (in parentheses) of the estimated grain heights at the four points tested in Situation 3 for the range of distance exponents tested; red cells indicate the mean error was outside the desired accuracy range, yellow cells indicate the mean was inside the desired range but ±1 standard deviation extended beyond the range, and green cells indicate the mean error ±1 standard deviation was completely contained by the desired accuracy range.

	Cart Location				All Locations	
Distance Weighting Exponent	MID_5 $\bar{\epsilon}_{MID_5}$ $(\sigma_{\epsilon_{MID_5}})$ (cm)	FAR_4 $\bar{\epsilon}_{FAR_4}$ $(\sigma_{\epsilon_{FAR_4}})$ (cm)	FAR_5 $\bar{\epsilon}_{FAR_5}$ $(\sigma_{\epsilon_{FAR_5}})$ (cm)	FAR_6 $\bar{\epsilon}_{FAR_6}$ $(\sigma_{\epsilon_{FAR_6}})$ (cm)	$\overline{\lvert\bar{\epsilon}_{j,\dots}\rvert}$ (cm)	$\bar{\sigma}_{\epsilon_{j,\dots}}$ (cm)
0	-44 (11) A	6 (18) A	-1 (18) A	0 (16) A	13	16
1	-37 (10) A	9 (15) A	4 (17) A	6 (13) A	14	14
2	-27 (9) AB	10 (11) A	8 (15) A	10 (10) A	14	11
3	-18 (9) B	8 (9) A	11 (14) A	10 (7) A	12	10
4	-13 (9) B	6 (10) A	12 (13) A	9 (6) A	10	9
5	-10 (9) B	4 (10) A	12 (12) A	7 (7) A	8	9
6	-9 (9) B	3 (11) A	12 (11) A	6 (7) A	8	9
7	-8 (9) B	3 (11) A	11 (11) A	6 (7) A	7	9
8	-8 (9) B	2 (11) A	11 (11) A	6 (7) A	7	9
9	-7 (9) B	2 (11) A	10 (10) A	6 (7) A	6	9
10	-7 (9) B	2 (11) A	9 (10) A	6 (7) A	6	9

FAR_4 also experienced a minimum error at zero, but its mean error reached a lower value when the distance exponent was greater than four. FAR_5 experienced more overestimation error than FAR_4 and FAR_6 because the model shifted more weight to points in the delivery area. The closest points to FAR_5 along the far edge (2 cell widths) were nearly the same distance away as points in the delivery area (2.2 cell widths). Similar distances to points along the far edge and points in the delivery area also explained why the mean error of FAR_5 did not appear to reach steady-state when the distance exponent reached a value of ten. The inverse distance weighting model appeared to perform best when the distance exponent was large so tests were setup with the distance exponent at that value that compared accuracy under diverse grain delivery conditions.

5.3.3.1 520 cm Lateral Distance between Vehicles

A test was conducted with the lateral distance between the combine and the grain cart reduced from 590 cm to 520 cm (Table 27). Changing the lateral distance from 590 cm to 520 cm showed no significant differences in the error of the estimated points. The mean error increased at FAR_4, decreased at MID_5 and FAR_5, and stayed neutral at FAR_6. Changes in the mean error at these points were less than 10 cm.

Table 27: Comparison of the effect of the lateral distance between vehicles of 590 cm and 520 cm on the mean errors and standard deviations (in parentheses) of the estimated grain heights at the four points tested in Situation 3 with a distance exponent of ten; yellow cells indicate the mean was inside the desired range but ±1 standard deviation extended beyond the range and green cells indicate the mean error ±1 standard deviation was completely contained by the desired accuracy range.

Grain Delivery Conditions			Cart Location			
Lateral Vehicle Distance	Filling Order	Number of Fill Zones	MID_5 $\dot{\epsilon}_2\,(\sigma_{\dot{\epsilon}_2})$ (cm)	FAR_4 $\dot{\epsilon}_3\,(\sigma_{\dot{\epsilon}_2})$ (cm)	FAR_5 $\dot{\epsilon}_4\,(\sigma_{\dot{\epsilon}_4})$ (cm)	FAR_6 $\dot{\epsilon}_5\,(\sigma_{\dot{\epsilon}_5})$ (cm)
590cm	F - M - B	3	-5 (11) A	1 (12) A	10 (11) A	6 (6) A
520cm	F - M - B	3	-10 (6) A	9 (10) A	2 (7) A	6 (7) A

The standard deviation decreased in three of the points. This was believed to be a result of the points along the far edge and in the delivery area being at similar elevations because grain was delivered about halfway between the rows of sensors. The mean error at all points was within the accuracy goal of -15 cm to +25 cm. Points along the far edge included ±1 standard deviation within the accuracy range. The estimation of MID_5 was expected to be less accurate than the estimations of points along the far edge because of the results observed in Situation 1 and Situation 2.

5.3.3.2 Middle-Front-Back Filling Order

Changing the filling order to Middle-Front-Back showed no significant changes in the error of all four estimated points. The MID_5 was underestimated in the control subset and the Middle-Front-Back subset (Table 28). This was expected based on the results of previous sections for points that directly received grain. The far edge points were overestimated or had a mean error of zero in both data sets because fewer points were known along the far edge to calculate an estimate. The mean of all estimated points were within the target range so the model's performance was confirmed with the Middle-Front-Back filling order as expected.

Table 28: Comparison of the effect of the filling order on the mean errors and standard deviations (in parentheses) of the estimated grain heights at the four points tested in Situation 3 with a distance exponent of ten; yellow cells indicate the mean was inside the desired range but ±1 standard deviation extended beyond the range and green cells indicate the mean error ±1 standard deviation was completely contained by the desired accuracy range.

Grain Delivery Conditions			Cart Location			
Lateral Vehicle Distance	Filling Order	Number of Fill Zones	MID_5 $\dot{\epsilon}_2\,(\sigma_{\dot{\epsilon}_2})$ (cm)	FAR_4 $\dot{\epsilon}_3\,(\sigma_{\dot{\epsilon}_2})$ (cm)	FAR_5 $\dot{\epsilon}_4\,(\sigma_{\dot{\epsilon}_4})$ (cm)	FAR_6 $\dot{\epsilon}_5\,(\sigma_{\dot{\epsilon}_5})$ (cm)
590cm	F - M - B	3	-5 (11) A	1 (12) A	10 (11) A	6 (6) A
590cm	M - F - B	3	-13 (5) A	0 (9) A	9 (8) A	3 (6) A

5.3.3.3 Seven Fill Zones

Changing the number of fill zones from three to seven did not show a significant impact on the error of the estimated points. In previous modeling situations when seven fill zones were used, a significant impact was detected at FAR_2 and FAR_8, but these locations did not comprise the points being analyzed (Table 29). A significant difference was expected to be found if FAR_2 or FAR_8 had been included in this test.

Table 29: Comparison of the effect of 3 fill zones and 7 fill zones on the mean errors and standard deviations (in parentheses) of the estimated grain heights at the four points tested in Situation 3 with a distance exponent of ten; yellow cells indicate the mean was inside the desired range but ±1 standard deviation extended beyond the range and green cells indicate the mean error ±1 standard deviation was completely contained by the desired accuracy range.

Grain Delivery Conditions			Cart Location			
Lateral Vehicle Distance	Filling Order	Number of Fill Zones	MID_5 $\dot{\epsilon_2}\,(\sigma_{\dot{\epsilon_2}})$ (cm)	FAR_4 $\dot{\epsilon_3}\,(\sigma_{\dot{\epsilon_2}})$ (cm)	FAR_5 $\dot{\epsilon_4}\,(\sigma_{\dot{\epsilon_4}})$ (cm)	FAR_6 $\dot{\epsilon_5}\,(\sigma_{\dot{\epsilon_5}})$ (cm)
590cm	F - M - B	3	-5 (11) A	1 (12) A	10 (11) A	6 (6) A
590cm	F - M - B	7	-2 (7) A	-1 (9) A	15 (7) A	7 (10) A

The mean error ±1 standard deviation was completely within the desired accuracy range for all points estimated in this test. The previous tests placed MID_5 in the yellow accuracy category, but MID_5 was expected to be more accurate when seven fill zones were used based on results from previous sections. FAR_5 was also expected to be more accurate, but its mean error was overestimated by an extra 5 cm. This occurred because the closest known points along the far edge were slightly closer than the closest known points in the delivery area. In previous tests the closet known points to FAR_5 in the delivery area (MID_4 and MID_6) were valleys of the three fill zones, but in this test those points were also peaks. Although the mean error increased at FAR_5, the mean errors of all points met the accuracy goal and the model and did not show a significant affect when more zones were used. The model was validated to perform consistently whether three or seven fill zones were used to fill the cart.

5.3.4 Situation 4 Modeling

It was important to include Situation 4 in the modeling analysis so the case when the entire far row of data points was missing could be evaluated. The data in Table 30 was produced using the combined delivery conditions of the four data subsets. All estimated points along the far edge showed the same behavior. The error in the estimated value was most accurate based on the mean error of each point when the distance exponent was zero. As the exponent increased, the

overestimation of the unknown points increased. A ceiling in the error was approached as the distance exponent increased.

Table 30: Mean errors and standard deviations (in parentheses) of the estimated grain heights in Situation 4 at each column of the fill grid for the range of distance exponents tested; the lowest magnitude mean errors for each column are highlighted in blue.

	Cart Location						
Distance Weighting Exponent	FAR_2 $\dot{\epsilon_2}$ (σ_{ϵ_2}) (cm)	FAR_3 $\dot{\epsilon_3}$ (σ_{ϵ_2}) (cm)	FAR_4 $\dot{\epsilon_4}$(σ_{ϵ_4}) (cm)	FAR_5 $\dot{\epsilon_5}$ (σ_{ϵ_5}) (cm)	FAR_6 $\dot{\epsilon_6}$(σ_{ϵ_6}) (cm)	FAR_7 $\dot{\epsilon_7}$(σ_{ϵ_7}) (cm)	FAR_8 $\dot{\epsilon_8}$(σ_{ϵ_8}) (cm)
0	10 (23) A	4 (26) A	7 (21) A	0 (22) A	1 (20) A	-4 (23) A	7 (20) A
1	15 (22) A	10 (26) A	13 (21) A	7 (22) A	10 (20) AB	5 (22) A	15 (19) A
2	20 (21) A	17 (25) A	20 (21) A	15 (22) A	19 (19) AB	15 (21) A	25 (18) A
3	25 (21) A	22 (25) A	26 (21) A	21 (21) A	27 (19) AB	23 (21) A	33 (18) A
4	28 (21) A	26 (25) A	31 (21) A	27 (21) A	33 (19) AB	29 (21) A	38 (17) A
5	30 (21) A	29 (25) A	34 (21) A	30 (21) A	37 (19) AB	32 (20) A	40 (17) A
6	31 (21) A	30 (25) A	35 (21) A	32 (21) A	39 (19) AB	34 (20) A	42 (17) A
7	31 (21) A	31 (25) A	36 (21) A	34 (21) A	41 (19) B	35 (20) A	42 (17) A
8	31 (22) A	32 (25) A	37 (21) A	34 (21) A	41 (19) B	36 (20) A	42 (17) A
9	30 (22) A	32 (25) A	37 (21) A	35 (21) A	42 (19) B	37 (20) A	42 (17) A
10	30 (22) A	32 (25) A	37 (21) A	35 (21) A	42 (19) B	37 (20) A	42 (17) A

The standard deviation of the error started large and decreased slightly, but it remained larger than the situations that were modeled. It was expected for the points along the far edge to be overestimated because these points were located at the spatial edge of the data set. When using the inverse distance method to estimate points at the edge of a data set, the values of the estimated points reached a ceiling nearly equal to the value of the closest point(s) in the spatial data set. Isaaks and Srivastava (1989) state the inverse distance weighting method should not be used to estimate unknown points in a spatial data set outside the area where points are known. The governing equation of the inverse distance weighting method does not extrapolate beyond known points. Its estimates reach a ceiling or floor that never exceeds the value of the closest known point.

The mean error of the estimated points along the far edge were within the target range when the distance weighting exponent was zero or one, but the standard deviation was very high (Table 31). An acceptable range was not specified for the standard deviation of the error, but the standard deviations of 20-30 cm were too much variability in the estimated points for adequate the decision support structure to perform adequately. This test showed the inverse distance weighting model with any exponent failed to adequately estimate unknown points along the far edge when all points along the far edge are simultaneously unknown.

Table 31: Mean errors and standard deviations (in parentheses) of the estimated grain heights in Situation 4 at each point in along the far edge for the range of distance exponents tested; red cells indicate the mean error was outside the desired accuracy range and yellow cells indicate the mean was inside the desired range but ±1 standard deviation extended beyond the range.

Distance Weighting Exponent	Cart Location						
	FAR_2 $\dot{\epsilon_2}(\sigma_{\epsilon_2})$ (cm)	FAR_3 $\dot{\epsilon_3}(\sigma_{\epsilon_2})$ (cm)	FAR_4 $\dot{\epsilon_4}(\sigma_{\epsilon_4})$ (cm)	FAR_5 $\dot{\epsilon_5}(\sigma_{\epsilon_5})$ (cm)	FAR_6 $\dot{\epsilon_6}(\sigma_{\epsilon_6})$ (cm)	FAR_7 $\dot{\epsilon_7}(\sigma_{\epsilon_7})$ (cm)	FAR_8 $\dot{\epsilon_8}(\sigma_{\epsilon_8})$ (cm)
0	10 (23) A	4 (26) A	7 (21) A	0 (22) A	1 (20) A	-4 (23) A	7 (20) A
1	15 (22) A	10 (26) A	13 (21) A	7 (22) A	10 (20) AB	5 (22) A	15 (19) A
2	20 (21) A	17 (25) A	20 (21) A	15 (22) A	19 (19) AB	15 (21) A	25 (18) A
3	25 (21) A	22 (25) A	26 (21) A	21 (21) A	27 (19) AB	23 (21) A	33 (18) A
4	28 (21) A	26 (25) A	31 (21) A	27 (21) A	33 (19) AB	29 (21) A	38 (17) A
5	30 (21) A	29 (25) A	34 (21) A	30 (21) A	37 (19) AB	32 (20) A	40 (17) A
6	31 (21) A	30 (25) A	35 (21) A	32 (21) A	39 (19) AB	34 (20) A	42 (17) A
7	31 (21) A	31 (25) A	36 (21) A	34 (21) A	41 (19) B	35 (20) A	42 (17) A
8	31 (22) A	32 (25) A	37 (21) A	34 (21) A	41 (19) B	36 (20) A	42 (17) A
9	30 (22) A	32 (25) A	37 (21) A	35 (21) A	42 (19) B	37 (20) A	42 (17) A
10	30 (22) A	32 (25) A	37 (21) A	35 (21) A	42 (19) B	37 (20) A	42 (17) A

5.3.5 Evaluating Different Estimation Model Parameters

Investigation into which distance exponent produced the best model was conducted. Overall, the smallest magnitude of error when estimating an unknown point in the grain delivery area or along the far edge with any distance exponent and delivery condition was with seven fill zones and a distance exponent of ten. This indicated the inverse distance weighting method of modeling was best suited for modeling missing points when the grain delivery was dispersed evenly in the cart or rough field conditions did not allow peaks to form. There was no significant impact to this model's performance when the lateral distance between vehicles changed or the order in which the zones of the cart were filled because neither of these delivery conditions changed the shape of the surface profile along the middle row of the cart. A significant impact was only detected when the cart was filled with seven fill zones because the shape of the grain profile had seven peaks instead of nine. The significant impact improved the accuracy of the estimation in those scenarios.

The absolute value of the mean error of the estimated unknown point was averaged across all points that were tested for each level of the distance exponent. This number was used as a summary statistic to evaluate the accuracy of each model, where small numbers were more accurate and large numbers were less accurate. The most accurate model that estimated unknown points in the grain delivery area had an exponent of four. The most accurate estimation model along the far edge had a distance exponent of ten. The most accurate distance exponent when

points in the middle and far rows were unknown at the same time was also ten. The fourth situation was not considered because the inverse distance model failed under all exponent values.

The standard deviation was also averaged across all points that were tested for each level of the distance exponent. This number was used to qualitatively gauge the precision of each model. In the first modeling situation, the standard deviation started out very high and reached a local minimum when the distance exponent was four. The standard deviation increased slightly for distance exponents larger than four. This trend was true for estimations in the delivery area and for estimations along the far edge in the second situation. The averaged standard deviation was always decreasing as the distance exponent increased in the third situation.

Another summary statistic was created by adding the two previous summary statistics together (absolute value of the mean error averaged across all points in the cart and the standard deviation of each point averaged across the length of the cart). This index roughly represented the maximum absolute value of the mean error of the estimated points averaged across all points being modeled in a situation. The purpose of this index was to qualitatively evaluate which estimation model was the best for this application. The index was plotted over the range of distance weighting exponents tested in the modeling situations (Figure 45). The curves for Situations 1-3 showed the highest index value when the exponent was zero followed by a decrease in the index value as the distance exponent increased. The index reached a local minimum around a distance exponent of four in the first two situations and increased very slightly as the exponent increased. Situation 3 saw the index value decrease constantly through the tested range.

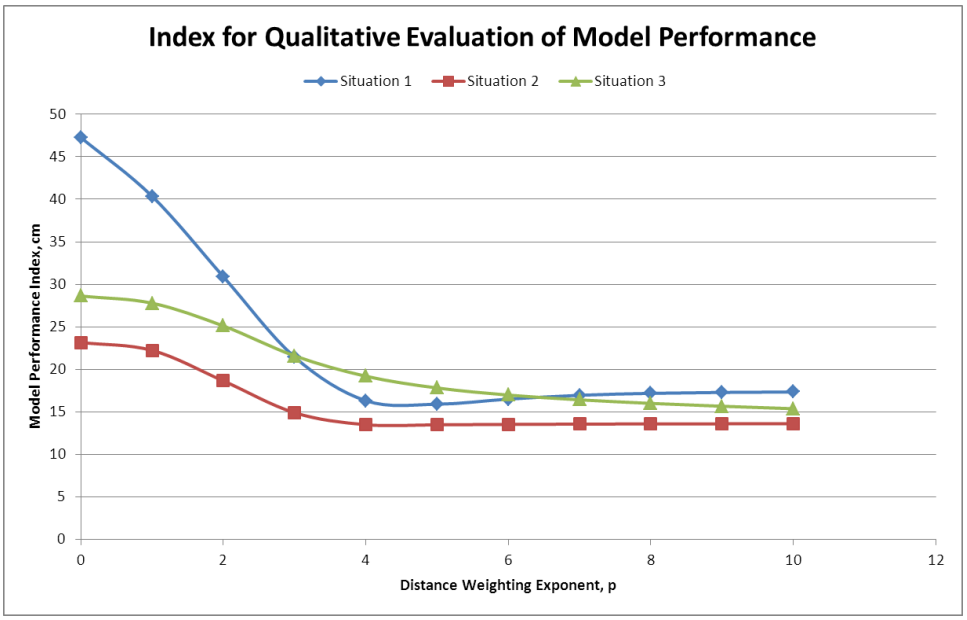

Figure 45: Index for qualitative evaluation of the inverse distance weighting model of the situations modeled

The best model for estimating points in the fill grid of a grain cart when values become unknown was found to be the inverse distance weighting method with a distance exponent of ten. This model was chosen because the mean index value across the three situations was smallest at ten and there was the smallest risk of experiencing a significant change in the index value if the shape of the index curves changed slightly. If a distance exponent of four was chosen and the local minima of Situations 1 and 2 shifted to the right, the plot indicates the error of the estimation model could increase substantially. The shape of the curves was likely influenced by environmental factors, such as rough and smooth terrain. A different crop type, such as rice, that has a larger angle of repose than most crops could also shift the local minimum so choosing a model with a high distance exponent was expected to reduce risks associated with different environments.

5.4 Summary and Conclusions

During this experiment, the inverse distance weighting model was used to estimate four situations where points in a fill grid commonly became unknown. The first situation was modeling a single point in the grain delivery area. It experienced mean errors in the estimates of unknown points ranging from -46 cm to +15 cm and a standard deviation of 7 cm to 16 cm. The distance exponent of the model was limited to a value of ten, and the ranges shrank to -8 cm to +15 cm for the mean error and 6 cm to 11 cm for the standard deviation. The mean errors were within the goal

of -15 cm to +25 cm. The value of the distance exponent was responsible for the most significant effects on the mean error and standard deviation. The height differences of the peaks and valleys between fill zones contributed to the remaining overestimation and underestimation errors. The number of fill zones was the only delivery conditions to have a significant impact on the model's ability consistently estimate unknown points. The impact of using seven fill zones improved the accuracy of the model.

The second situation involved modeling a single point along the far edge of the cart. It experienced mean errors from -8 cm to +16 cm and a standard deviation of 6 cm to 21 cm. When the distance exponent was limited to a value of ten, the ranges shrank to -8 cm to +11 cm for the mean error and 6 cm to 11 cm for the standard deviation. The mean errors were within the goal of -15 cm to +25 cm. The value of the distance exponent was responsible for the most significant effect on the mean error of the estimates and the standard deviation of the error of the estimates. Peaks and valleys between fill zones were responsible for the remaining range in the mean error. The standard deviation was consistent regardless of whether a point was a peak or valley. The number of fill zones was the only delivery conditions to have a significant impact on the model's ability consistently estimate unknown points. Like the previous modeling situation, the impact of using seven fill zones improved the accuracy at locations where a significant difference was detected.

The third situation required modeling four unknown points in the fill grid at the same time. One point was in the grain delivery area, and the others were the closest three points along the far edge. The mean error of the point in the delivery area ranged from -44 cm to -7 cm and a standard deviation of 9 cm to 11 cm. The mean error of the points along the far edge ranged from -1 cm to +12 cm with a standard deviation of 6 cm to 18 cm. When the distance exponent was limited to ten, the middle point was under estimated by 7 cm and had a standard deviation of 9 cm. The mean error of the far edge points was +2 cm to +9 cm with a standard deviation of 7 cm to 11 cm.

The fourth situation involved modeling all the points along the far edge simultaneously. The inverse distance weight model failed to meet the accuracy goal of -15 cm to +25 cm at all locations, regardless of the value of the distance exponent. The best accuracy was achieved with an exponent of zero, but the variation was extremely high. The points were overestimated by 30 cm to 42 cm with a standard deviation of 17 cm to 22 cm.

An Estimation Model Index was formed to evaluate distance exponent values against each other. Using the results of Situations 1-3, the model with the best accuracy was achieved when the distance exponent was at the highest value tested in this research.

Chapter 6 Grain Weight Estimation

6.1 Introduction

The objective of this phase of the research was to quantify the impact of sensor placement and grain delivery conditions on the ability to calculate the weight of grain in a grain cart. The average grain height measured by the ultrasonic sensors was expected to be a robust and accurate predictor of the weight against different sensor configurations and delivery conditions due to the high number points available to calculate the average grain height.

6.2 Materials and Methods

Of the 5x9 fill grid used in the previous chapters, only 21 cells possessed dedicated sensors. The cells without a sensor were modeled deterministically by using a constant offset from a neighboring cell that did have a dedicated sensor. Offset values were determined experimentally during preliminary testing. Figure 46 shows a completed fill grid with the modeled cells. Cells with orange and red blocks were calculated using the blocks at the tail of the arrows. The value inside each red and orange block is the number of centimeters added to the source block to estimate the grain height. For example, if the measured grain height by Sensor 1 (top-left) was -20 cm, the estimated height of the cell to the left would be -30 cm.

A deterministic model was used to describe cells without a dedicated sensor instead of a statistical model, such as inverse distance weighting, because cell values in the first and last columns of the fill grid would involve extrapolation. Several texts have dismissed extrapolation as an appropriate application of inverse distance weighting. This conclusion was also made in the previous chapter.

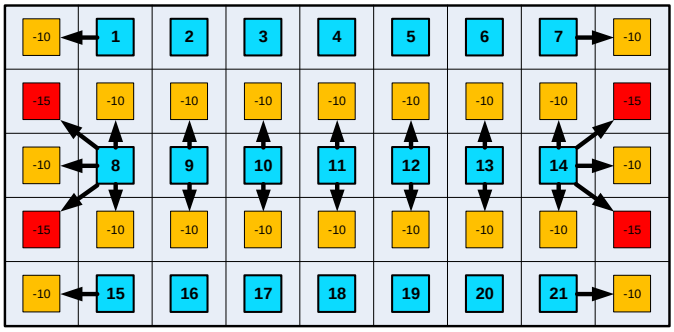

Figure 46: Fill grid depicting how cells that do not have a dedicated sensor are calculated

The simple deterministic modeling technique was used to fill in the remaining 24 cells of the fill grid for all tests. A more advanced model was not developed to estimate these points because the most important values to estimate in the fill grid were the sensor height readings. They were the only points which reflected known grain heights.

6.2.1 Sensor Configuration

Three sensor configurations were tested to investigate the effect of sensor placement on the ability to accurately predict the weight of grain in a cart. Each method used the average height of cells of specific columns of the fill grid to calculate the average grain height:

1. Columns 2-8 (Figure 47)
2. Columns 3, 5, and 7 (Figure 48)
3. Columns 2, 4, 6, and 8 (Figure 49)

Fill Grid	-57	-47	-40	-55	-43	-48	-37	-51	-61
	-46	-41	-29	-37	-29	-38	-30	-43	-48
	-41	-31	-19	-27	-19	-28	-20	-33	-43
	-46	-41	-29	-37	-29	-38	-30	-43	-48
	-98	-88	-82	-86	-79	-75	-80	-83	-93
Column Average	-58	-50	-40	-49	-40	-45	-40	-51	-59
Cart Average	-45								

Figure 47: Example grain heights in centimeters of a fill grid, column averages, and cart average where Columns 2-8 were used to calculate the average grain height of the cart

Fill Grid	-57	-47	**-40**	-55	**-43**	-48	**-37**	-51	-61
	-46	-41	**-29**	-37	**-29**	-38	**-30**	-43	-48
	-41	-31	**-19**	-27	**-19**	-28	**-20**	-33	-43
	-46	-41	**-29**	-37	**-29**	-38	**-30**	-43	-48
	-98	-88	**-82**	-86	**-79**	-75	**-80**	-83	-93
Column Average	-58	-50	**-40**	-49	**-40**	-45	**-40**	-51	-59
Cart Average	**-40**								

Figure 48: Example grain heights in centimeters of a fill grid, column averages, and cart average where Columns 3, 5, and 7 were used to calculate the average grain height of the cart

Fill Grid	-57	**-47**	-40	**-55**	-43	**-48**	-37	**-51**	-61
	-46	**-41**	-29	**-37**	-29	**-38**	-30	**-43**	-48
	-41	**-31**	-19	**-27**	-19	**-28**	-20	**-33**	-43
	-46	**-41**	-29	**-37**	-29	**-38**	-30	**-43**	-48
	-98	**-88**	-82	**-86**	-79	**-75**	-80	**-83**	-93
Column Average	-58	**-50**	-40	**-49**	-40	**-45**	-40	**-51**	-59
Cart Average	**-48**								

Figure 49: Example grain heights in centimeters of a fill grid, column averages, and cart average where Columns 2, 4, 6, and 8 were used to calculate the average grain height of the cart

Each method used a different number of cells to calculate the average grain height in the cart. This was done to determine the minimum resolution of the fill grid that could be used before the variation in the predicted grain weight showed a significant change. The second and third methods used the locations of the peaks and valleys, respectively, of fill zones when three fill zones were used to fill the cart. The average grain height calculated using these methods represented the minimum and maximum the average grain height could be with any arrangement of sensors in the cart.

Regression analysis was conducted to investigate the relationship between the average grain height and the weight of grain in the cart. The only input to the regression analysis was the average grain height calculated from the fill grid. The average grain height was calculated using three methods. The first method included all columns of the fill grid that contained sensors (Columns 2-8). The second method used the height of cells in Columns 3, 5, and 7. This method used the peaks of the cart when three fill zones were used to fill the cart. The third method used

cells in Columns 2, 4, 6, and 8 to calculate the average grain height. This method used the valleys of the cart when three fill zones were used to fill the cart.

A linear relationship was expected between the recorded weight and the average grain height, regardless of which columns of the fill grid were used to calculate the average. This was because the trough at the bottom of the grain cart was already filled when each filling test began. Figure 50 shows the typical starting fullness of the grain cart designated by the black line. Once a peak was established, grain delivered to the cart stacked in layers that were easily measured by the sensors. As additional grain was delivered to the cart, the grain spread out evenly across the top of the existing peaks once the slope of the pile reached the angle of repose.

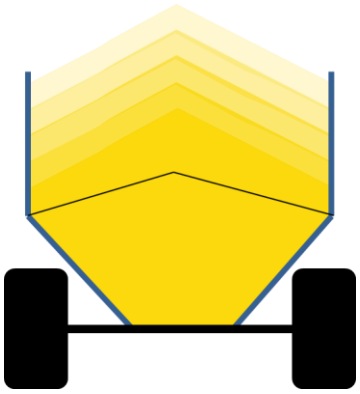

Figure 50: Cross-section of a grain cart where delivered grain accumulates evenly across the width of the cart once the angle of repose has been reached

6.2.2 Delivery Conditions

Different delivery conditions were tested to determine if the error of the predicted weight was impacted when grain was delivered to the cart under corner conditions in the field. Three specific treatment factors of the delivery conditions were tested:

1. Lateral distance between the combine and the grain cart
2. Order in which the zones of the grain cart were filled
3. Number of discrete zones the grain cart was divided

Grain height and weight data were collected with the data acquisition system described in Chapter 4. At the start of each test, the cart was partially filled with grain, as shown in Figure 50, until all sensors registered a valid height measurement. The cart was filled using the delivery conditions in Figure 51 that corresponded to the test that was conducted. The total number of fill

grids collected was 333. Test ID 1 represented each delivery condition at its baseline level. Subsequent tests changed each delivery condition one at a time so the effect of each condition could be analyzed independently.

Test ID	Number of Fill Grids	Lateral Distance Between Vehicles		Filling Order		Number of Zones	
		590cm	520cm	Front-Middle-Back	Middle-Front-Back	3 Zones	7 Zones
1	106	X		X		X	
2	77		X	X		X	
3	79	X			X	X	
4	71	X		X			X

Figure 51: Grain delivery conditions and the level of each condition tested

6.3 Results

6.3.1 Sensor Configuration

An equation did not exist that related grain height to grain weight in a cart. The grain height averaged across Columns 2-8 was the only input for a regression model created to predict the weight of grain in the grain cart (blue in Figure 52). Since no model previously existed that correlated average grain height to grain weight in a cart, the model using Columns 2-8 was assumed to be the true relationship between average grain height and actual grain weight for this study.

The regression model using sensors at the peaks of each zone (Columns 3, 5, 7) consistently over predicted the weight of the cart through the full range of tested grain heights compared to the model that used Columns 2-8 (Figure 52). The weight was expected to be over predicted in this case because sensors in the valleys were not included in the average height calculation to decrease the average.

The regression model using sensors at the valleys of each zone (Columns 2, 4, 6, 8) consistently under predicted the weight of the cart through the entire range of tested grain heights compared to the model that used all columns. The under prediction error was expected because height measurements at the peaks were not included to increase the average height calculation.

According to Figure 52, all three models converged at low average grain heights and spread apart as the average grain height increased. This behavior was caused by the cart not having

significant peaks at the start of the tests when the grain heights were low so there was minimal height difference between the peaks and valleys. As the cart filled with grain, more pronounced peaks and valleys formed so the regression models diverged.

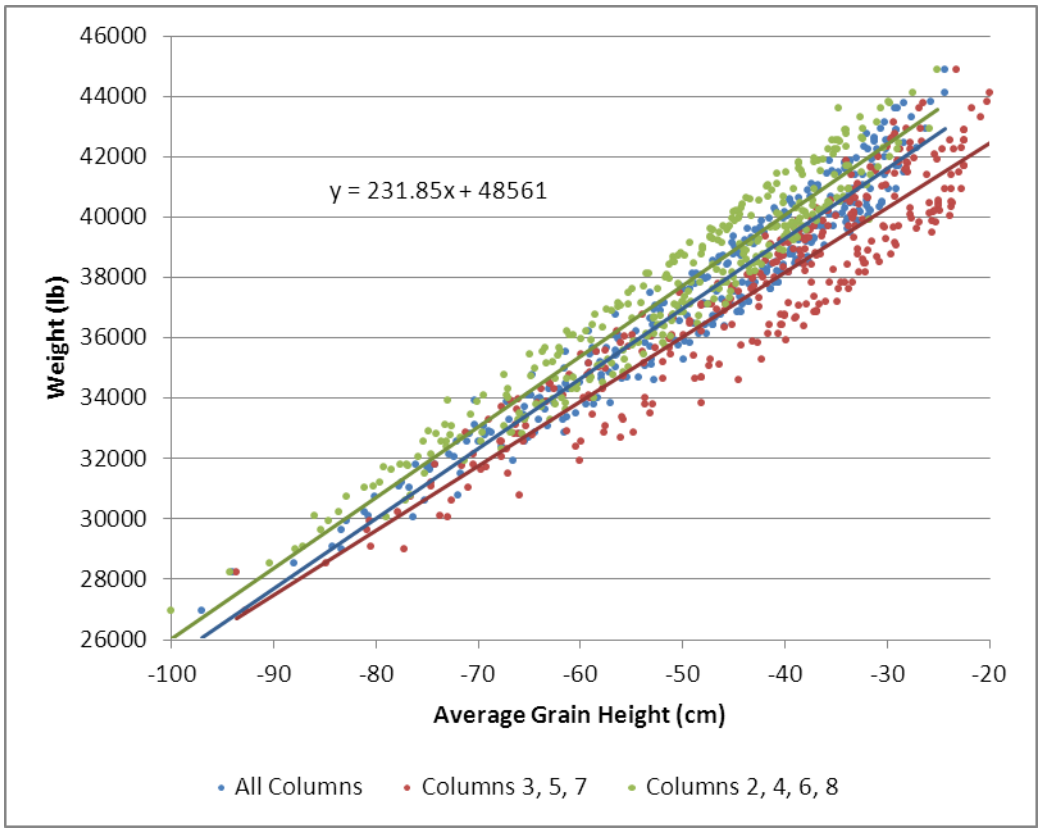

Figure 52: True weight plotted against the average grain height in the cart using three methods to calculate the average grain height; the equation shown corresponds to the method using all columns of the fill grid (middle line)

The determination coefficients (R-squared values) of each method showed a small increase as more points were included to calculate the average grain height (Table 32). Greater numbers of points were expected to yield coefficients of determination closer to one, but the changes in the coefficient of determination were small enough that the effect of more points did not conclusively increase the value of the coefficient.

Table 32: Coefficients of determination (R-squared) for each method of calculating the average grain height

Average Height Calculation Method	Coefficient of Determination, R^2
Columns 3, 5, 7	0.89
Columns 2, 4, 6, 8	0.93
All Columns	0.94

Residuals for each method of calculating the average grain height were found using the height-weight equation in Figure 52; the true weight of each captured fill grid was known from the experiment using the scales discussed in Chapter 4. An interval plot of the residual errors using each method of calculating the average grain height was created to analyze the significance of sensor location on the predicted weight in the cart (Figure 53). The error bars in Figure 53 are ±1 standard deviation from the mean residual of the respective method. The mean residual using Columns 2, 4, 6, and 8 to calculate the average grain height was negative. This supported the visual interpretation of Figure 52. The mean residual of the predicted weight using Columns 3, 5, and 7 was positive which also supported Figure 52. The mean residual using all columns was exactly zero because, by definition, a regression equation sets the mean residual of the population that was regressed equal to zero.

The interval plot indicated no significance in the predicted weight existed between using all columns of the fill grid to calculate the average weight or using Columns 2, 4, 6, and 8. The plot also indicated no significance existed between using all columns of the fill grid and using Columns 3, 5, and 7. This is strongly indicated by zero residual falling within one standard deviation of both methods for calculating the average grain height. Conclusive evidence did not support a significance existed between using Columns 2, 4, 6, and 8 versus using Columns 3, 5, and 7. The means residuals of these groups were different by 1800lb (32bu of corn at 15.5%MC_{wb}). In the context of a grain cart typical to North American agriculture with a capacity of 1000bu, this difference was not significant.

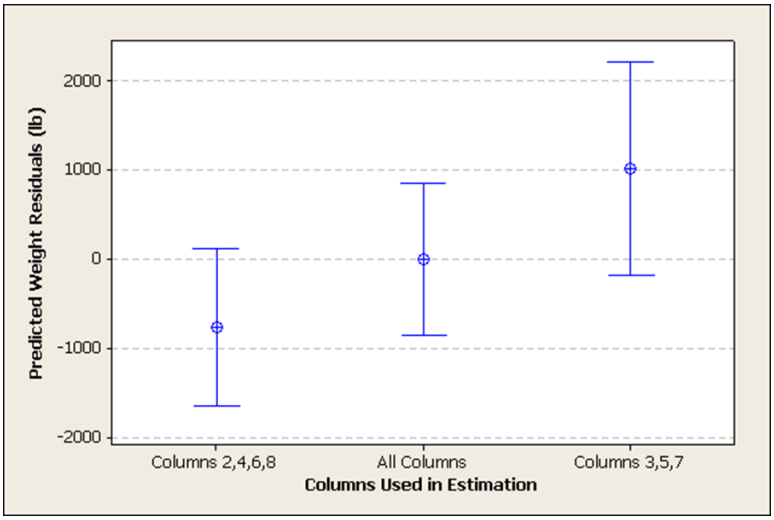

Figure 53: Residuals of the predicted weight for each method of calculating the average grain height using the same regression model for each method; intervals are ±1 standard deviation in length

The standard deviation of the residuals of each group decreased as more cells of the fill grid were used to calculate the average grain height (Table 33). The number of values used to analyze the error in the weight prediction did not vary from 333 for each group, but the number of points used to calculate each average grain height did change. The standard deviation improved by more than 300 lb when twenty points of the fill grid were used instead of fifteen, but the standard deviation improved by less than 40 lb when the number of points used was increased to 35. This indicated the minimum number of sensors required to calculate an accurate weight in the grain cart used without experiencing a substantial increase in variation was between 20 and 35.

Table 33: Number of points used in a fill grid by each method of calculating the average grain height and the standard deviation of the residuals of the predicted grain weight

Average Height Calculation Method	Number of Points in Fill Grid Used	Standard Deviation (lb)
Columns 3, 5, 7	15	1203
Columns 2, 4, 6, 8	20	885
All Columns	35	853

When the result of each method of calculating the average grain height versus the true cart weight was plotted on separate graphs (Figure 54), the true grain weights in Figure 52 appeared to form two clusters separated by a line parallel to the regression equation in Figure 52. This pattern was not expected since each plot only consisted of points from a single average grain height calculation method.

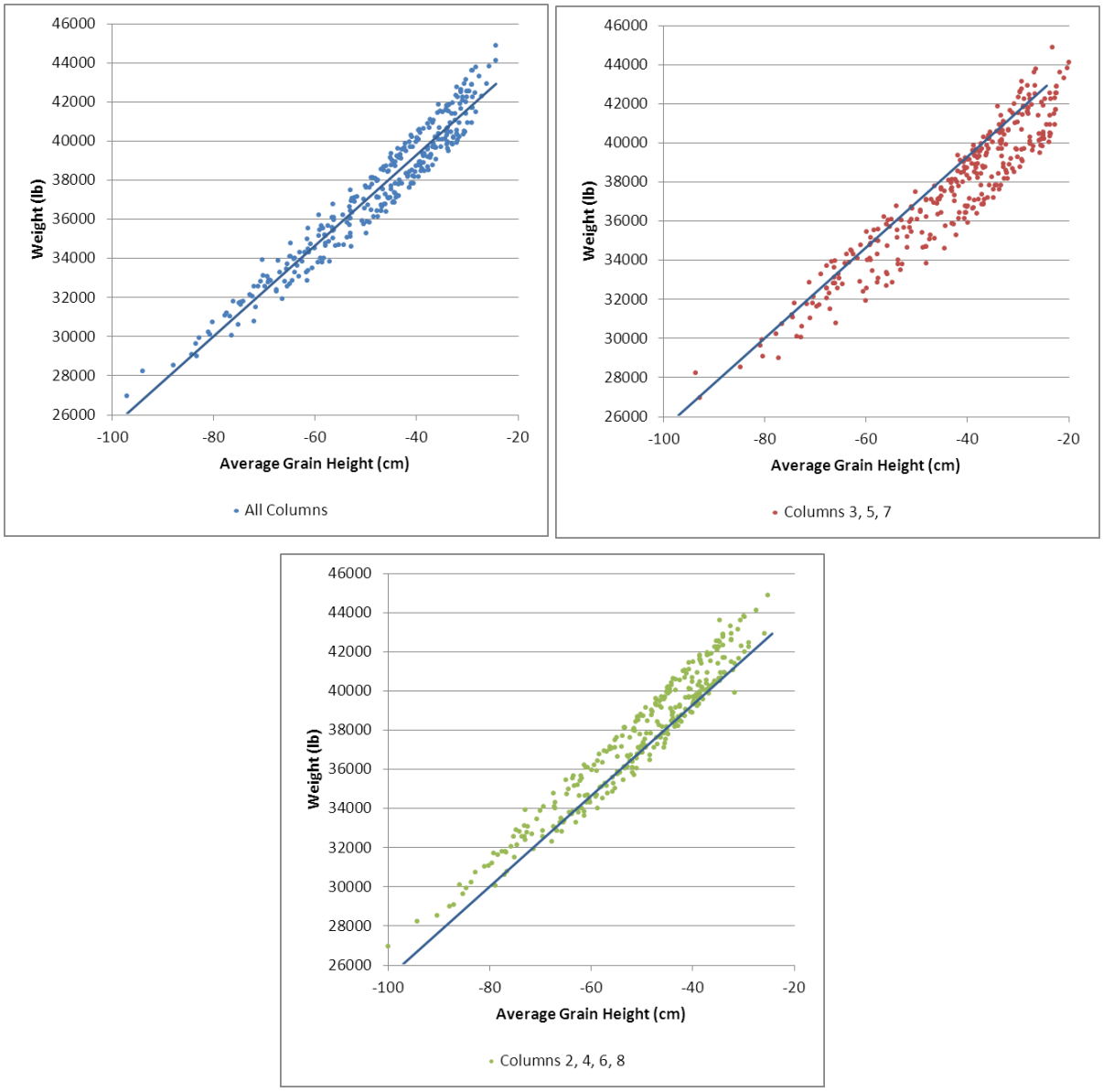

Figure 54: True weight plotted against the average grain height using data points in all columns that had sensors (top-left), Columns 3, 5, and 7 (top-right), and Columns 2, 4, 6, and 8 (bottom-center) with the regression line for the assumed true height-weight relationship overlaid in each plot; true grain weights in all plots appeared to form two clusters separated by a line parallel to the regression line

Histograms were created for each average grain height calculation method of the residual error of the predicted weight. The histograms of each method showed a bi-modal distribution in the residuals (Figure 55). The peaks of each histogram distribution were separated by 1500-2500lb indicating other factors were influencing the error of the weight prediction model. Since the data set used in this chapter included 333 fill grids combining all delivery conditions (baseline conditions,

smaller lateral offset, different filling order, and more fill zones), it was hypothesized the delivery conditions caused the bi-modal error distribution.

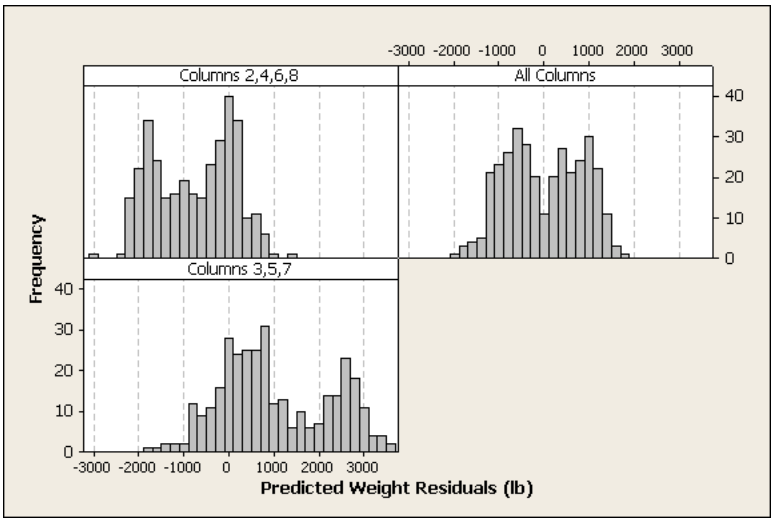

Figure 55: Histogram of the residuals of the predicted grain weights for each method of calculating the average grain height; bi-modal distributions were visually present in each method

6.3.2 Delivery Conditions

To investigate the impact of delivery conditions on the weight prediction model, the population of 333 calculated average grain heights and respective scale weights were analyzed by delivery conditions.

6.3.2.1 520 cm Lateral Distance between Vehicles

Tests were conducted with the lateral distance between the combine and the grain cart shortened from 590 cm at the baseline level to 520 cm. The blue line in Figure 56 represents the regression equation using all data points (true relationship between average grain height and grain weight), and the green line is the regression equation using data from tests with a 520 cm offset distance. The regression of the 520 cm offset group showed the difference in predicted weight and actual weight was small when carts contained less grain, and the difference increased as the cart filled with grain.

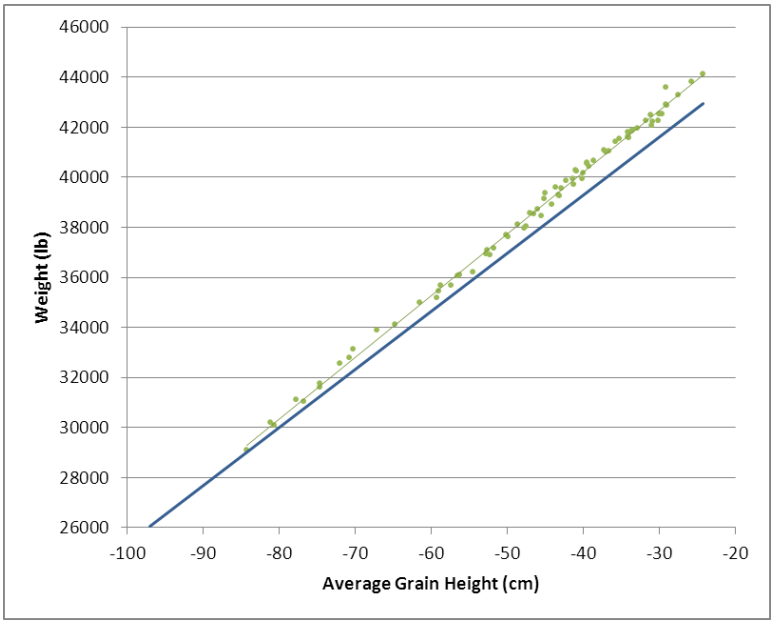

Figure 56: True weight versus average grain height for fill grids tested with a 520 cm later distance between the combine and grain cart; the blue line indicates the equation for the assumed true height-weight relationship, and the green line is the regression model using only the group of points tested with a 520 cm offset

An increasing significance between the data sets was expected because the model used to estimate the grain height in cells that did not have a dedicated sensor relied on the assumption that the delivery location was in the lateral center of the grain cart. When grain was delivered a substantial distance away from the center, a large peak accumulated between the far and middle rows of the sensors was not accounted for. The green volume in Figure 57 represents the unaccounted for volume of grain that would result from filling with a smaller lateral distance between vehicles because the second and fourth rows were assumed a constant height lower than the middle row. Using the grain height measurement along the near edge to estimate the height in the second column proved inaccurate and highly variable in previous testing compared to the middle row of sensors because the minimum sensing threshold of sensors mounted along the near and far edges breached early in the process of filling the cart.

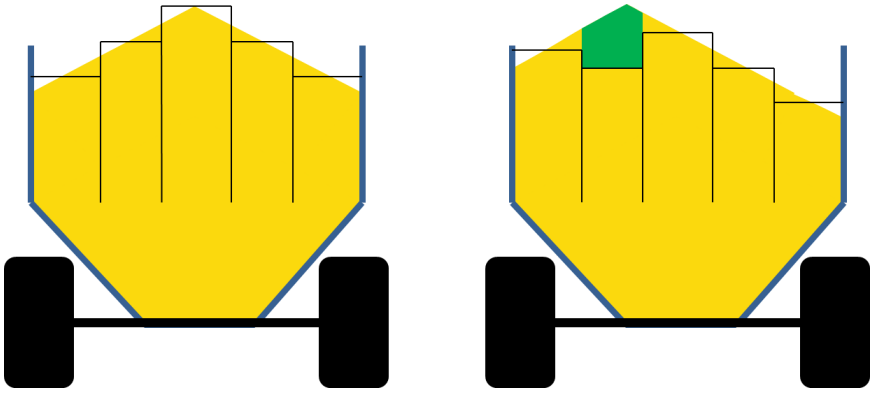

Figure 57: Comparison of the modeled grain height at when grain is delivered to the lateral center of the cart (left) and when it is delivered closer to the far edge; the green area represents the unacounted for volume of grain

A histogram of the 520 cm offset weight prediction residuals overlaying the residuals of the entire population was created (Figure 58). A mean residual of -830 lb. with a standard deviation of 300 lb. was calculated for the 520 cm offset group. A difference in means of 830 lb. represented the average weight of grain left unaccounted for in the green volume at each column of the fill grid along the length of the cart. Figure 56 visually showed a significant difference in the error could have been present when filling with a smaller lateral offset. It was apparent from the histogram that the majority of the most negative residuals of all 333 data points were attributed to the data set from the 520 cm offset delivery condition. The interval plot in Figure 58 supported the strong presence of a difference in the residual means. With a 95% confidence interval the difference in means was 600 lb. Although the difference was statistically significant, 600 lb. represented less than 1.5% of the total weight delivered to this size of grain cart when it was full.

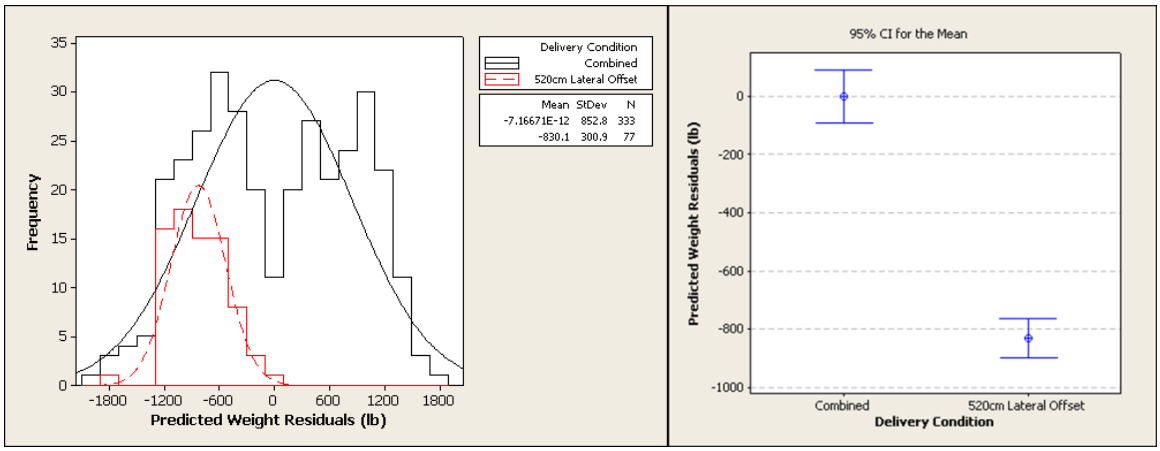

Figure 58: Histogram (left) and interval plot (right) of the residuals of the predicted grain weight for the combined data set (black) and the 520 cm lateral offset data set (red)

6.3.2.2 Middle-Front-Back Filling Order

Tests were conducted with the filling order of the three fill zones changed from the baseline filling order of Front-Middle-Back to the test level Middle-Front-Back. The blue line in Figure 59 represents the regression equation of average grain height calculated using Columns 2-8 versus the true grain weight, and the purple line is the regression equation using data from tests with a Middle-Front-Back filling order. Regression of the predicted weight using Middle-Front-Back tests showed almost no difference in the slopes of each regression equation, but the weight of Middle-Front-Back tests were consistently over estimated. The filling order was not expected to influence the predicted weight of grain; however, analysis conducted in the previous chapter indicated the Middle-Front-Back tests could have abnormally steeper peaks in the grain cart compared to other tests that used three fill zones. The behavior shown in Figure 59 supports the hypothesis that steeper peaks were present when the Middle-Front-Back tests were conducted. It was assumed the steep peaks were a result of human inconsistencies in the experiment conduction, not a result of using a different filling order.

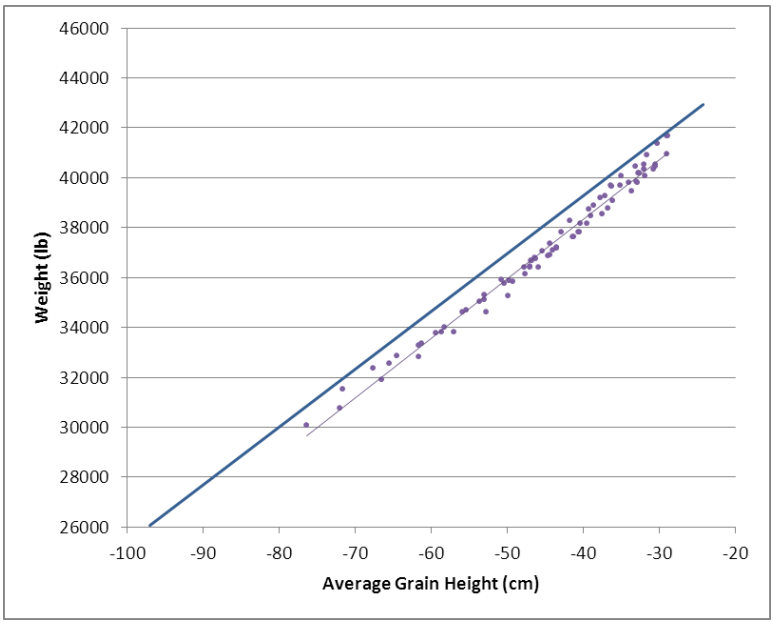

Figure 59: True weight versus average grain height for fill grids tested with a Middle-Front-Back filling order; the blue line indicates the equation for the assumed true height-weight relationship, and the purple line is the regression model using only the group of points with a Middle-Front-Back filling order

A histogram of the residuals of the Middle-Front-Back filling order weight prediction model were overlaid on a histogram of the residuals for the all delivery conditions (Figure 60). The mean

residual of the Middle-Front-Back filling order was almost 1000 lb. with a standard deviation of 340 lb.

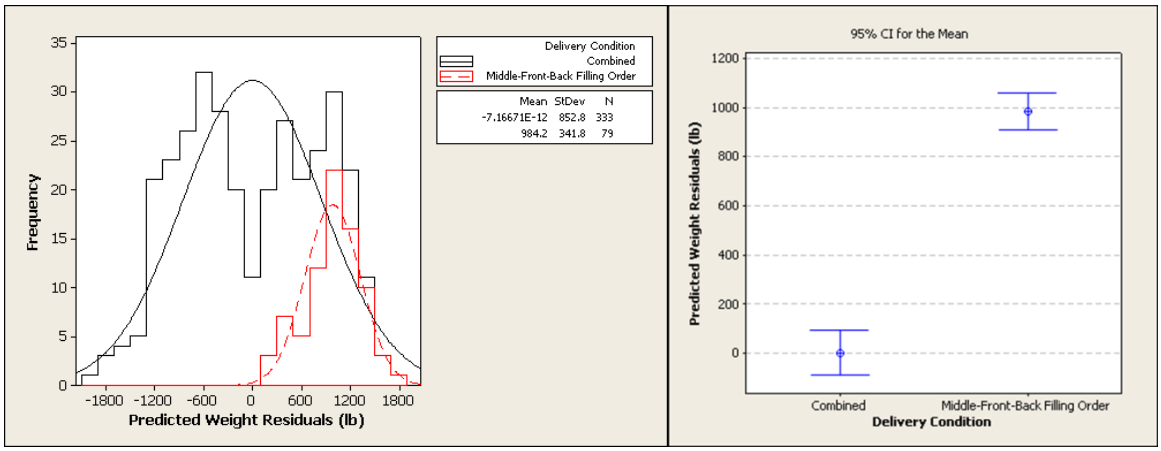

Figure 60: Histogram (left) and interval plot (right) of the residuals of the predicted grain weight for the combined data set (black) and the Middle-Front-Back filling order data set (red)

The mean residual was expected to be 0 lb. for this delivery condition, and excessively steep peaks and valleys did not likely comprise 1000 lb. The cause of the large mean error was unknown. It was apparent from the histogram that the majority of the most positive residuals of the model came from the Middle-Front-Back filling order.

The interval plot in Figure 60 supported the strong difference in the residual means, but magnitude of the differences was around 800 lb. This difference accounted for less than 2% of the total cart weight so the impact on the ability to estimate the weight of grain in the cart was not significant to the purpose of the model.

6.3.2.3 Seven Fill Zones

The last delivery condition test was conducted using seven fill zones instead of the baseline level of three. The blue line in Figure 61 represents the regression equation of average grain height calculated using Columns 2-8 versus the true grain weight, and the teal line is the regression equation using data from tests with seven fill zones. Regression of the predicted weight using data from carts filled with seven fill zones showed almost no difference in the regression equation, and the weight showed almost no difference in the combined data set. The slopes and intercepts were nearly identical.

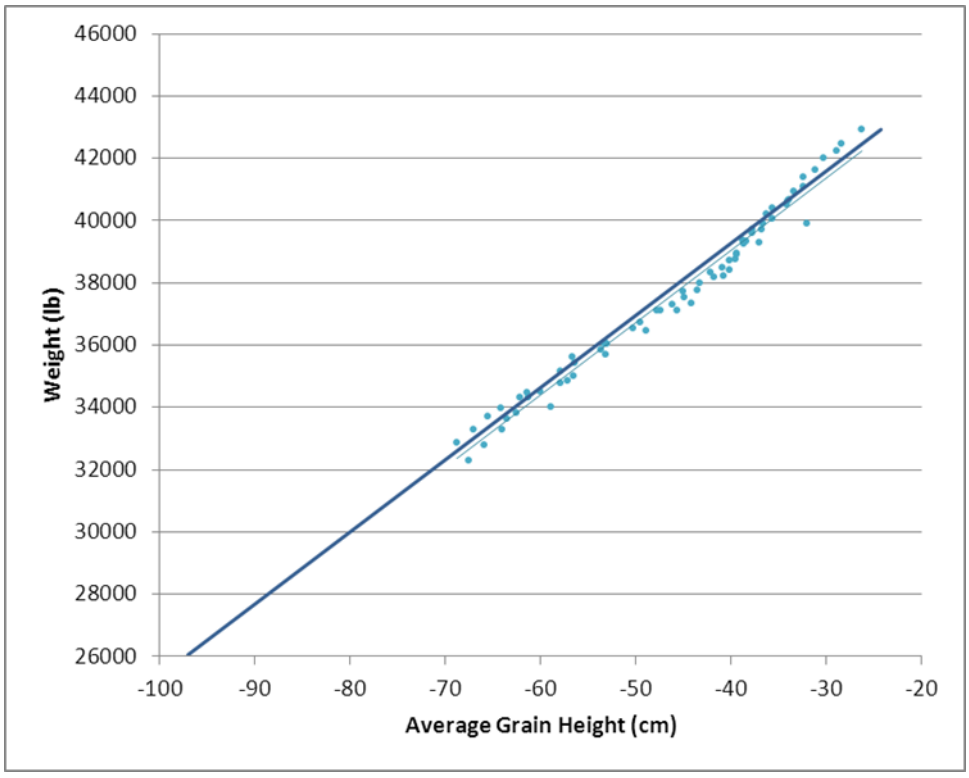

Figure 61: True weight versus average grain height for fill grids tested with seven fill zones; the blue line indicates the equation for the assumed true height-weight relationship, and the teal line is the regression model using only the group of points with seven fill zones

A histogram of the residuals of the predicted weight using data from carts filled with seven fill zones was overlaid with the histogram of the combined data set (Figure 62). The histogram showed the mean error with seven zones was less than 300 lb. The standard deviation was about the same as with a 520 cm offset or a Middle-Front-Back filling order: 300-400 lb. The mean residual and standard deviation of the residual strongly supported that the number of fill zones did not impact the estimation model that used the combined delivery conditions.

The interval plot in Figure 62 supported the presence of a difference in the residual means with a 95% confidence interval. The difference was around 100 lb, which represented less than 1% of the total grain weight in the cart so the effect of seven fill zones was not significant to the application of the model.

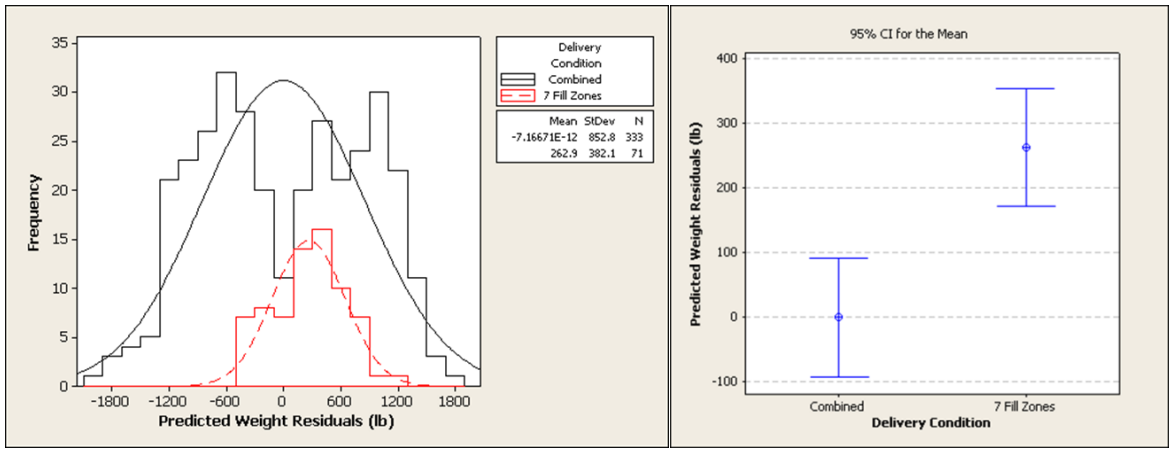

Figure 62: Histogram (left) and interval plot (right) of the residuals of the predicted grain weight for the combined data set (black) and the seven zones data set (red)

6.4 Conclusions

The average grain height using Columns 2-8 of the fill grid was calculated and regressed against the true grain weight. Several repetitions were conducted under different delivery conditions. A linear regression model produced a satisfactory level of fit for the predicted weight as a linear function of the average grain height; this model was used as the true weight for all calculated average grain heights. The average grain height was calculated using two methods in addition to this method: only using Columns 2, 4, 6, and 8 and only using Columns 3, 5, and 7. These columns were selected in an attempt to detect a difference in the predicted weight based on whether peaks or valleys were used to calculate the average grain height. The residual errors of the predicted weight of each method for calculating the average grain height revealed no significance among any methods. This indicated the number of sensors in each row of the grain cart potentially could have been reduced from seven to three or four without significantly impacting the predicted weight. The standard deviation of the residuals decreased from 1200 lb. to 800 lb. when the average grain height was calculated with Columns 2-8 or 2, 4, 6, and 8 instead of using Columns 3, 5, and 7. This suggested the number of sensors in each row of the fill grid should be at least four to keep the standard deviation of the weight below 1000 lb. If less variation was desired, it is expected that more than seven sensors per row would be required before the variation decreased by a measureable amount.

A bi-modal distribution of the residuals was discovered in the predicted weight of the cart for all methods of calculating the average grain height. The cause was hypothesized to be the

delivery conditions because the data set that was regressed to define the relationship between the average grain height and the grain weight included four different delivery conditions. The mean residuals of the predicted weights of the data set utilizing seven fill zones did not show a bias in the residuals. The residuals of the predicted weight when the lateral distance between vehicles decreased from 590 cm to 520 cm under predicted the weight, and the Middle-Front-Back filling order over predicted the weight. All delivery conditions demonstrated a difference in the mean residuals compared to the combined data set. However, the difference in the mean residuals was less than 2% of the weight of a full cart, which was not significant to the application of a weight prediction model.

Chapter 7 Dynamic Field Testing of the Decision Support System

7.1 Introduction

The purpose of this phase of the research was to identify a decision support system that automatically filled a grain cart and quantify the repeatability of the system during dynamic field testing.

7.2 Materials and Methods

The decision support system was designed in Simulink and operated as part of the larger autonomous unloading system on the combine. It required input information that was supplied by two sources:

1. Grain height information from a stereovision camera
2. System settings and parameters from a user interface

The stereovision camera was mounted on the auger of the combine and provided grain heights in the form of fill grids similar to the format of ultrasonic sensors used in previous chapters. The main difference was a cell size of 25 cm by 25 cm was produced by the stereovision camera instead of 67 cm by 59 cm produced by the ultrasonic system.

7.2.1 Decision Support System

Diverse features were incorporated into the decision support system that could be tuned by operators to meet their functional desires of the system. Regardless of operator preferences, the support system needed to output two requests that were sent to the rest of the autonomous control system. These outputs were:

1. Positional change of the end of the auger in number of fill grid cells forward or backward
2. Auger engagement/disengagement

The decision support system reached the values of these outputs in six steps. The first step of the decision support system was to condense the input data from the stereovision camera from a fill grid to a single row of the average grain heights of each column (Figure 63). These values were sent to the next subsystem of the decision support system as a one-dimensional array. The average

grain height of the entire fill grid was also calculated and converted to a percentage before being transmitted to the user interface.

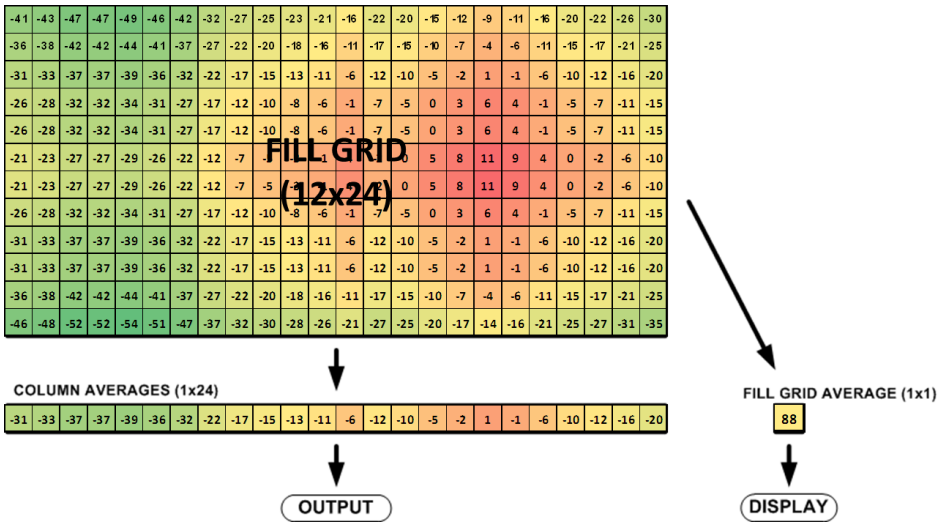

Figure 63: Example fill grid from a stereovision camera with grain heights (in centimeters) that was condensed into a 1D array of average fill levels; average fullness of the fill grid was also calculated and expressed as a percentage for feedback to the user on the user interface

The second step of the support system compared the average grain height of each column to the desired fill level. Values lower than the desired level were assigned a "1" (acceptable), and values higher than the desired level were assigned a "0" (not acceptable) (Figure 64). Regardless of the measured grain heights at the front and rear of the cart, No-fill Zones at the front and rear were overridden with 0s. The resulting 1s and 0s were packed into an array sent to the next subsystem.

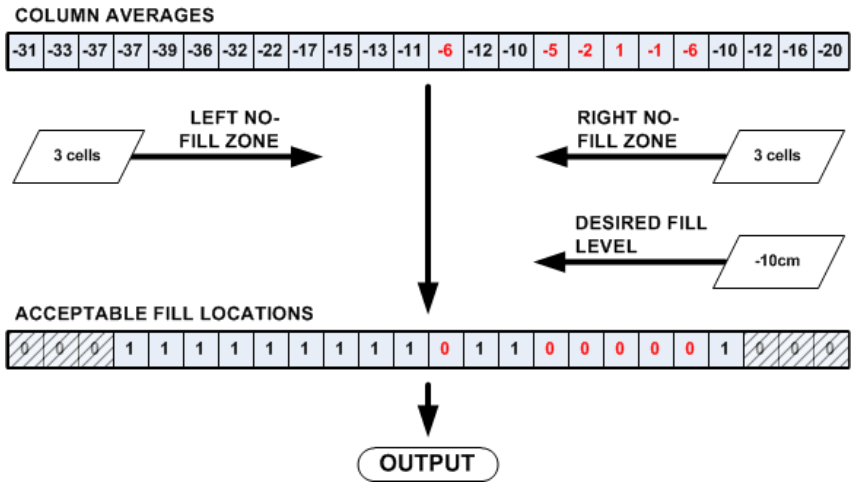

Figure 64: Example step in the decision support system where average fill levels of each column were compared to the desired fill level and expressed as 1s (acceptable) and 0s (not acceptable); no-fill zones of three cells were applied to the front and back of the output array

The purpose of the next step of the process was to mitigate the effects of variation in the grain height measurement by implementing hysteresis in the comparison of each average fill level to the desired fill level. Cells already designated not acceptable were passed directly to the output array (Figure 65). Historical data was checked for cells that were acceptable. If the cell was judged not acceptable in a previous program loop, a hysteresis margin was added to the desired level before that cell could become acceptable again (Figure 66).

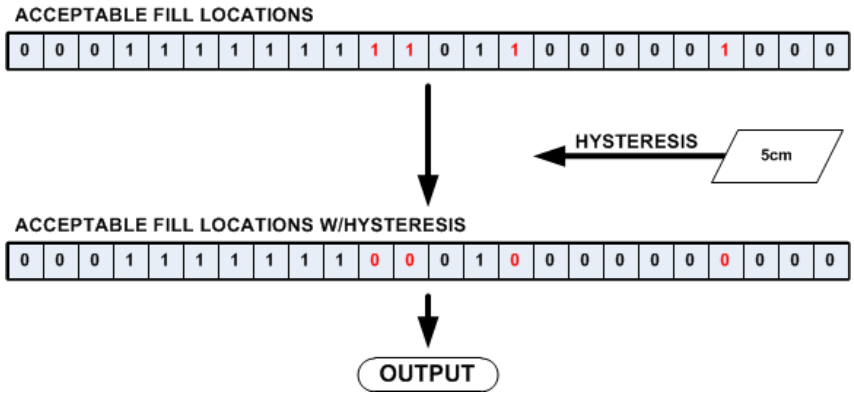

Figure 65: Example step in the decision support system where a 5 cm hysteresis was applied to the acceptable fill locations to mitigate the effects of noise in the grain height measurement

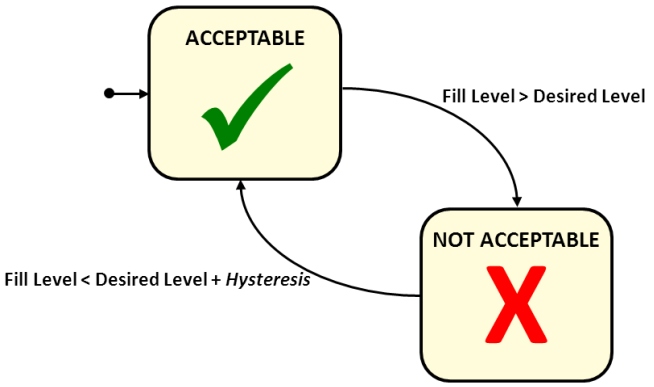

Figure 66: Logic of the decision support system showing each cell that was not acceptable was required to have a fill level lower than the desired fill level and a hysteresis value in order to become acceptable again

The next step was to create fill zones in the cart. The length of the cart (except No-fill Zones) was divided into discrete fill zones. A required number of acceptable cells per zone was included to decide whether a fill zone was acceptable to receive grain or not. The number of acceptable cells in each zone was summed and compared to the required number of acceptable cells per zone. If a zone met this requirement, the output array was packed with the zone number in each cell of the zone (Figure 67). Zones that did not meet the requirement were packed with 0s.

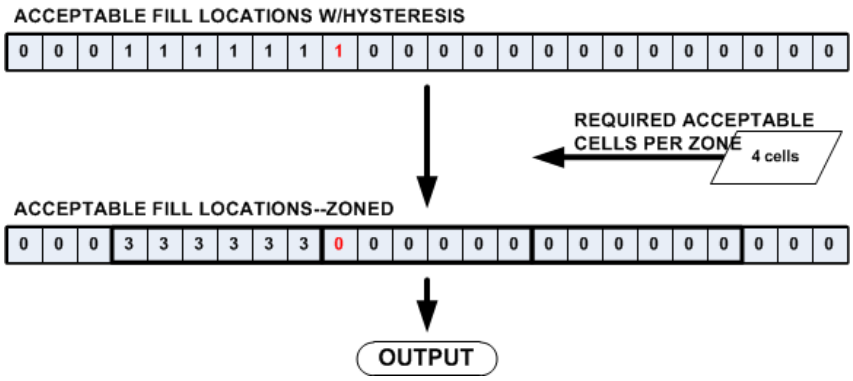

Figure 67: Example step in the decision support system where zoning was applied to the acceptable fill locations; starting from the front of the cart (right side) Zone 1 and Zone 2 did not meet the minimum number of acceptable cells per zone, but Zone 3 did meet the requirement and contains 3s in the cells within that zone

The next step of the decision support system determined the best location to deliver grain based on the chosen fill mode. A Front-Back fill mode targeted the center of the front-most acceptable zone, and a Back-Front fill mode targeted the center of the rear-most acceptable zone. The first-last zone offset was implemented to nudge the targeted center of the first and last zones outward to spread the grain peaks farther apart. The output of this step was a positional nudge

request in the positive or negative (forward or backward) direction relative to the current position of the end of the auger (Figure 68). An output of 0 cells meant the decision support system did not request any movement from the auger.

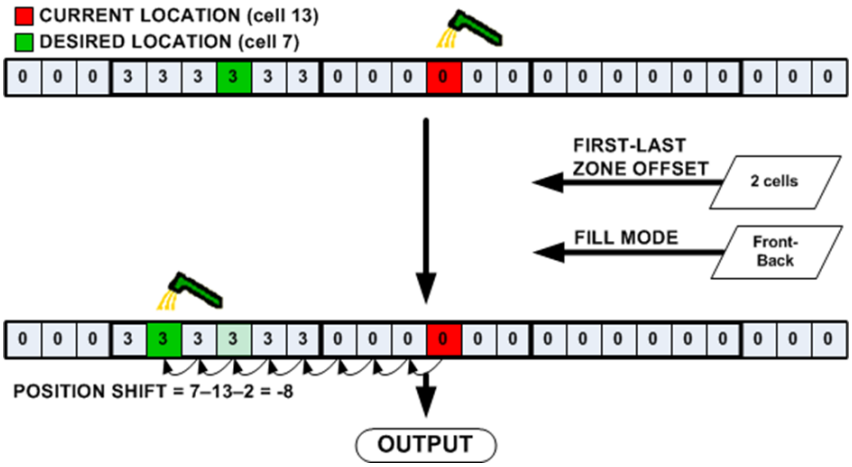

Figure 68: Example step in the decision support system where the zoned acceptable fill locations were analyzed with the fill mode and first-last zone offset to calculate a desired change in the current location of the end of the auger; the output was calculated by subtracting the current location from the center point of the desired zone and adding (if front-most zone) or subtracting (if rear-most zone) the First-last Zone Offset

The last step of the decision support system output a request to engage or disengage the auger based on the fill level of the current position and the desired fill level. An overfill allowance was added to the desired fill level when attempting to disengage the auger so it remained engaged while the system moved to a new position (Figure 69). Without the overfill allowance the auger momentarily disengaged when a new position was requested causing excessive wear on machine hardware.

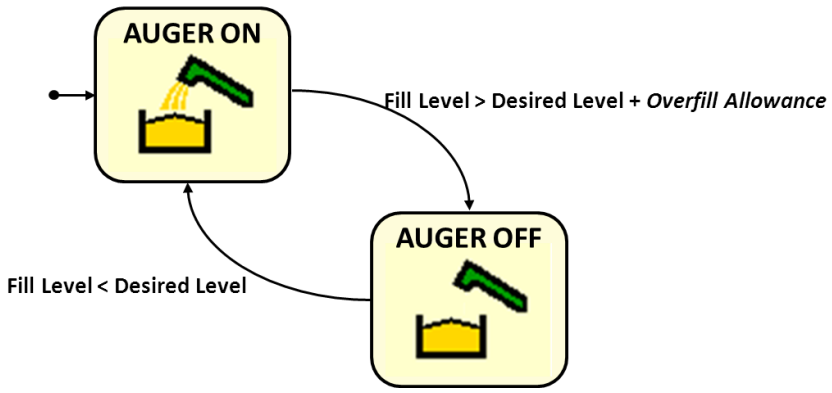

Figure 69: Logic of the decision support system where the request to disengage or engage the auger was made; an overfill allowance was added to the requirement to disengage the auger so it would remain engaged when a new position was requested

7.2.2 Decision Support System Features

It was critical to test four features of the decision support system dynamically because they possessed long-term viability as the most important features of an autonomous unloading system.

1. Fill Mode
2. Number of Fill Zones
3. Desired Fill Level
4. First-last Zone Offset

Most features were tested with two brands of grain carts: a Kinze 840 and a Brent 1088 (Figure 70). Tests were conducted with a different desired fill level or different number of fill zones for each cart because the geometries were different. Each test had at least three repetitions; more than three repetitions were collected in many test cases to validate dynamic performance of the autonomous unloading system.

Figure 70: Brent 1088 grain cart used during dynamic field testing of the decision support system

7.2.2.1 Fill Mode

Front-Back or Back-Front fill modes were selected to determine which area of the cart was given higher priority to receive grain. Both fill modes were commonly used during harvesting. A Front-Back fill mode transferred more weight to the hitch of the tractor to limit potential traction issues in wet fields. A Back-Front mode positioned the cart to give the combine operator the best possible view of the cart while unloading on-the-go. Both models of grain carts were tested with a Front-Back and Back-Front fill mode (Figure 71).

Repetitions	Grain Cart Manufacturer		Fill Mode		Number of Fill Zones				Desired Fill Level			First-Last Zone Offset	
	Kinze	Brent	Front-Back	Back-Front	One	Two	Three	Four	95% (-7.5cm)	100% (+0cm)	105% (+7.5cm)	1 cell	2 cells
3	X		X			X				X			X
3	X			X		X				X			X
6		X	X				X			X			X
4		X		X			X			X			X

Figure 71: Decision support system settings for testing the fill mode with the Kinze and Brent grain carts

7.2.2.2 Number of Fill Zones

The number of zones was increased or decreased with the intent to change the amount of space left between peaks of the fill zones. The number of zones also affected the amount of wear on the combine as more zones required more effort from the actuation control circuit to maintain a certain location within a fill zone. The Kinze cart was tested with one, two, and three fill zones, and the Brent cart was tested with three and four zones (Figure 72). The carts were tested with different fill modes and different desired fill levels to gain diversity in the test conditions.

Repetitions	Grain Cart Manufacturer		Fill Mode		Number of Fill Zones				Desired Fill Level			First-Last Zone Offset	
	Kinze	Brent	Front-Back	Back-Front	One	Two	Three	Four	95% (-7.5cm)	100% (+0cm)	105% (+7.5cm)	1 cell	2 cells
3	X		X		X				X				X
6	X		X			X			X				X
4	X		X				X		X				X
4		X		X			X			X			X
3		X		X				X		X			X

Figure 72: Decision support system settings for testing the desired fill level; the Kinze and Brent cart were used with different number of fill zones

7.2.2.3 Desired Fill Level

The desired fill level was changed to have the system delivery more or less grain into the cart. This was the level targeted by the decision support system that directed swing and engagement requests. Weight measured by the scales on the cart did not drive requests by the decision support system because the scales were only accurate when the cart was stationary on flat ground. If the grain cart was not stationary and on flat ground, several thousand pounds of error could result. The Kinze was tested at desired fill levels from 95% (-7.5 cm) to 105% (+7.5 cm) (Figure 73). The Brent cart was tested at 95% and 100%.

Repetitions	Grain Cart Manufacturer		Fill Mode		Number of Fill Zones				Desired Fill Level			First-Last Zone Offset	
	Kinze	Brent	Front-Back	Back-Front	One	Two	Three	Four	95% (-7.5cm)	100% (+0cm)	105% (+7.5cm)	1 cell	2 cells
6	X		X			X			X				X
3	X		X			X				X			X
5	X		X			X					X		X
3		X	X				X		X				X
6		X	X				X			X			X

Figure 73: Decision support system settings for testing the desired fill level; the Kinze and Brent cart were used with different number of fill zones each

7.2.2.4 First-last Zone Offset

The center-point of the fill zones farthest to the front and farthest to the rear were offset outward to distribute the locations of the grain peaks farther apart. The goal of this feature was to achieve fuller carts in the field. The Brent cart was not included in tests on the first-last zone offset (Figure 74).

Repetitions	Grain Cart Manufacturer		Fill Mode		Number of Fill Zones				Desired Fill Level			First-Last Zone Offset	
	Kinze	Brent	Front-Back	Back-Front	One	Two	Three	Four	95% (-7.5cm)	100% (+0cm)	105% (+7.5cm)	1 cell	2 cells
5	X		X			X					X	X	
7	X		X			X					X		X

Figure 74: Decision support system settings for testing the first-last zone offset distance

7.2.2.5 Grain Cart Manufacturer

The manufacturer of the grain cart being unloaded into was not required by the decision support system and was not an input to the algorithm. The use of diverse carts was critical to investigate in order to discover any unintended reliance on specific grain cart geometries. Filling repeatability was compared on both carts at 95% and 100% (Figure 75).

Repetitions	Grain Cart Manufacturer		Fill Mode		Number of Fill Zones				Desired Fill Level			First-Last Zone Offset	
	Kinze	Brent	Front-Back	Back-Front	One	Two	Three	Four	95% (-7.5cm)	100% (+0cm)	105% (+7.5cm)	1 cell	2 cells
4	X		X				X		X				X
3		X	X				X		X				X
5	X		X				X			X			X
6		X	X				X			X			X

Figure 75: Decision support system settings for testing grain cart manufacturers at two desired fill levels

Repeatability of the system was measured by the final grain weight in the cart when the decision support system defined the cart had met the desired fill level. Weight was not input directly to the decision support system to determine when a cart was full. The system's interpretation of the measured grain heights decided when the cart was full. The weight and moisture content of the grain were used to calculate the volume delivered to the cart in bushels. A volumetric comparison was used for this portion of the research to mitigate the effects of varying moisture content throughout the harvesting season when data collected. Weight was used in previous chapters because the same sample of grain was used to collect data over just a few day's time.

7.3 Results

7.3.1 Fill Mode

Fill mode tests with the Kinze grain cart indicated the final cart volume was not significantly impacted when a Front-Back or Back-Front fill mode was used (Figure 76). It was desirable for the decision support system to not be impacted by the chosen fill mode. The fill mode was not expected to be significant because the fill mode did not change the locations in the cart that grain was targeted for delivery. Slightly more variation in the final cart volume was observed with a Front-Back fill mode. The higher variation was believed to be caused by varying levels of experience of machinery operators. All Back-Front tests were conducted at the end of the harvest season while Front-Back tests were conducted throughout the harvest season.

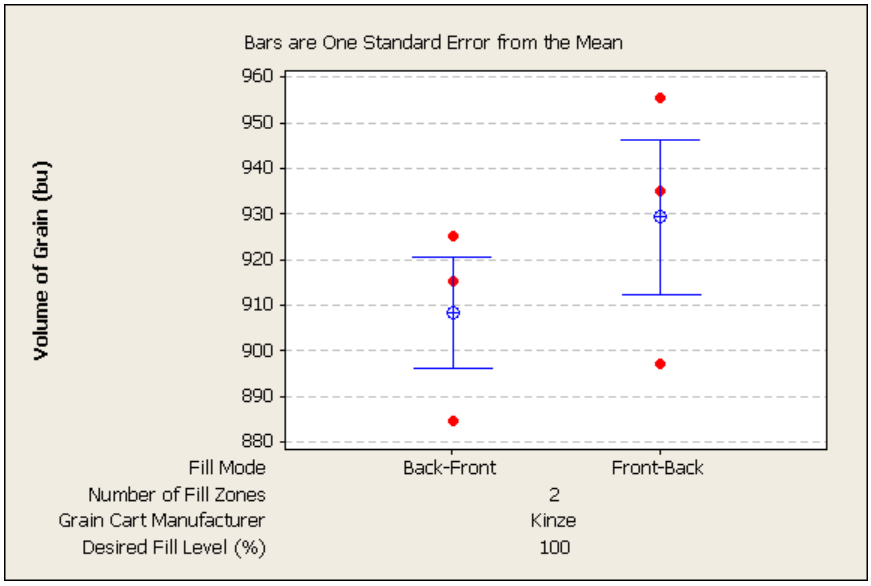

Figure 76: Interval plot for the final volume of grain delivered to the Kinze grain cart using Front-Back and Back-Front fill modes

Fill mode tests with the Brent grain cart indicated the cart received significantly more grain when a Front-Back fill mode was used instead of a Back-Front (Figure 77). A significant impact on the final cart volume by the fill mode was not expected in one cart but not the other. A potential cause of this inconsistency between the Brent and Kinze grain carts was the Brent had a longer opening to deliver grain (5.4 m on the Kinze vs. 6.5 m on the Brent). A longer opening of the cart meant the combine or tractor operators were required to change their relative positions for the front-most and rear-most fill zones to receive grain. The more time that elapsed before an operator recognized the desired fill location was outside the swing range of the auger, the more grain that

accumulated well above the desired fill level due to the overfill allowance feature of the decision support system.

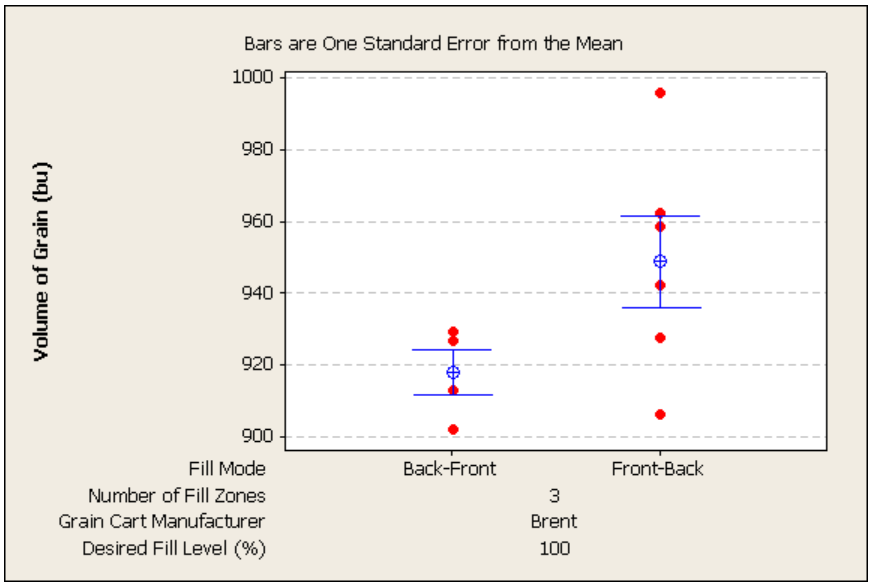

Figure 77: Interval plot for the final volume of grain delivered to the Brent grain cart using Front-Back and Back-Front fill modes

7.3.2 Number of Fill Zones

The Kinze grain cart was divided into one, two, and three fill zones to test the impact of the number of fill zones on the final cart volume. Tests indicated the final cart volume was impacted by increasing the number of zones from one to two, but increasing from two to three fill zones showed no significance (Figure 78). The significance from one to two zones was expected, but the addition of more zones was also expected to show a significant impact on the final cart volume. Visual observation of the tests indicated going from one to two fill zones substantially increased the amount of grain delivered to the front and rear of the cart (Figure 79). Three fill zones appeared to reduce the empty space between peaks that was left with two zones, but the additional grain did not appear to be significant, supporting the statistical data.

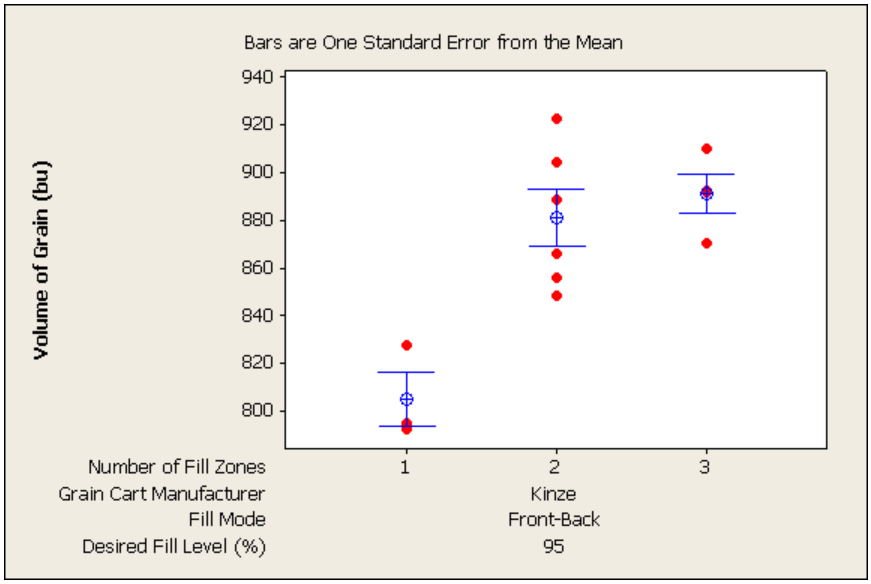

Figure 78: Interval plot for the final volume of grain delivered to the Kinze grain cart using one, two, and three fill zones

Figure 79: Kinze grain cart filled with one (left), two (center), and three (right) fill zones

The Brent grain cart showed no significance when the number of fill zones was increased from three to four (Figure 80). The Brent cart was not tested using one fill zone. Significance was expected to appear when four zones were used, but a visual inspection of the Brent carts during the testing suggested the volume of grain was not impacted with more zones (Figure 81), supporting the statistical data.

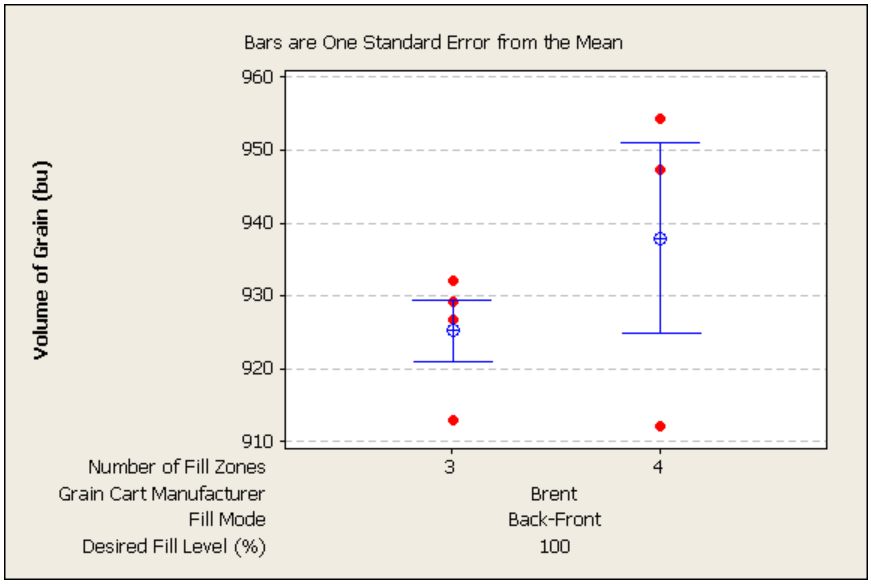

Figure 80: Interval plot for the final volume of grain delivered to the Brent grain cart using three and four fill zones

Figure 81: Brent grain cart filled with three (left) and four (right) fill zones

7.3.3 Desired Fill Level

The Kinze grain cart was filled to 95% (-7.5 cm), 100% (0 cm), and 105% (+7.5 cm) to test the impact of the desired fill level on the final cart volume. Tests indicated the final cart volume was significantly impacted by increasing the desired fill level from 95% to 100%, but going from 100% to 105% showed no significance (Figure 82). There was also a significant impact in the final cart volume by changing the desired fill level from 95% to 105%. A significant impact was expected between 95% and 105%, but no significance was expected for a 5% (7.5 cm) change in the desired fill level because a hysteresis of 8% (10 cm) was used in all tests. Since significance was detected at a 5% change in desired fill level, this indicated the grain measurement may have been highly stable so hysteresis did not have to play a significant role in reducing noise in the grain height

measurement. Visually, it was difficult to determine if a cart filled to 95% had a volume different from carts filled to 100% or 105% (Figure 83).

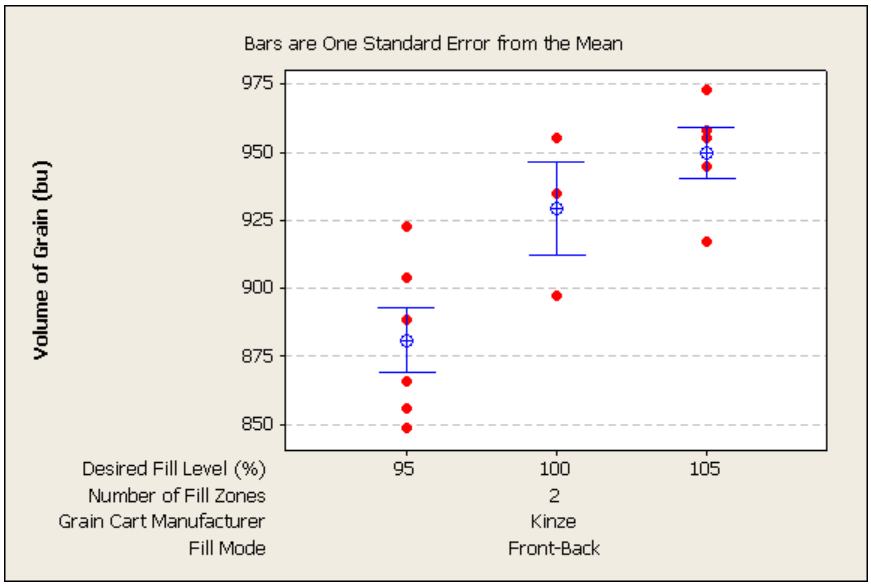

Figure 82: Interval plot for the final volume of grain delivered to the Kinze grain cart using a 95%, 100%, and 105% desired fill levels

Figure 83: Kinze grain cart filled with a 95% (left), 100% (center), and 105% (right) desired fill level in the decision support system

The Brent grain cart was tested at 95% and 100% to determine if the desired fill level impacted the final cart volume in a different cart. It was not tested at 105%. At intervals of ±1 standard error from the mean final cart volume, less than 5 bu of difference was detected (Figure 84), indicating a slight significance for a 5% change in desired fill level. The Brent was not expected to show a significant impact until the desired fill level changed by 10% because 8% hysteresis was implemented. Since a slight significance was detected, this indicated the hysteresis served a small

role in the grain measurement. Visually, the final cart volume of the Brent did not appear to change from 95% to 100% (Figure 85).

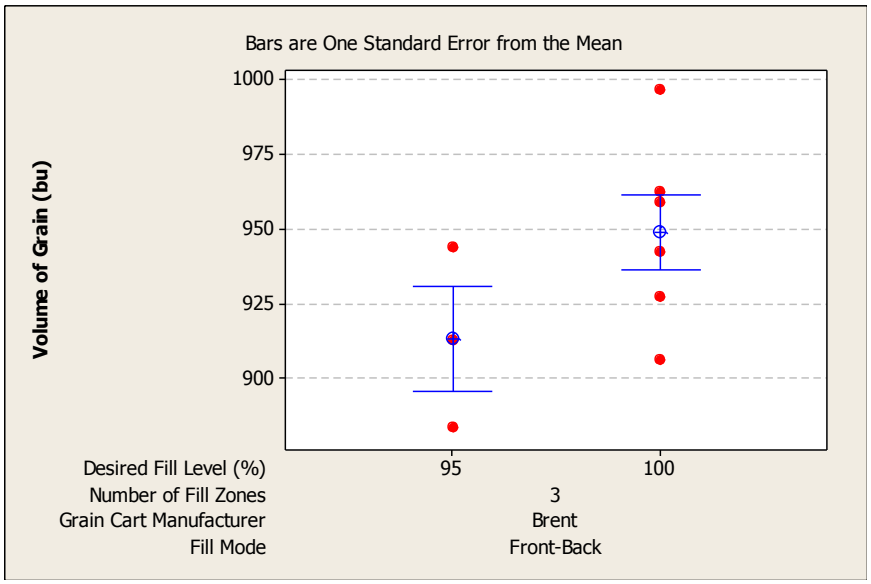

Figure 84: Interval plot for the final volume of grain delivered to the Brent grain cart using a 95% and 100% desired fill level

Figure 85: Brent grain cart filled with a 95% (left) and 100% (right) desired fill level in the decision support system

7.3.4 First-last Zone Offset

Tests offsetting the center point of the first and last fill zones from one cell (25 cm) to two cells (50 cm) significantly increased the final cart volume (Figure 86). The final cart volume was expected to show a significant impact from changing the first-last zone offset based on visual observations of the cart in the field (Figure 87) which often showed one large pile in the middle of

the cart because the delivery locations within each zone were close to one another. When the offset increased, substantially more grain was delivered to the front and rear of the cart. Tests on the first-last zone offset were only conducted on the Kinze grain cart.

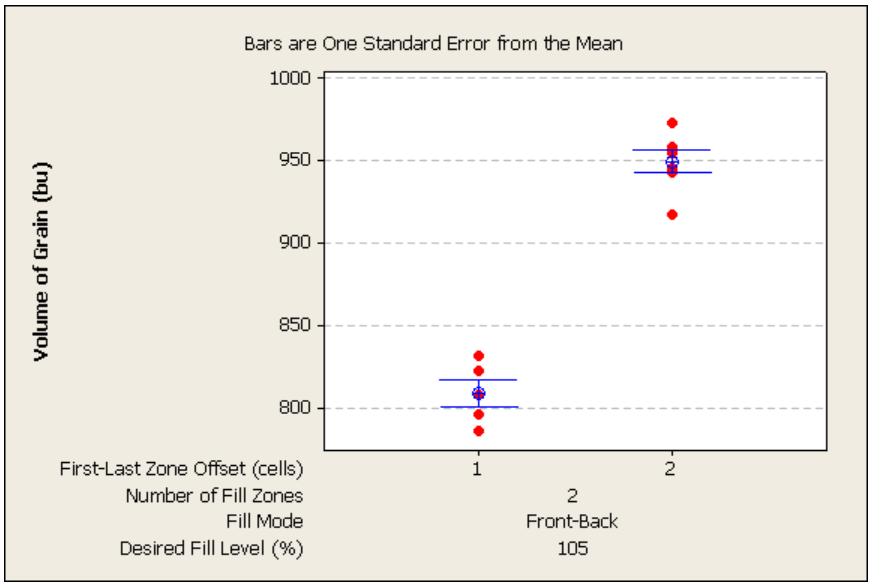

Figure 86: Interval plot for the final volume of grain delivered to the Kinze grain cart using a first-last fill zone offset of one cell (25 cm) and two cells (50 cm)

Figure 87: Kinze grain cart filled with the center point of the first and last fill zones offset one cell (25 cm) outward from the actual center of the zones; grain is piled toward the middle with empty space at the front and back

7.3.5 Grain Cart Manufacturer

No significant impact was found in the final cart volume for the data sets comparing the Kinze and Brent (Figure 88) with a 95% desired fill level. The same test was conducted at 100% to determine if the impact was significant at higher desired cart fullness levels (Figure 89). The final

cart volumes showed no significance between the carts. This suggested the Kinze and Brent carts shared similar geometries within the range of desired fill levels tested (0-10 cm below the opening). The Brent cart had a pyramid base with short sidewalls while the Kinze had a shorter length with tall side walls. The lack of differences in the final volume between carts was likely caused by the top several feet of depth in the carts containing straight sidewalls.

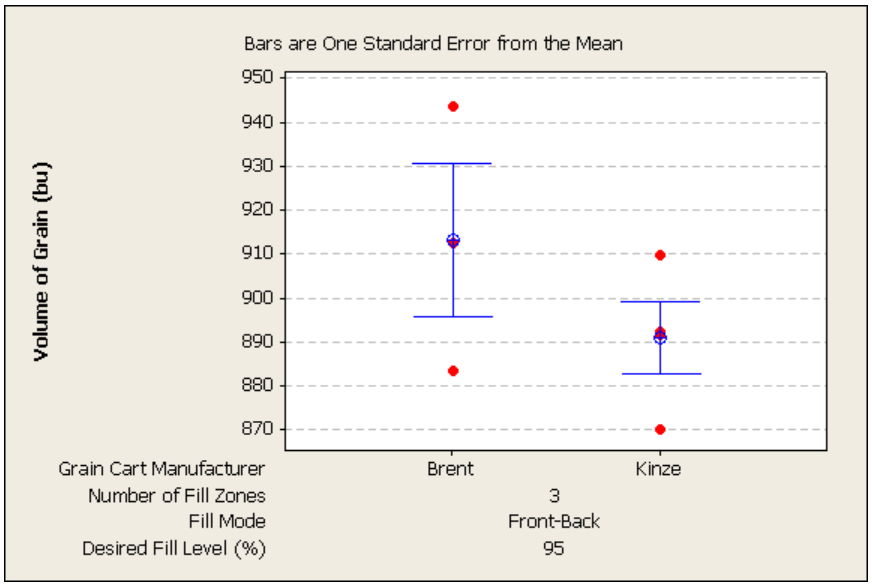

Figure 88: Interval plot for the final volume of grain delivered to the Kinze and Brent grain carts a 95% desired fill level

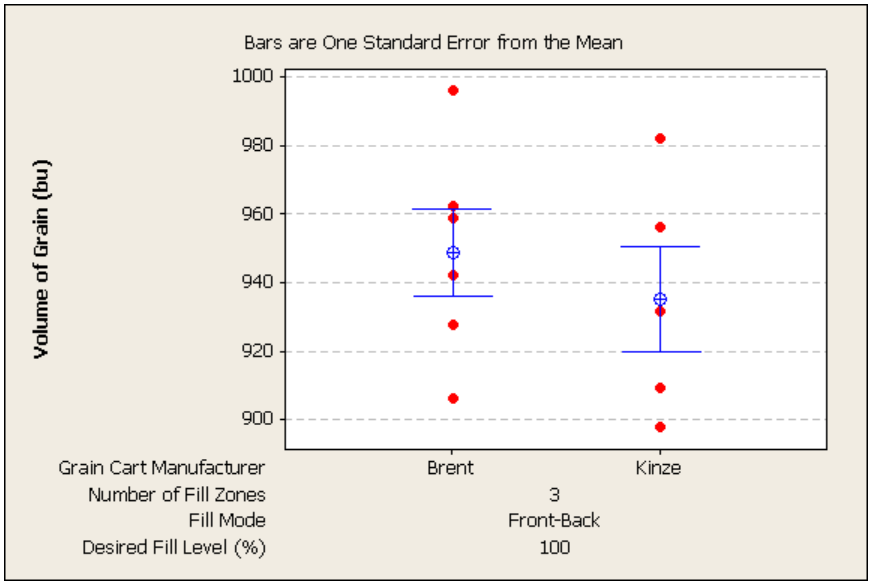

Figure 89: Interval plot for the final volume of grain delivered to the Kinze and Brent using a 100% desired fill level

7.4 Conclusions

A significant impact in the final cart volume was not detected in the Kinze grain cart when switching from a Front-Back to a Back-Front fill mode, but a small impact was measured with the same fill modes on the Brent cart. A strong conclusion was not formed from the results regarding the effect of the fill mode on the final cart volume.

When the number of fill zones was changed, one fill zone left substantial empty space at the front and back of the cart. Two fill zones showed a strong impact on the final cart volume by delivering grain to these areas. Additional fill zones above two did not significantly add to the final fullness of the grain cart on both models that were tested.

The resolution of the desired fill level, in order to demonstrate a significant change in the final cart volume was 5-10% (7.5-15 cm), depending on the cart manufacturer. This was within the 8% (10 cm) hysteresis applied to the grain height measurement during all testing indicating the hysteresis effectively reduced noise in the grain height measurement.

The first-last zone offset showed it had a very strong impact on the final cart volume when the offset changed from one cell to two cells. The impact on the cart volume was expected to continue being significant as the offset increased until the center point was adjusted to the boundary of the first and last fill zones.

The final cart volumes of the Kinze and Brent were statistically the same when subjected to the same delivery conditions. It was assumed a coincidence that the carts contained the same amount of grain while being designed of different geometries.

Chapter 8 Conclusions

The inverse distance weighting method was investigated as a modeling technique to estimate points of a fill grid in four situations prone to producing grain height measurements that were missing or highly variable. Higher distance exponents were shown to produce greater accuracy than lower exponents when grain was unloaded under extreme circumstances. The mean error of each estimated point in each of the four modeling situations is capable of achieving an accuracy of -15 cm to +25 cm with a distance exponent of ten in the inverse distance weighting equation. A distance exponent of ten caused the inverse distance weighting method to closely resemble the polygon estimation method. This indicated the polygon method is also a viable method for modeling points on the surface of a grain cart when a simpler method is required.

The average grain height of the fill grid was used to predict the weight of grain in a cart against four delivery conditions and using a dataset that included all the delivery conditions tested in this research. Different methods to calculate the average grain height in a cart indicated the calculated height was not significantly different whether points at the peaks or valleys of grain piles were used. Variation in the error of the predicted grain weight increased when 15 cells of the fill grid were used instead of 20 or 35. A bi-modal distribution of the error in the predicted grain weights appeared in the results of the testing indicating different delivery conditions can cause an average grain height model to over- or under-predict the weight of grain in the cart. The differences in the mean errors of each delivery condition were found to be statistically significant in the tests that were conducted, but the difference was less than 2% of a full cart weight so the impact of different delivery conditions was deemed insignificant to the application of using the average grain height to predict the weight of grain in a grain cart.

A decision support system was developed as part of an autonomous filling system for unloading on-the-go into grain carts. Dynamic field testing validated critical features of the algorithm, and performance was at a level of robustness and accuracy expected of an autonomous system. Increasing the number of fill zones used to fill the cart from one to two significantly increased the amount of grain added to the cart, but additional fill zones above two did not significantly add to the amount of grain the system delivered to the cart. Offsetting the center point

of the first and last fill zones of the cart by 50 cm also significantly increased the amount of grain the system delivered to the cart by distributing more grain to the front and rear of the cart.

Chapter 9 Future Work

The inverse distance weighting method was not able to achieve the desired accuracy of -15 cm to +25 cm when all far edge points were unavailable. A derivative of the inverse distance weighting method coupled with other modeling techniques could be investigated to produce more accurate estimates along the far edge. For simplicity, historic data and time-based modeling were not considered to estimate missing points. These techniques could be viable alternatives in situations where the inverse distance weighting method produced unexpected results.

The inverse distance weighting method was not used with other grain height measurement sensors, such as the stereovision cameras used for the dynamics field tests in Chapter 7. The next logical step in this research would be to apply inverse distance weighting to data produced by other types of sensors, such as stereovision cameras.

Chapter 6 highlighted the ability to predict the weight of grain in a cart based on the calculated average grain height. Investigation could be conducted into the a calibration procedure for determining the grain weight and assessing the risks associated with a decision support system designed to fill to a calibrated weight instead of a height. Research could also be conducted into the ability to use information from the grain moisture sensor on the combine to mitigate risks from highly variable grain moisture content across the field.

Vision systems are a relatively new technology to agriculture, especially in grain cart height sensing with stereovision. Continuous development of the decision support system will be essential as stereovision algorithms develop and better cameras are produced. Error bars in the final cart weight at the end of an unloading period are expected to shrink as the decision support system and stereovision algorithms improve.

Bibliography

Bern, C. J., Hurburgh, C. R., & Brumm, T. J. (2010). *Managing Grain After Harvest.* Ames, Iowa, USA: Iowa State University.

Blackmore, B. S., & Marshall, C. J. (1996). Yield Mapping: Errors and algorithm. In P. C. Robert, R. H. Rust, & W. E. Larson (Ed.), *Proceedings of the 3rd International Conference on Precision Agriculture* (pp. 403-415). Madison, WI: ASA, CSSA, SSSA.

CNH Global N.V. (2010, December 6). *Case IH Wins Gold and Silver Medals at SIMA Innovation Awards*. Retrieved September 21, 2011, from CNH Investors Site News Releases: http://investors.cnh.com/phoenix.zhtml?c=61651&p=irol-news&nyo=0

Deere & Company. (2011, August 25). *John Deere Introduces New Machine Sync Technology to Optimize Harvesting in the Field*. Retrieved September 21, 2011, from John Deere 2011 News Releases and Information: http://search.deere.com/DDC/en_US/News/

Enander, F. A. (1984). *Patent No. 4437497.* United States.

Han, S., Goering, C. E., Hummel, J. W., & Cahn, M. D. (1993). A Robust Method for Estimating Soil Properties in Unsampled Cells. *Transactions of the ASAE, 36*(5), 1363-1368.

Han, S., Schneider, S. M., Evans, R. G., & Davenport, J. R. (2004). Block Esimating of Spatial Yield Data and its Uncertainty. *Precision Agriculture, 5*, 73-84.

Happich, G., Lang, T., & Harms, H.-H. (2009). Loading of Agricultural Trailers using a Model-Based Method. *Agricultural Engineering International: The CIGR EJournal, XI*.

Happich, G., Lang, T., & Harms, H.-H. (2010). Parallel Operated Loading Using a Spatial Descriptive Model. *Proceedings of the 2nd International Conference on Machine Control and Guidance*, (pp. 187-195). Bonn, Germany.

Happich, G., Lang, T., & Harms, H.-H. (2010). Spatial Modeling of Agricultural Crops for Parallel Loading Operations. *Proceedings of the 10th International Conference on Precision Agriculture.* Denver, CO, USA: International Society of Precision Agriculture.

Isaaks, E. H., & Srivastava, R. M. (1989). *An Introduction to Applied Geostatistics.* New York: Oxford University Press.

Moller, J. (2010). *Computer Vision - A Versatile Technology in Automation of Agricultural Machinery.* Bologna: EIMA International.

Pollklas, M. (1996). *Patent No. 5575316.* Germany.

Pulli, R., Jasu, J., & Kallio, J. (2010, July 6). *Patent No. 7751927.* United States.

Srivastava, A. K., Goering, C. E., Rohrbach, R. P., & Buckmaster, D. R. (2006). *Engineering Principles of Agricultural Machines* (2 ed.). St. Joseph, Michigan, USA: ASABE.

United States Department of Agriculture. (2011). *World Agricultural Supply and Demand Estimates.* Office of the Chief Economist. Washington, D.C.: United States Department of Agriculture.

Webster, K. E. (2011). *Master's Thesis: Single-pass corn stover harvest system productivity and cost analysis.* Ames, Iowa, USA: Keith Edward Webster.